Study on the Biosynthetic Pathway of Polyunsaturated Fatty Acids in Unicellular Marine Eukaryotes Aiming for Industrial Applications

松田, 高宜
九州大学大学院生物資源環境科学府

https://doi.org/10.15017/21692

Study on the Biosynthetic Pathway of Polyunsaturated Fatty Acids in Unicellular Marine Eukaryotes Aiming for Industrial Applications

Takanori Matsuda

2012

CONTENTS

GENERAL INTRODUCTION 1

CHAPTER 1. The development of a transformation system for thraustochytrids
1-1. INTRODUCTION 22
1-2. MATERIALS AND METHODS 24
1-3. RESULTS 29
1-4. DISCUSSION 31
1-5. SUMMARY 33
FIGURES AND TABLES 34

CHAPTER 2. Molecular cloning of a *Pinguiochrysis pyriformis* oleate-specific microsomal Δ12-fatty acid desaturase and functional analysis in yeasts and thraustochytrids
2-1. INTRODUCTION 38
2-2. MATERIALS AND METHODS 40
2-3. RESULTS 46
2-4. DISCUSSION 51
2-5. SUMMARY 54
FIGURES AND TABLES 55

CHAPTER 3. The analysis of Δ12-fatty acid desaturase function revealed that two distinct pathways are active for the synthesis of polyunsaturated fatty acids in *Thraustochytrium aureum* ATCC 34304
3-1. INTRODUCTION 65
3-2. MATERIALS AND METHODS 68
3-3. RESULTS 75
3-4. DISCUSSION 82
3-5. SUMMARY 86
FIGURES AND TABLES 87

GENERAL DISCUSSION 106

REFERENCES 112
ACKNOWLEDGEMENTS 130

Abbreviations

ACP: acyl carrier protein

ARA: arachidonic acid (C20:4 n-6)

ATCC: American Type Culture Collection

Bla^r: blasticidin resistance

cDNA: complementary DNA

CoA: coenzyme A

DHA: docosahexaenoic acid (C22:6 n-3)

EF-1α: elongation factor-1α

EPA: eicosapentaenoic acid (C20:5 n-3)

FAME: fatty acid methyl ester

FAS: fatty acid synthse

GC: gas chromatography

GC-MS: gas chromatography mass spectrometry

GFP: green fluorescence protein

GL: glycolipid

GLA: γ-linolenic (C18:3 n-6)

Hyg^r: hygromycin resistance

LA: linoleic acid (C18:2 n-6)

Neo^r: neomycin resistance

NL: neutral lipid

OA: oleic acid (C18:1 n-9)

ORF: open reading frame

PCR: polymerase chain reaction

PKS: polyketide synthase

PL: phospholipid

PUFA: polyunsaturated fatty acid

RACE: rapid amplification of cDNA ends

SFA: saturated fatty acid

SDS-PAGE: sodium dodecyl sulfate polyacrylamide gel electrophoresis

TLC: thin-layer chromatography

GENERAL INTRODUCTION

In this thesis, the author describes the establishment of a transformation system for thraustochytrids and analysis of pathway for fatty acid production in thraustochytrids for industrial applications. Before the experimental details are discussed, some background and fundamental information are given as part of a general introduction. Finally, the scope of this research is summarized at the end of this chapter.

What are Thraustochytrids and Pinguiochrysis?

Thraustochytrids, widely distributed in marine and estuarine environments, are heterotrophic eukaryotic microorganisms. They are classified into the kingdom *Stramiipila*, class *Labyrinthulomycetes*, family *Thraustochytriaceae*, and four genera *Aurntiochytrium* (formerly *Schizochytrium*), *Thraustochytrium*, *Parientichytrium* and *Schizochytrium*. Thraustochytrids are characterized by the presence of an ectoplasmic network generated by one or more unique cell surface organelles called sagenogenetosomes, a cell wall with noncellulosic scales and a life cycle consisting of vegetative cells, zoosporangia, and zoospores (1, 2). Unlike *Thraustochytrium* vegetative cells, *Schizochytrium* vegetative cells divide into halves prior to releasing zoospores from zoosporangia (Fig. gi-1). Interestingly, zoospores of thraustochytrids show a chemotactic response to carbohydrates, amino acids and leaf extracts (3). Therefore, thraustochytrids can be isolated from environments through the chemotactic response toward pine pollen.

Thraustochytrids play a major role in the degradation and mineralization of detritus in

the ocean. They are able to produce extracellular enzymes such as cellulases, proteases, lipases and xylanases, decomposing organic matter as nutrients (4). Thraustochytrids are also known to be associated with marine invertebrates. Some thraustochytrids are pathogens to juvenile abalone and hard-shell clam (*Mercenaria mercenaria*) (5, 6). In addition, some species are found on the surface and in the mucus of reef-building coral species such as *Favia* sp. and *Fungia granulose*, with which they have mutualistic associations (7, 8).

Particular attention has been given to the thraustochytrids as potential sources of valuable bioactive compounds, such as fatty acids, carotenoids and squalene (9-11). Thraustochytrids are also expected to be a material for biofuel. Thraustochytrids possess prominent lipid bodies (lipid droplets) and accumulate a great amount of polyunsaturated fatty acids (PUFAs). Therefore, they are expected to be an alternative source of PUFAs, especially docosahexaenoic acid (DHA). Indeed, several products including DHA are now distributed in the USA and European markets. Thraustochytrids are also used commercially as feed for rotifers (*Brachionus* sp.) and brine shrimp (*Artemia* sp.), enriching them with PUFAs.

Many efforts to enhance the production of PUFAs in thraustochytrids have been conducted by changing growth conditions, such as temperature and concentrations of dissolved oxygen (12-16). However, the molecular breeding of thraustochytrids has yet to be fully conducted for the production of PUFAs. There are several basic demands for engineering thraustochytrids as potential sources of beneficial PUFAs: (1) uncovering the full scope of the biosynthetic pathway and, therefore, of the enzymes/genes involved; (2) cloning of the genes necessary for the selective production of specific PUFAs; (3) development of a transformation system for molecular breeding

of thraustochytrids.

Studies have proposed two distinct pathways involved in PUFA synthesis in thraustochytrids. One is the desaturase/elongase (standard) pathway, found widely in eukaryotes, in which PUFAs are produced by a series of alternating desaturation and elongation steps from saturated fatty acids. Several genes encoding desaturases and elongases have been cloned from thraustochytrids and functionally characterized in yeasts and plants (17-23). The other is the polyketide synthase-like (PUFA synthase) pathway, which is found in specific marine bacteria (24-26). This pathway, catalyzed by a complex enzyme machinery composed of multi-subunit enzymes homologous to enzymes in the polyketide synthase (PKS) pathway, has been found in *Schizochytrium* sp. (24-26). However, some enzymes essential for the standard pathway have not been identified in thraustochytrids. Therefore, further investigation is needed to elucidate the full scope of the pathways for PUFA production in thraustochytrids.

Pinguiochrysis pyriformis is an unicellular marine microalga classified into the kingdom *Stramiipila*, phylum *Ochrophyta*, and class *Pinguiophyceae* (27). *Pinguiophyceae* is a new class including five genera, *Pinguiochrysis*, *Glossomastix*, *Phaeomonas*, *Pinguiococcus* and *Polypodochrysis* (28). All five genera produce large amounts of PUFAs, especially EPA. *P. pyriformis* cells are typically pear-shaped and frequently change to a subspherical shape. The name of *P. pyriformis* is based on the large amounts of PUFAs (pingue = fat, grease) and the cell shape (pyriform = pear-shaped). Extracellular structures such as a cell wall and polysaccharide layer are not found around the cells of *P. pyriformis*. *P. pyriformis* has an ovoid chloroplast surrounded by a chloroplast endoplasmic reticulum and contains more than three thylakoids. It is suggested that EPA is mainly incorporated into glycolipids, structural

components of both envelop membranes and thylakoids in the chloroplast, in *Glossomastix chrysoplasta* (29).

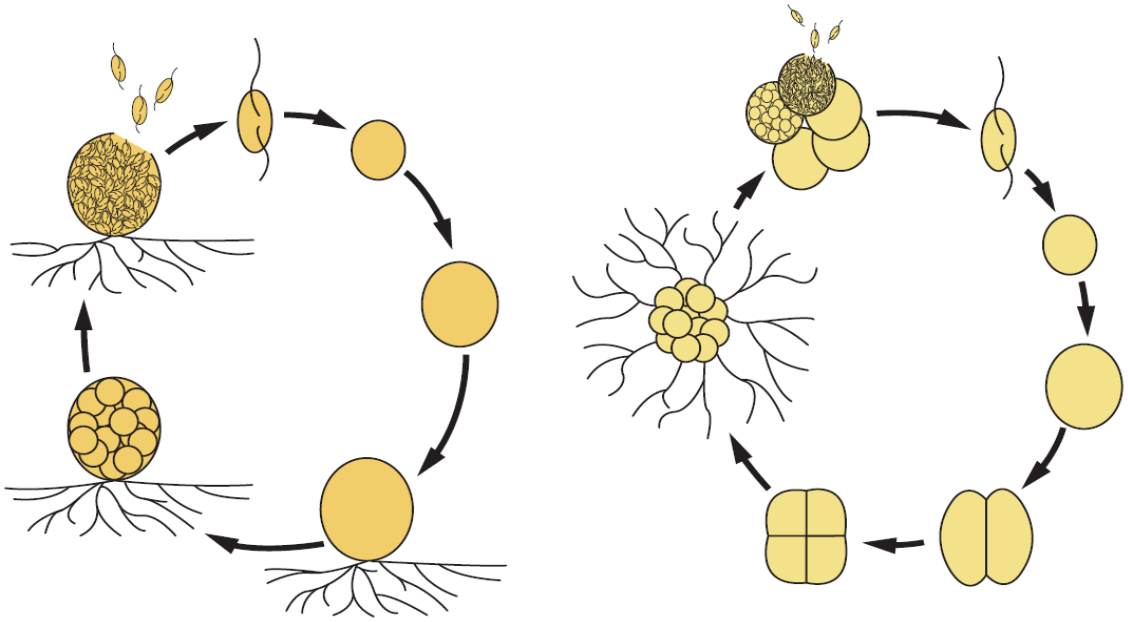

Fig. gi-1. Life cycles of *Thraustochytrium* and *Aurantiochytrium*.

Polyunsaturated fatty acids (PUFAs)

PUFAs are fatty acids that contain more than one double bond. Fatty acids are often abbreviated as $CX:Y^{\Delta z}$, where X stands for the number of carbon atoms of the acyl-chain, Y for the number of double bonds, and Z for the position of the double bond counted from the carboxyl end (Fig. gi-2A). For example, γ-linolenic acid (GLA), abbreviated as $C18:3^{\Delta 6, 9, 12}$, is an 18-carbon fatty acid with *cis* double bonds between carbons 6 and 7, carbons 9 and 10 and carbons 12 and 13. PUFAs are also classified into the omega-X form, depending on the position of the first double bond counted from the methyl terminus of the fatty acids. In this way, eicosapentaenoic acid (EPA, $C20:5^{\Delta 5, 8, 11, 14, 17}$) is abbreviated as C20:5ω3 or C20:5 n-3.

In most eukaryotic and prokaryotic organisms, PUFAs are biosynthesized by the desaturase/elongase (standard) pathway. On the other hand, some marine bacteria produce PUFAs by the polyketide synthase-like (PUFA synthase) pathway (30-34). In mammals, several PUFAs are recognized as essential fatty acids, because they lack the Δ12- and Δ15-fatty acid desaturases necessary to insert a double bond at the ω6 or ω3 position. PUFAs play important roles in many cellular functions as structural membrane components, gene regulatory elements and precursors of eicosanoids such as prostaglandins, thromboxanes, and leukotrienes (Fig. gi-2B) (35-39). For example, EPA and DHA have anti-inflammatory effects through their metabolic products or the stimulation of G protein-coupled receptors, thereby preventing chronic diseases such as coronary heart disease, diabetes, arthritis and cancer (40-44). DHA is also essential for neurological growth and development in infants and for the maintenance of adequate cellular function in the adult brain (45, 46). The eicosanoids from arachidonic acid

(ARA, C20:4 n-6) are mediators of acute inflammation and several diseases such as allergic disorders, asthma and cancer.

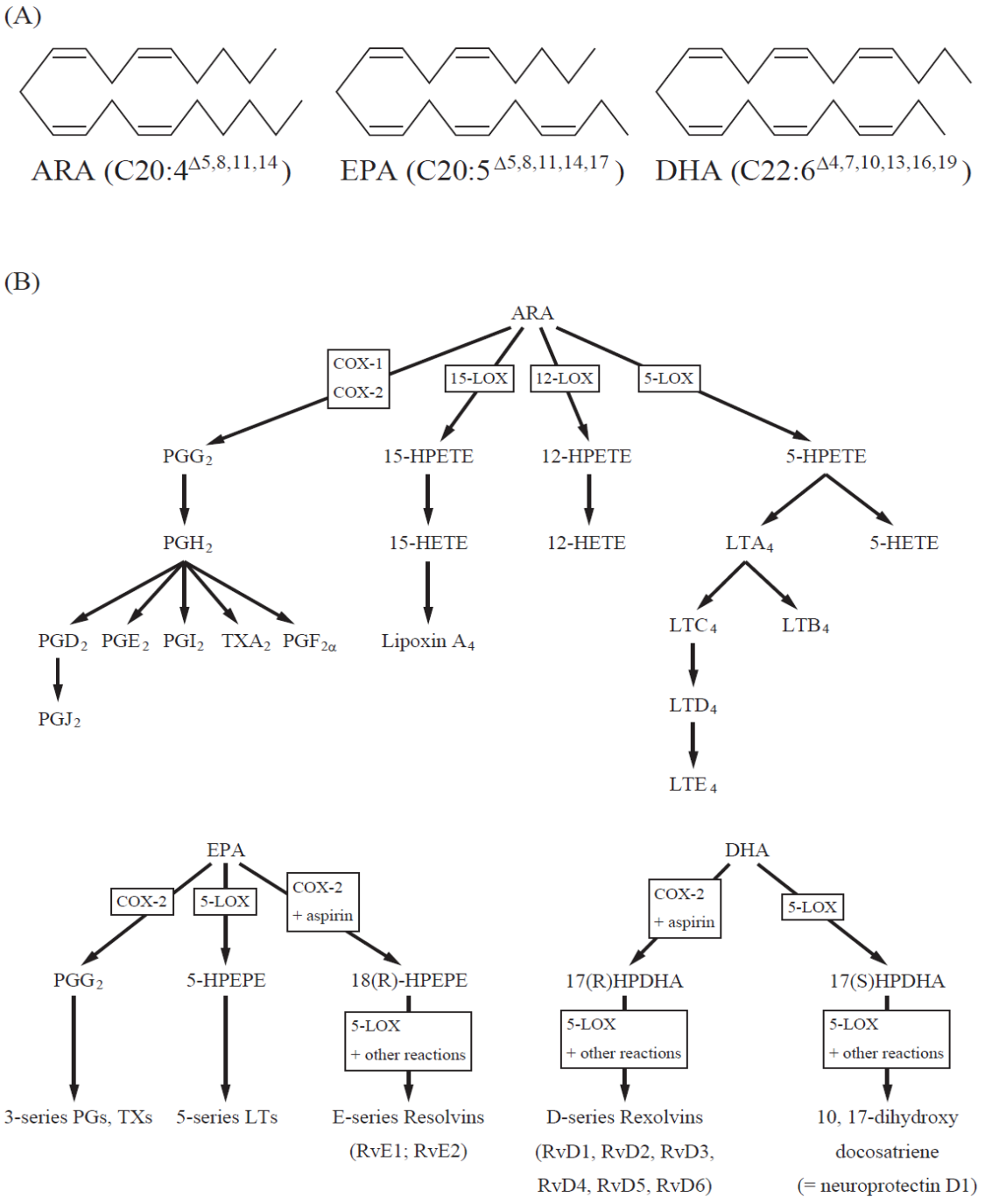

Fig. gi-2. Structure of several PUFAs and their metabolic pathways.

(A) Structures of ARA, EPA and DHA. (B) Outline of the pathways of production of eicosanoids and docosanoids. COX, cyclooxygenase; HETE, hydroxyl-eicosatetraenoic acid; HPETE, hydroperoxy-eicosatetraenoic acid; HPDHA, hydroperoxy-docosahexaenoic acid; HPEPE, hydroperoxy-eicosapentaenoic acid; LOX, lipoxygenase; LT, leukotriene; PG, prostaglandin; TX, thromboxane; Rv, resolvin.

Desaturase/elongase (standard) pathway

This pathway consists of alternating desaturation and elongation steps, with molecular oxygen required for the desaturation (Fig. gi-3). The initial step of this pathway occurs with the production of palmitic acid (C16:0) or stearic acid (C18:0) by fatty acid synthase (FAS). The palmitic acid is elongated to form stearic acid and then desaturated to produce oleic acid (OA, C18:$1^{\Delta 9}$) by a Δ9 -fatty acid desaturase. Next, a Δ12-fatty acid desturase converts the oleic acid into linoleic acid (LA, C18:$2^{\Delta 9,\ 12}$), which is further desaturated into α-linolenic acid (ALA, C18:$3^{\Delta 9,\ 12,\ 15}$) by a Δ15-fatty acid desaturase. Subsequently, the LA and ALA are desaturated by a Δ6-fatty acid desaturase. The products of the Δ6-fatty acid desaturation, γ-linolenic (GLA, C18:$3^{\Delta 6,\ 9,\ 12}$) and stearidonic acid (C18:$4^{\Delta 6,\ 9,\ 12,\ 15}$), are elongated to form dihomo-γ-linolenic acid (DGLA, C20:$3^{\Delta 8,\ 11,\ 14}$) and eicosatetraenoic acid (ETA, C20:$4^{\Delta 8,\ 11,\ 14,\ 17}$), respectively. This elongation is followed by Δ5-fatty acid desaturation to produce arachidonic acid (ARA, C20:$4^{\Delta 5,\ 8,\ 11,\ 14}$) and eicosapentaenoic acid (EPA, C20:$5^{\Delta 5,\ 8,\ 11,\ 14,\ 17}$). In some fungi, ARA is desaturated to produce EPA by a ω3-fatty acid desaturase (Δ17-fatty acid desaturase). Then, ARA and EPA are elongated to form docosatetraenoic acid (DTA, C22:$4^{\Delta 7,\ 10,\ 13,\ 16}$) and ω3 docosapentaenoic acid (ω3 DPA, C22:$5^{\Delta 7,\ 10,\ 13,\ 16,\ 19}$), respectively. Finally, these elongation products are subjected to further desaturation at the Δ4 position to produce ω6 docosapentaenoic acid (ω6 DPA, C22:$5^{\Delta 4,\ 7,\ 10,\ 13,\ 16}$) and docosahexaenoic acid (DHA, C22:$6^{\Delta 4,\ 7,\ 10,\ 13,\ 16,\ 19}$).

With regard to the biosynthesis of DHA, a Δ4-fatty acid desaturase-independent pathway has been proposed in mammals (47-49). This “Sprecher pathway” involves two consecutive elongation steps, Δ6-fatty acid desaturation and C2 unit shortening via

β-oxidation in the peroxisome. In addition, an alternate pathway for C20 PUFA production has been demonstrated in some organisms, which is independent of Δ6-fatty acid desaturation (50, 51). In the first step of this pathway, LA and ALA are elongated to form eicosadienoic acid (EDA, C20:$2^{\Delta 11, 14}$) and eicosatrienoic acid (ETrA, C20:$3^{\Delta 11, 14, 17}$). In turn, these elongation products are further desaturated to produce DGLA and ETA, respectively, by Δ8-fatty acid desaturase. The DGLA and ETA are then subjected to desaturation and elongation to produce final products in the conventional pathway. A schematic diagram of the desaturase/elongase pathway is shown in Fig. gi-3.

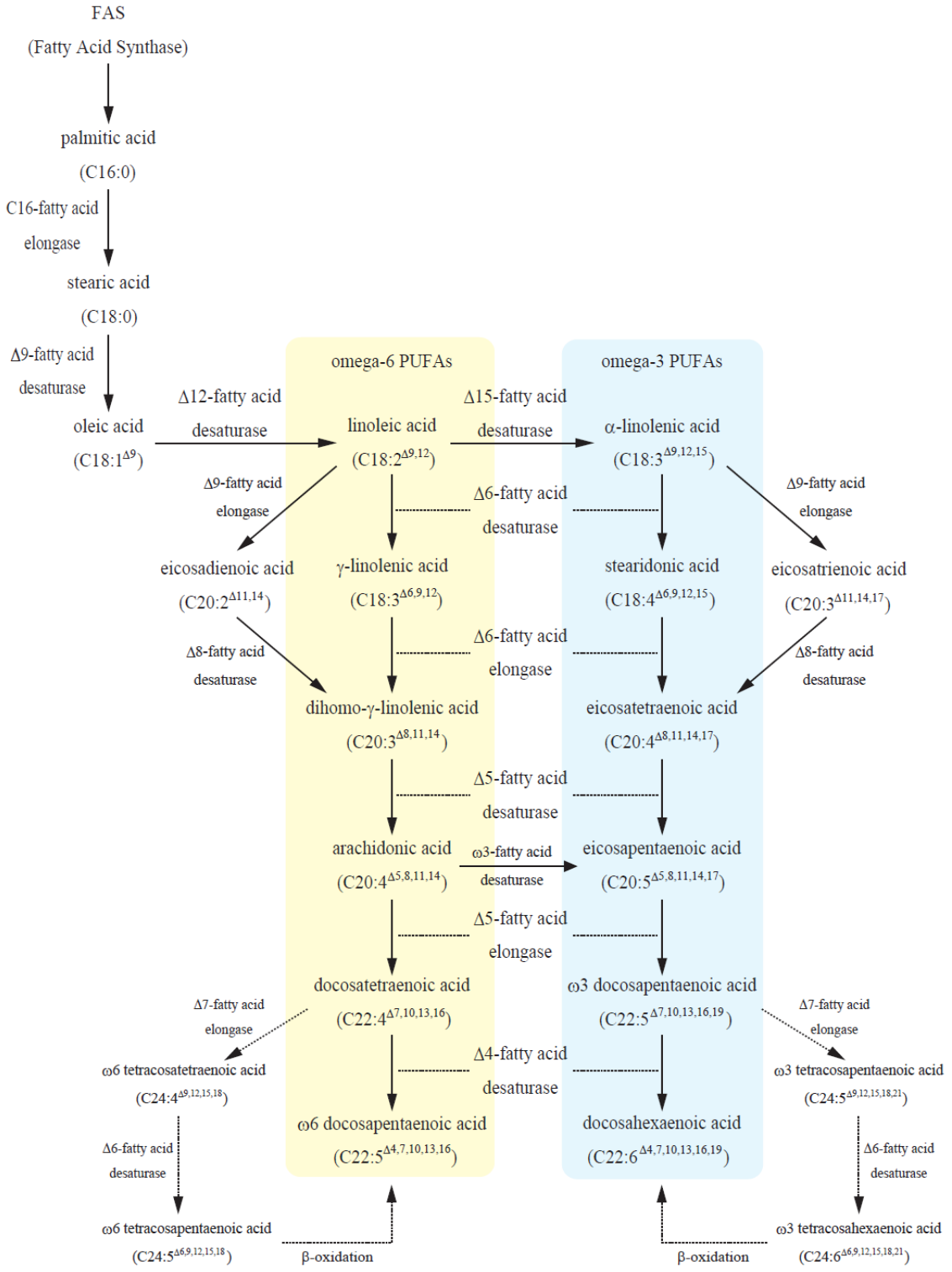

Fig. gi-3. Schematic diagram of desaturase/elongase (standard) pathway.
Dashed arrows indicate the "Sprecher pathway" found in mammals but not thraustochytrids.

Fatty Acid Desaturase

Fatty acid desaturases, iron-containing enzymes, introduce a double bond at a specific position in fatty acids (Fig. gi-4) (52). These enzymes require molecular oxygen and an electron transport system (usually ferredoxin-NADPH reductase and ferredoxin, or cytochrome *b5* reductase and cytochrome *b5*) for their reactions. Fatty acid desaturases use activated molecular oxygen to extract hydrogens from the substrate creating a double bond in a fatty acid. Except for the soluble acyl-acyl carrier protein (ACP) desaturase in plant plastids (53), all of these enzymes have several transmembrane domains and contain three histidine boxes, which act as di-iron coordinating centers for catalytic activity (54).

In terms of their regioselectivity or acyl substrate specificity, desaturases are categorized into several groups. Four regioselective classes have been proposed for these fatty acid desaturases (Fig. gi-5). Δx-fatty acid desaturases introduce a double bond at position x from the carboxyl end of a fatty acid (17, 51). ωx-fatty acid desaturases introduce a double bond between the x and x + 1 carbons from the methyl end (55). The ν + x fatty acid desaturases introduce a double bond at x carbons from the pre-existing double bond (ν) toward the methyl end, while ν – x fatty acid desaturases introduce a double bond at x carbons from the pre-existing double bond ν toward the carboxyl end (56, 57). Δ4, Δ5, Δ6 and Δ8-fatty acid desaturases are also classified as 'front-end' desaturases (58). These desaturases introduce a new double bond between the pre-existing double bond and the carboxyl end of fatty acids. Front-end desaturases are characterized by the presence of cytochrome *b5*-domain in their amino acid sequences, which is predicted to serve as an electron donor during

desaturation.

With regard to the acyl substrate specificity, fatty acid desaturases are separated into three types. The acyl-Coenzyme A (CoA) desaturases use fatty acids esterified to CoA as a substrate, and this type of desaturase is found in animals, insects and microalgae (57, 59, 60). The acyl-ACP desaturases are soluble enzymes, and desaturate fatty acids linked to ACP. The acyl-lipid desaturases introduce a double bond into lipid-bound fatty acids such as glycerophospholipids and sphingolipids (61, 62).

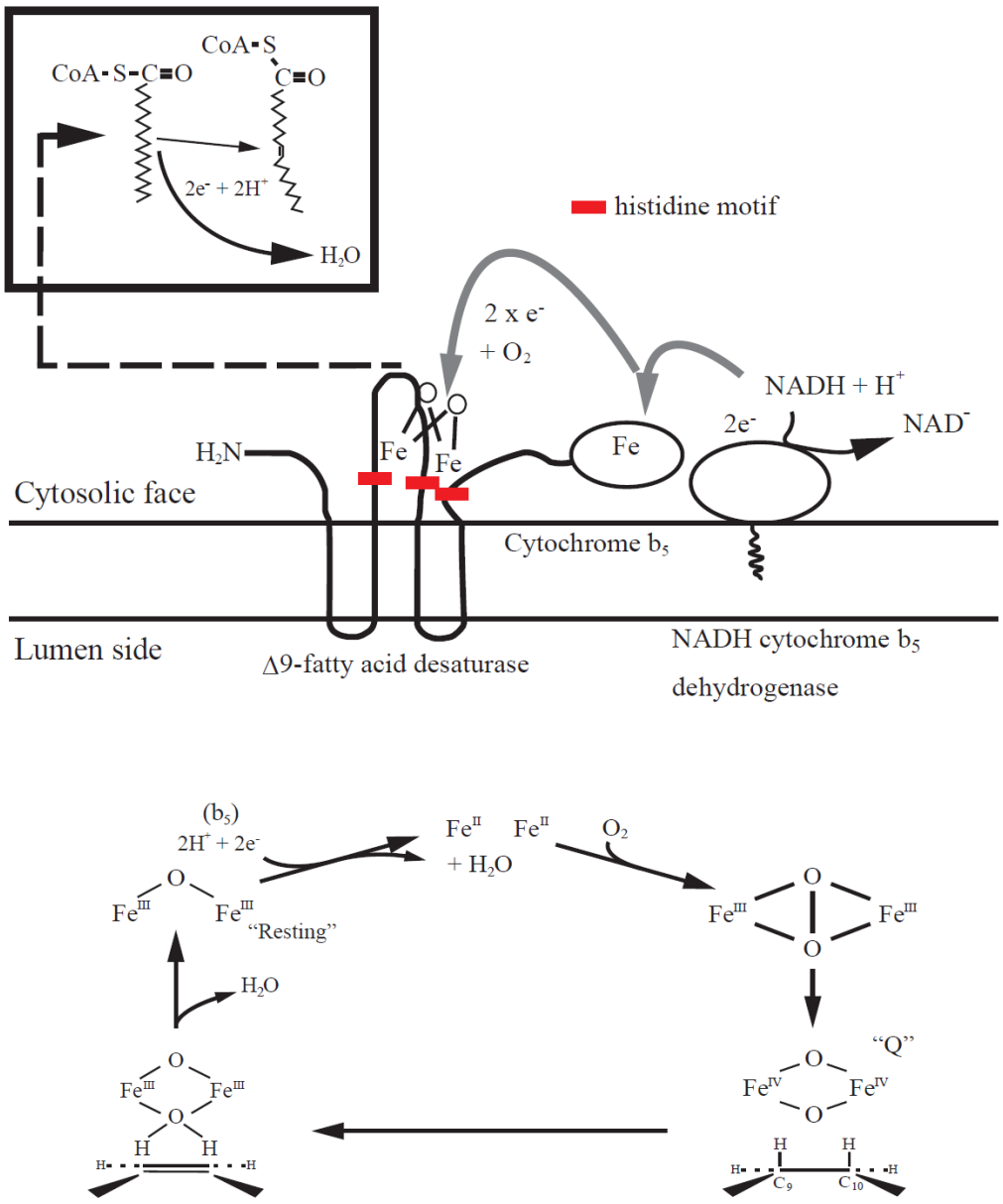

Fig. gi-4. Proposed trans-membrane form and mechanism of the Δ9-fatty acid desaturase.

The transfer of 2 electrons and 2 protons from the hydrocarbon chain to water results in the formation of the cis-double bond in the substrate fatty acid. Reducing equivalents were transferred from NADH to the diiron-oxo raction center (gray arrow) through NADH cytochrome *b5* dehydrogenase and cytochrome *b5*. Reducing equivalents reduce the iron atoms to the ferrous state with the release of the oxygen atom as water. The red boxes indicate the positions of the histidine clusters that form di-iron coordinating centers for catalytic activity.

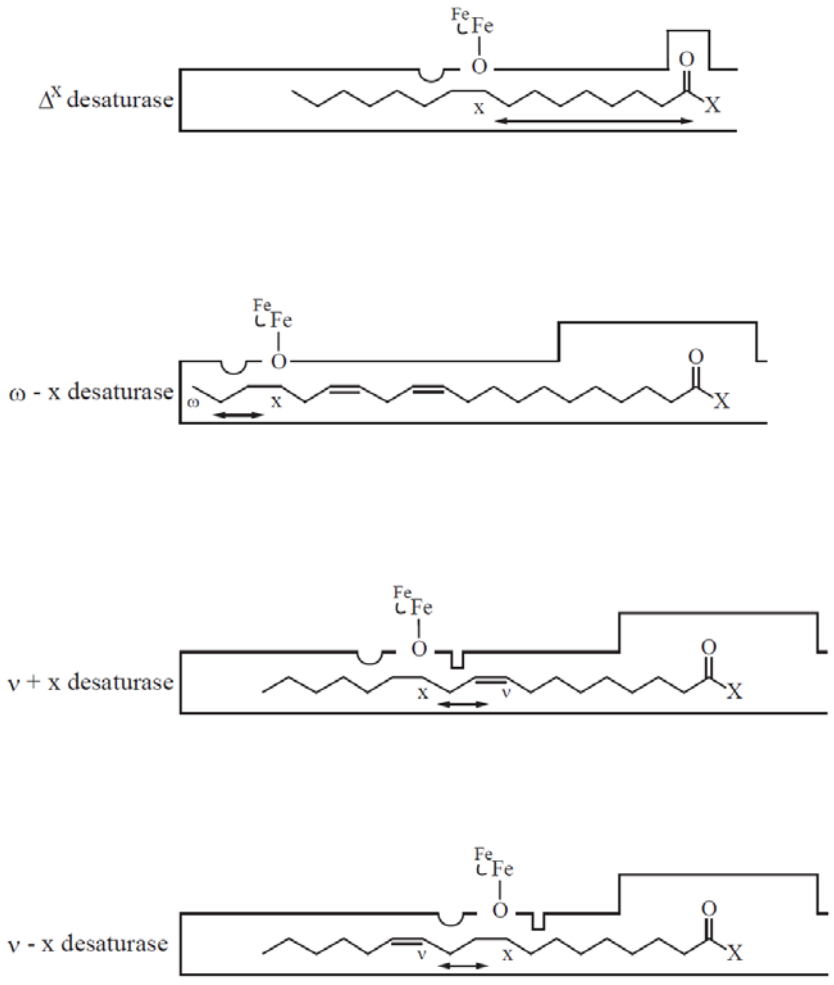

Fig. gi-5. The type of fatty acid desaturase based on their regioselectivity.

Elongase

Fatty acid elongation consists of four reactions catalyzed by a multi-enzyme complex composed of four enzymes (Fig. gi-6) (63). The initial step is the condensation of malonyl-CoA with the acyl primer to form β-ketoacyl-CoA catalyzed by β-ketoacyl-CoA synthase (called elongase, ELOVL, KCS or FAE), which is the rate-limiting step in the elongation process. Next, the β-ketoacyl-CoA is reduced to β-hydroxyacyl-CoA by β-ketoacyl-CoA reductase in the presence of NAD(P)H. Subsequently, dehydraion of the β-hydroxyacyl-CoA to trans-2-enoyl-CoA is mediated by β-hydroxyacyl-CoA dehydratase. Then, reduction of the enoyl-CoA by enoyl-CoA reductase in the presence of NAD(P)H generates a fatty acyl-CoA that is two carbons longer. The substrate specificity in the elongation reaction is determined by the β-ketoacyl-CoA synthase, and predicted elongation activity is restored by the expression of only this enzyme in heterologous hosts (64). The three other enzymes are ubiquitously expressed and shared by diverse elongation systems.

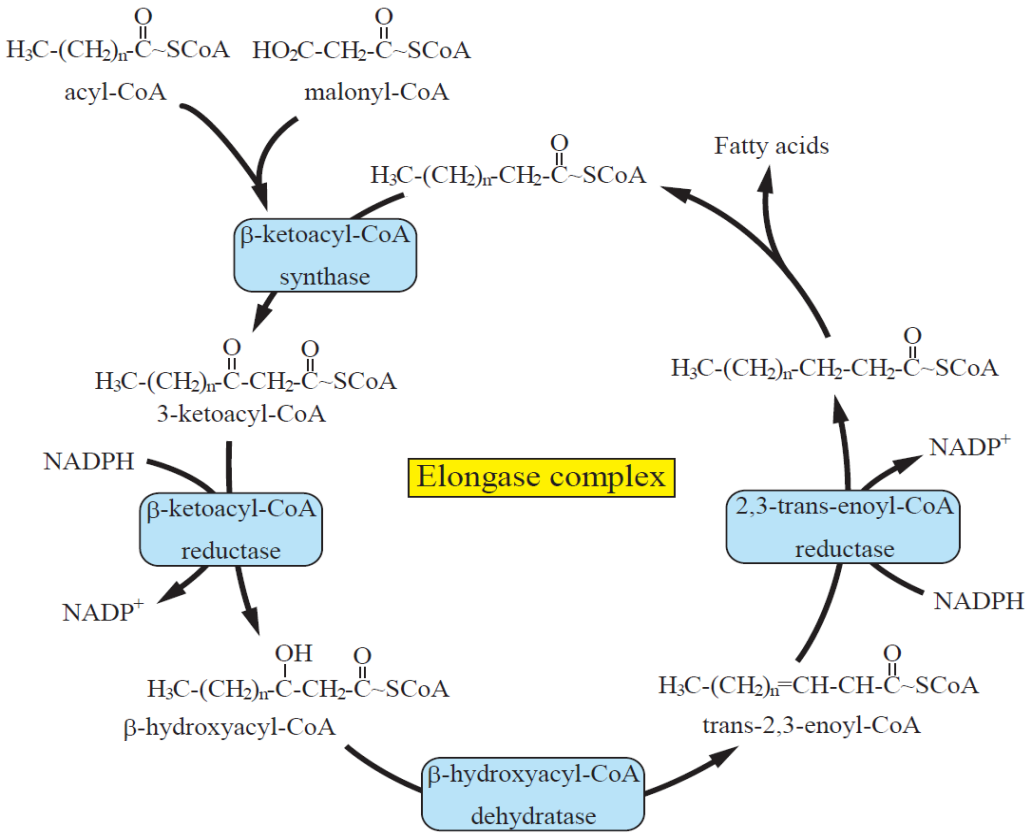

Fig. gi-6. Schematic diagram of the fatty acid elongation system.

Polyketide synthase-like (PUFA synthase) pathway

The genes involved in this pathway were cloned from an EPA-producing bacterium, *Shewanella* sp. strain SCRC-2738, in 1996 (65). After this discovery, homologs were cloned from both prokaryotic and eukaryotic marine organisms (30-34). Among eukaryotes, this pathway has been reported only in thraustochytrids (24-26). Since the pathway does not require molecular oxygen, PUFAs are biosynthesized under both anaerobic and aerobic conditions. This process involves a large multi-domain enzyme complex. Several domains closely resemble homologs of polyketide synthase (PKS) and fatty acid synthase (FAS). The mechanism of action of the PUFA synthase has been predicted by several researchers (66, 67). As shown in Fig. gi-7, the initial step of this pathway is the condensation of an acyl-ACP and a malonyl-ACP to produce a ketoacyl-ACP by ketosynthase. Next, the ketoacyl-ACP is reduced to hydroxyacyl-ACP by ketoreductase, followed by dehydration/isomeration to produce an enoyl-ACP by dehydratase/isomerase. Then, the enoyl-ACP is subjected to reduction to saturated fatty acid by enoyl reductase. Unlike FAS, the PUFA biosynthetic pathway often omits processes such as dehydration/isomeration and reduction.

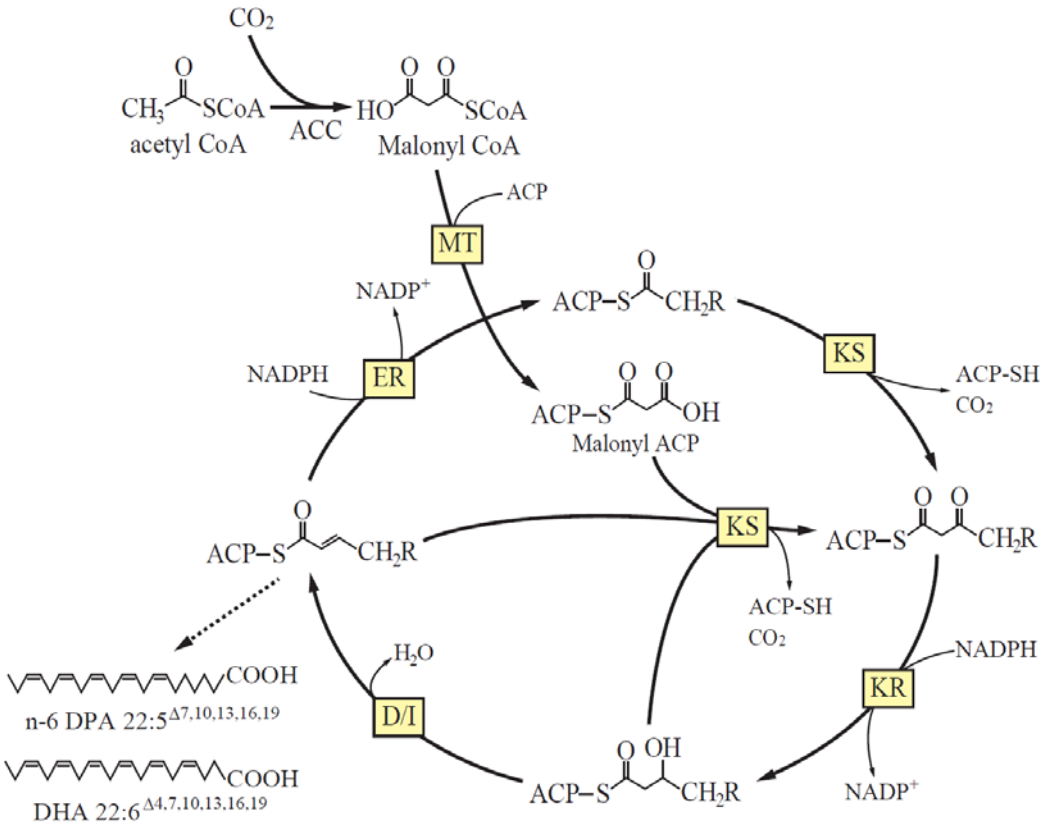

Fig. gi-7. Predicted PUFA biosynthesis in the PUFA synthase pathway.

ACC, Acetyl-CoA carboxylase; MT, Malonyl transferase; ACP, Acyl carrier protein; KR, Ketoreductase; ER, Enoyl reductase; KS, Ketosynthase; D/I, Dehydratase/Isomerase

The scope of this study

As described above in this CHAPTER, the development of a transformation system and elucidation of the PUFA biosynthesis pathway are necessary for the selective production of PUFAs using thraustochytrids. This thesis describes the development of a transformation system for thraustochytrids and evaluates the biosynthetic pathway for PUFA production in two typical genera of thraustochytrids, *Aurantiochytrium* and *Thraustochytrium*.

CHAPTER 1 describes a transformation system developed for thraustochytrids, which uses the neomycin-resistance (Neo^r) gene and enhanced-green fluorescence protein (EGFP) as transformation markers. The system is applicable to the genetic manipulation of thraustochytrids as shown in the following chapters.

CHAPTER 2 describes the heterozygous expression of a fatty acid desaturase in *Aurantiochytrium limacinum* mh0186. The gene encoding a Δ12-fatty acid desaturase was cloned from the marine alga *Pinguiochrysis pyriformis*, expressed in *Saccharomyces cerevisiae*, and characterized. This enzyme was expressed functionally in thraustochytrids as well as yeasts. In this chapter, the author discusses the PUFA biosynthesis in *A. limacinum* mh0186 in terms of Δ12-fatty acid desaturase activity.

Finally, the molecular cloning and characterization of a Δ12-fatty acid desaturase from *Thraustochytrium aureum* ATCC 34304 are described in CHAPTER 3. This enzyme adopted not only oleic acid (C18:1) but also odd-numbered monounsaturated fatty acids such as C17:1 and C19:1. Disruption of the Δ12-fatty acid desaturase gene in *T. aureum* resulted in significant changes in fatty acid profiles without decreasing the

content of DHA. This result may indicate that the standard pathway functions to produce PUFAs, whereas DHA is mainly produced by the PUFA synthase system. That is, two distinct pathways are present in *T. aureum* for production of PUFAs.

The transformation system developed in this study was successfully applied to transgene expression and targeted gene disruption in thraustochytrids. This is the first report describing the heterozygous expression and disruption of a fatty acid desaturase in thraustochytrids. This study also provides evidence that the mode of production of PUFAs differs depending on the genera/species in thraustochytrids. This study could facilitate the molecular breeding of thraustochytrids for the selective production of beneficial PUFAs.

CHAPTER 1

The development of a transformation system for thraustochytrids

1-1. INTRODUCTION

Many n-3 PUFAs such as eicosapentaenoic acid (EPA) and docosahexaenoic acid (DHA) function as therapeutic "nutraceuticals" in the prevention and treatment of cardiovascular and inflammatory diseases (41-43). EPA and DHA have historically been obtained from fish oils, but recent decreases in fish stocks make alternative sources desirable. Thraustochytrids are heterotrophic unicellular eukaryotes belonging to the class Labyrinthulomycetes. These organisms have been isolated from a wide range of habitats worldwide including deep-sea and estuarine environments. Because of their ability to accumulate high levels of PUFAs, thraustochytrids have received much attention as a potential commercial source of PUFAs. Considerable effort has been expended in modifying plants to produce desirable PUFAs through the expression of certain elongases and desaturases (68, 69). However, the genetic manipulation of thraustochytrids holds the potential for the accumulation of higher levels of PUFAs than those found in plants because thraustochytrids are capable of storing large amounts of PUFAs in their lipid droplets. Nevertheless, the basic information and tools required for genetic manipulation remain missing for thraustochytrids. Therefore, the development of a transformation system for thraustochytrids will facilitate not only the molecular breeding of thraustochytrids that are highly enriched for desirable PUFAs but also the elucidation of their PUFA biosynthetic pathway.

Since its discovery in the jellyfish *Aequorea aequorea* by Shimomura *et al* in 1962, green fluorescent protein (GFP) and its derivatives have been applied extensively in the biological sciences, e.g., in promoter assays, the monitoring of protein trafficking, the detection of viral infection and other labeling studies (70, 71). These proteins are also useful tools for evaluating the efficiency of transformation (72) because they are easily detected under a fluorescent microscope and do not require the addition of exogenous substrates.

In this chapter, the author describes the development of a transformation system for thraustochytrids using the neomycin-resistance (Neo^r) and enhanced-GFP (EGFP) genes as selection markers. These marker genes, driven by promoter/terminator systems derived from elongation factor-1α (EF–1α) or ubiquitin, were randomly integrated into the genomes of thraustochytrids and functionally expressed. This transformation system, which is applicable to transgene expression, will make it possible to obtain genetically engineered thraustochytrids for the selective production of beneficial PUFAs.

1-2. MATERIALS AND METHODS

Materials

Restriction enzymes and a Ligation-Convenience Kit were purchased from Nippon Gene (Tokyo, Japan). Synthetic oligonucleotides were obtained from Hokkaido System Science (Hokkaido, Japan) and GeneNet (Fukuoka, Japan). D-(+)-Glucose and dry yeast extract were purchased from Nacalai Tesque (Kyoto, Japan). SEA LIFE was purchased from MARINETECH Co., Ltd. (Tokyo, Japan). Neomycin (G418) was purchased from Nacalai Tesque. All other reagents were of the highest purity available.

Strains and culture

Thraustochytrium aureum ATCC 34304 was obtained from the American Type Culture Collection (USA). *Aurantiochytrium limacinum* mh0186 and *Thraustochytrium* sp. ATCC 26185, obtained from Dr. M. Hayashi at Miyazaki University, were identified based on the sequences of their 18S rRNA genes (DDJB, accession number: AB362211) (73). All these strains were maintained on potato dextrose agar (PDA) plates (0.8% potato dextrose and 1.2% agar in 50% artificial sea water). The thraustochytrids were cultivated on GY medium, consisting of 3% glucose and 1% yeast extract in 50% artificial sea water (ASW).

Isolation of the promoter and terminator regions of EF–1α

T. aureum ATCC 34304 was grown at 25°C in GY liquid medium with shaking at 150 rpm. Cells in the logarithmic growth phase were harvested by centrifugation (3,500 ×

g, 4°C, 10 min), and the total RNA was extracted using Sepasol RNA I Super (Nacalai Tesque). The poly(A)$^+$ RNA was purified using an Oligotex-dT Super mRNA Purification Kit (TaKaRa Bio, Shiga, Japan). First strand cDNA was prepared with a SMART RACE cDNA Amplification Kit (Clontech, CA, USA), and the 3′- and 5′-RACE PCRs were performed according to the manufacturer's instructions. PCR was then performed using a degenerate primer targeting the conserved region of EF–1α, EF-F1 (5′-THG AYG CNC CNG GNC AYM G-3′). The sequence of the 980-bp 3′-RACE product was highly homologous to EF–1α, and thus the primer EF-1r (5′-GTG AAG GCC AGA AGG GCG TG-3′) was designed to perform 5′-RACE PCR. Consequently, we identified a 1,396-bp region of the EF–1α cDNA derived from *T. aureum* ATCC 34304 that included a 1,023-bp ORF encoding 341 amino acid residues. Subsequently, the 5′- and 3′-flanking sequences of the gene, assumed to be the functional EF–1α promoter and terminator regions, were isolated using an LA PCR *in vitro* Cloning Kit (TaKaRa Bio) according to the manufacturer's instructions. The PCR primers used were as follows: r3 (5′-CCT CCT TCT CGA ACT TCT CGA TCG TG-3′) for the isolation of the EF–1α 5′-flanking sequences; EF-t-F1 (5′-CAT GGT CAA GAT GTA TCC CCT CCA A-3′) and EF-t-F2 (5′-TCA CCA AGG GCG ACA AAT AAA TTC T-3′) for the EF–1α 3′-flanking sequences. As a result, 615-bp and 1,414-bp EF–1α promoter and terminator regions, respectively, were identified.

Construction of the Neo^r and Neo^r/EGFP expression cassettes

The codons of the Neo^r gene were adjusted according to the codon usage of *T. aureum* (http://www.kazusa.or.jp/codon/) to achieve suitable expression in thraustochytrids. The Neo^r expression cassette (the Neo^r construct, Fig. 1-1A), driven

with an EF–1α promoter/terminator system, was prepared by fusion PCR. The Neo^r construct was subcloned into the *Ssp* I/*Pst* I sites of the pUC18 vector (TaKaRa Bio) to generate the plasmid pNeo^r. A linear DNA fragment of the Neo^r construct was amplified by PCR using 2F and 5R as the primers and used for the transformation of thraustochytrids. Prior to constructing the Neo^r/EGFP expression cassette (the EGFP construct, Fig. 1-2A) that is driven by an EF–1α or ubiquitin promoter/terminator system, the EGFP expression cassette was generated by fusion PCR. The PCR product was then subcloned into the *Kpn* I site of pNeo^r to generate the EGFP construct. The ubiquitin promoter and terminator were obtained from *T. aureum* ATCC 34304. A linear DNA fragment of the EGFP construct was amplified by PCR with the 2F and pUC18-R primers and used for thraustochytrid transformation. The primers used for the PCR amplification are listed in Table 1-1.

Transformation of *Thraustochytrium* sp. ATCC 26185

The Neo^r construct was introduced into *Thraustochytrium* sp. ATCC 26185 by electroporation. After culturing in GY medium, cells in the logarithmic growth phase were harvested by centrifugation (3,500 × *g*, 4°C, 10 min) and washed with distilled water plus 1.75% (w/v) SEA LIFE. The cells (5×10^6) were then resuspended in 75 μl of Nucleofector solution L (Amaxa Biosystems, MD, USA), 50 mM sucrose, 100 mM sucrose or 300 mM sorbitol. Subsequently, the suspended cells were mixed with 5 mg of highly purified DNA fragments and then transferred to a 0.1-cm-gap cuvette, which was pulsed twice using a Gene Pulser (Bio-Rad, CA, USA). After the pulses, 1 ml of GY medium was immediately added to the solution, which was incubated at 25°C for 1 day and then spread on a PDA plate (containing G418 at 2 mg/ml).

Expression of EGFP in thraustochytrids

The EGFP construct was introduced into *Thraustochytrium* sp. ATCC 26185 and *A. limacinum* mh0186 by electroporation using Nucleofector solution L as the suspending solution. The method for electroporation was described above (pulse conditions: 50 mF, 50 W, 7.5 kV/cm, 2 pulses).

The Biolistic PDS-1000/He system (Bio-Rad) was used for the transformation of *T. aureum* ATCC 34304. Gold particles (0.6 mm in diameter) coated with highly purified DNA fragments were prepared according to the manufacturer's instructions. Cells in the logarithmic growth phase were harvested by centrifugation (3,500 × *g*, 4°C, 10 min) and spread on a PDA plate (15 × 60 mm) without G418. The bombardment was performed in a Biolistic PDS-1000/He system with DNA-coated gold microcarriers according to the manufacturer's instructions using the following bombardment conditions: pressure, 7.58×10^6 Pa; target distance, 6 cm; vacuum, 8.80×10^4 Pa. After the bombardment, the plate was incubated at 25°C for 4 hours, after which the cells were collected and suspended in GY medium followed by respreading on a PDA plate containing G418. The concentrations of G418 added to the PDA plates were 2 mg/ml for *Thraustochytrium* sp. ATCC 26185 and *T. aureum* ATCC 34304 and 0.5 mg/ml for *A. limacinum* mh0186.

Genomic PCR and Southern blot hybridization of thraustochytrid transformants

Genomic DNA was prepared from transformants cultured in GY medium containing appropriate amounts of G418. PCR was then performed using the forward primer 2F and the reverse primers 5R or pUC18-R (Table 1-1). For the Southern blot analysis, 3 μg of genomic DNA was digested with *Pst* I or *Hin*d III and subjected to 0.7% agarose

gel electrophoresis. The DNA was then transferred to a nylon membrane (Hybond N^+, GE healthcare, Tokyo, Japan). The membrane was hybridized with a probe that was prepared using the PCR DIG Probe Synthesis Kit (Roche Diagnostics K.K., Mannheim, Germany). The 3F and 4R PCR primers were used for the Neo^r DNA probe synthesis. The genomic DNA hybridized with the probe was detected with an anti-digoxigenin-AP Fab fragment and an NBT/BCIP stock solution (Roche Diagnostics K.K.).

RT-PCR analysis

Total RNA was prepared from transformants grown in GY medium containing appropriate amounts of G418 using Sepasol RNA I Super, an RNeasy Mini Kit (QIAGEN, Tokyo, Japan) and DNase I (Takara Bio Inc.) and used to produce first-strand cDNA with PrimeScript^{TM} Reverse Transcriptase (Takara Bio Inc.). PCR was performed using the forward primer 3F and the reverse primer 4R for the amplification of Neo^r cDNA.

Fluorescence assay

Colonies grown on PDA plates containing appropriate amounts of G418 were observed by fluorescence microscopy (Leica Microsystems, Tokyo, Japan). EGFP-positive colonies were inoculated on GY medium containing appropriate amounts of G418 and incubated at 25°C with shaking at 150 rpm. Cells in the late logarithmic growth phase were harvested by centrifugation (3,500 × *g*, 4°C, 10 min) then washed and suspended in sterilized sea water. The harvested cells were then observed under a confocal laser-scanning microscope Digital Eclipse C1 (Nicon, Tokyo, Japan).

1-3. RESULTS

Transformation of *Thraustochytrium* sp. ATCC 26185 with the Neo^r construct

To develop a transformation system for *Thraustochytrium* sp. ATCC 26185, the author constructed a Neo^r expression cassette (Neo^r construct, Fig. 1-1A) driven with an EF–1α promoter/terminator system. The EF–1α gene with 5′ and 3′ flanking sequences was isolated from *T. aureum* ATCC 34304 as described in the MATERIALS AND METHODS. The Neo^r construct was introduced into *Thraustochytrium* sp. ATCC 26185 by electroporation. The transformants were obtained under several pulse conditions: 0.15 kV/50 Ω/1,000 μF, 0.3 kV/50 Ω/500 μF, 0.3 kV/50 Ω/1,000 μF and 0.75 kV/50 Ω/50 μF with Nucleofector solution L, or 0.15 kV/50 Ω/200 μF and 0.15 kV/50 Ω/1,000 μF with 50 mM sucrose. Transformants grown on GY medium containing G418 were subjected to genomic PCR to examine whether the full-length Neo^r construct was integrated into the chromosomal DNA. As illustrated in Fig. 1-1B, a 2,657-bp PCR product (corresponding to the Neo^r construct) was detected in these transformants. Southern blot hybridization using a Neo^r DNA probe confirmed that the Neo^r gene was randomly integrated into the genomes of the thraustochytrids (Fig. 1-1D). Furthermore, RT-PCR revealed the presence of 835-bp transcripts of the Neo^r gene in these transformants (Fig. 1-1C).

Expression of the EGFP gene in the thraustochytrids

To express EGFP in the thraustochytrids, the Neo^r/EGFP expression cassette (EGFP construct, Fig. 1-2A), driven with an EF–1α and ubiquitin promoter/terminator system, was constructed. The EGFP and Neo^r constructs were separately introduced into

Thraustochytrium sp. ATCC 26185, *A. limacinum* mh0186 and *T. aureum* ATCC 34304. Colonies transformed with the EGFP construct, but not the control Neo^r construct, showed EGFP-derived fluorescence under the fluorescence microscope. The transformants were also subjected to genomic PCR, and single bands corresponding to each full-length construct were detected (Fig. 1-2B, C). Furthermore, cells harboring the EGFP construct, but not the Neo^r construct, exhibited green fluorescence under the confocal laser-scanning microscope (Fig. 1-3).

1-4. DISCUSSION

Thraustochytrids are unicellular eukaryotic microorganisms that are grouped in the class *Labyrinthulomycetes* based on their 18S rDNA sequences and life cycles. Thraustochytrid PUFA profiles are used as identifying characteristics in their taxonomy because these profiles differ by strain (74). Because of their ability to synthesize and accumulate PUFAs, thraustochytrids have attracted attention as potential commercial sources of beneficial PUFAs. The development of a transformation system should enable the production of large amounts of desirable PUFAs in thraustochytrids. In addition, the alteration of the PUFA profiles in thraustochytrids by gene manipulation could elucidate the biosynthetic pathways and biological functions of the PUFAs. However, a transformation system has not yet been established for thraustochytrids.

In this study, the author attempted to develop a transformation system for thraustochytrids. The Neo^r expression cassette was integrated into the genome when introduced into *Thraustochytrium* sp. ATCC 26185 (Fig. 1-1B). Southern blot analysis revealed that the integration of the marker gene occurred at a different chromosomal site in each transformant (Fig. 1-1D). Furthermore, the Neo^r gene was effectively transcribed into Neo^r mRNA (Fig. 1-1C). To assess the transformation system developed in this study, the Neo^r/EGFP expression cassette was introduced into *Thraustochytrium* sp. ATCC 26185, *A. limacinum* mh0186 and *T. aureum* ATCC 34304. EGFP-expressing transformants, which are easily distinguished from wild-type and control mock transformants by fluorescence microscopy, were obtained in the experiments using *A. limacinum* and *T. aureum* as host cells. However, the author detected no EGFP-positive transformants when *Thraustochytrium* sp. ATCC 26185 was

used as the host, even when transformed with the Neo^r construct. The EGFP and Neo^r genes were confirmed to be integrated into the genomic DNA in *A. limacinum* and *T. aureum*.

The transformation efficiencies of *A. limacinum* and *T. aureum* with the EGFP construct were lower than that with the Neo^r construct (the control). Because the Neo^r/EGFP construct is longer than the Neo^r construct, these results suggest that the size of the expression cassette affected the transformation efficiency. Further studies will be required to improve the transformation efficiency. In conclusion, the author developed a transformation system for thraustochytrids by which exogenous genes can be functionally expressed in thraustochytrids. This result indicates that the genetic engineering of thraustochytrids can be performed using this method.

1-5. SUMMARY

Thraustochytrids are unicellular eukaryotic organisms with the potential to become an alternative source of useful PUFAs. Although gene manipulations would allow the accumulation of more abundant or specific PUFAs in thraustochytrids, a transformation system has not yet been established for thraustochytrids. In this work, the author reported the development of a transformation system for thraustochytrids. Neo^r and Neo^r/EGFP constructs, driven by either an EF-1α or a ubiquitin promoter/terminator system, were introduced into *Thraustochytrium* sp. ATCC 26185. The Neo^r gene was integrated into the host genomic DNA at random and then transcribed into Neo^r mRNA. However, the EGFP gene was not expressed in *Thraustochytrium* sp. ATCC 26185. In contrast, the EGFP gene was expressed in *T. aureum* ATCC 34304 and *A. limacinum* mh0186 when the Neo^r/EGFP expression cassette was introduced into these thraustochytrids. These results indicated that this transformation system is suitable for the expression of functional genes in certain thraustochytrids. This study opens the door to the generation of engineered thraustochytrids with a capacity for the selective production of beneficial PUFAs. Furthermore, the visual screening system using EGFP fluorescence may be useful for developing an optimized transformation system for various thraustochytrids.

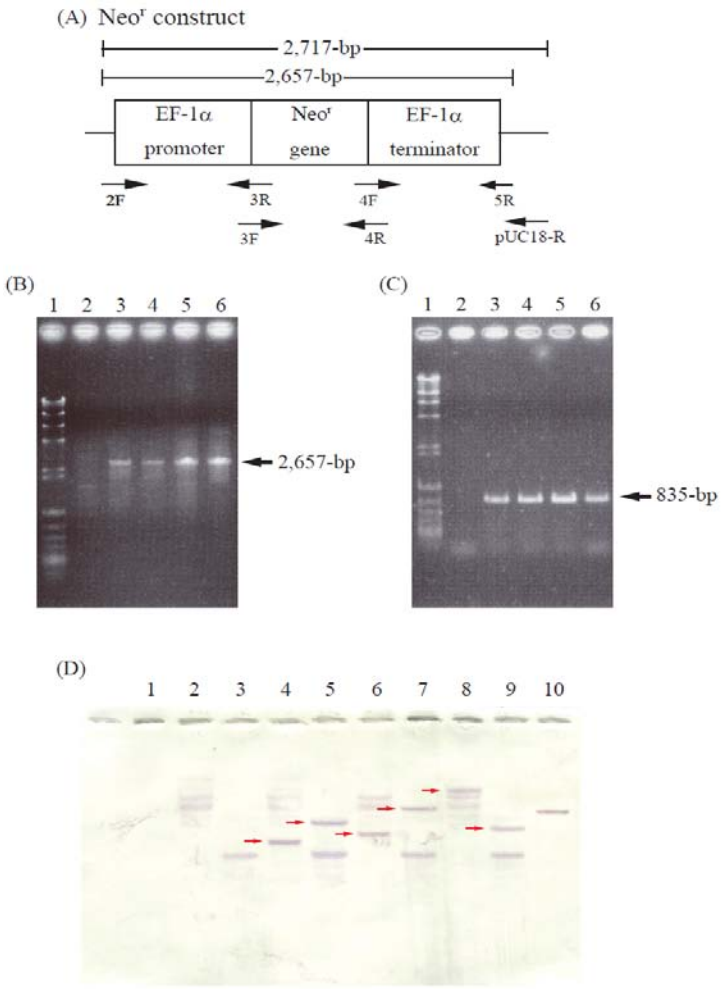

Fig. 1-1. Molecular characterization of transformants.

(A), thraustochytrid-specific exprerssion construct containing Neo^r gene (Neo^r construct, control vector) with sites for primers used. Neo^r gene was drived with thraustochytorid-derived EF-1α promoter/terminator. (B), Genomic PCR showing Neo^r construct. 1, λ*Hin*d III digest/ϕX174 *Hin*c II digest; 2, wild type (2F/5R); 3-5, Neo^r transformants (2F/5R); 6, pNeo^r (2F/5R). (C), RT-PCR analysis of transformants. 1, λ*Hin*d III digest/ϕX174 *Hin*c II digest; 2, wild type cDNA (3F/4R); 3-5, Neo^r transformants cDNA (3F/4R); 6, pNeo^r (3F/4R). (D), Southern blot hybridization using Neo^r gene-specific probe. 1, λ*Hin*d III digest/ϕX174 *Hin*c II digest; 2, wild type (*Hin*d III); 3, wild type (*Pst* I); 4, 6, 8, Neo^r transformants (*Hin*d III); 5, 7, 9, Neo^r transformants (*Pst* I); 10, positive control (pNeo^r, *Hin*d III). The details are shown in MATERIALS AND METHODS.

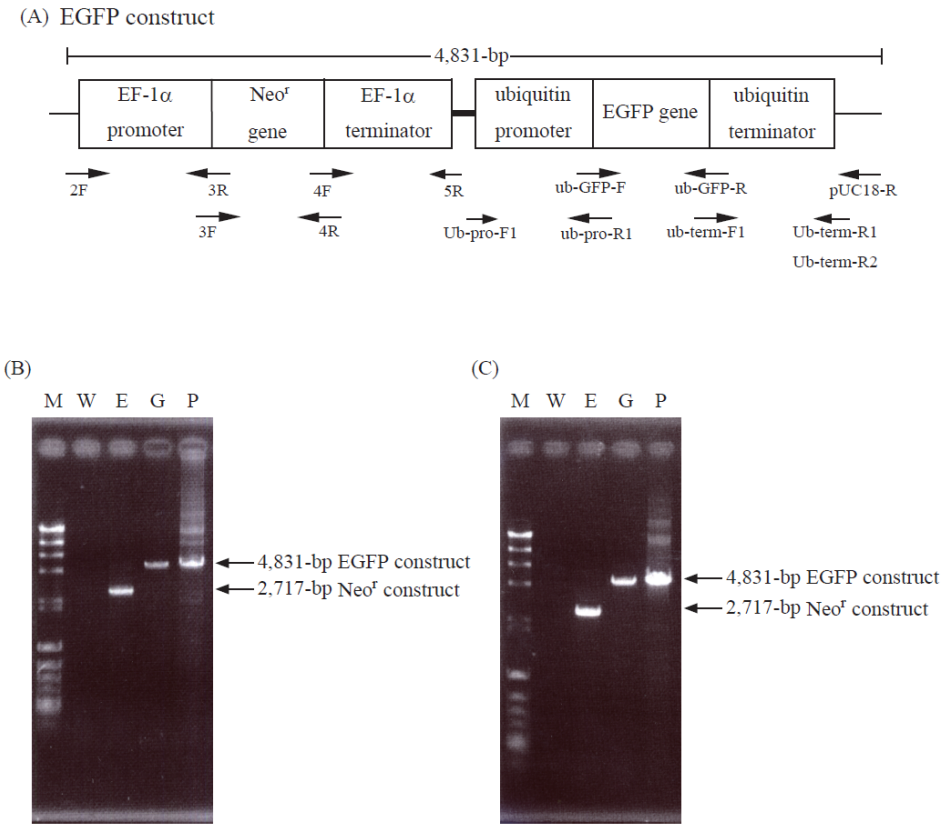

Fig. 1-2. Genomic PCR of transformants harboring EGFP gene.

(A), thraustochytrid-specific exprerssion construct containing Neo^r and EGFP genes (EGFP construct) with sites for primers used (arrows). Neo^r and EGFP genes were drived with thraustochytorid-derived EF-1α or ubiquitin promoter/terminator, respectively. (B), Genomic PCR of *A. limacinum* transformants. (C), Genomic PCR of *T. aureum* transformants. M, λ*Hin*d III digest/ϕX174 *Hin*c II digest; W, wild type of *A. limacinum* or *T. aureum*; E, Neo^r construct transformants; G, EGFP construct transformants; P, Positive control (EGFP construct). The details are shown in MATERIALS AND METHODS.

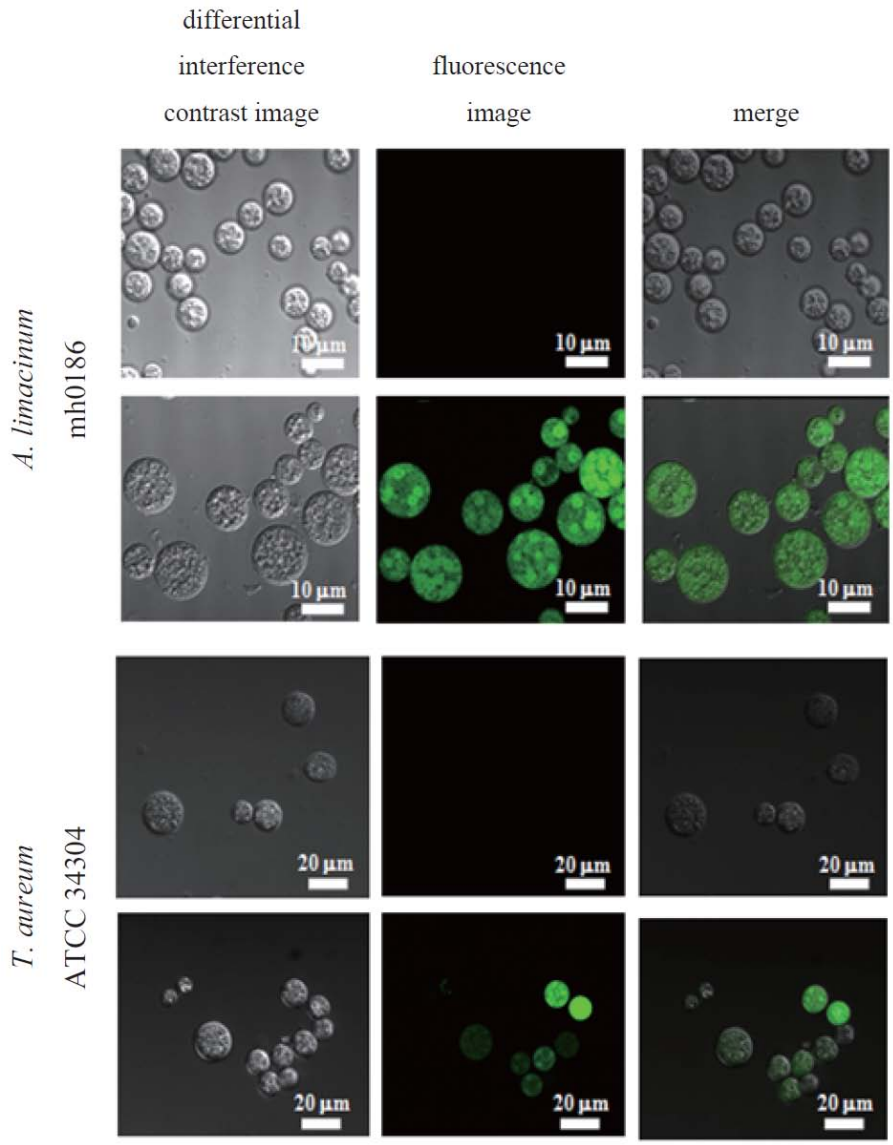

Fig. 1-3. Detection of EGFP-derived fluorescence in transformants.

Images of *A. limacinum* mh0186 and *T. aureum* ATCC 34304 transformed with the Neo^r construct (control, *upper*) or EGFP construct (*lower*). The details are shown in MATERIALS AND METHODS.

Table 1-1. PCR primers used in this chapter.

Name	Sequence	Direction
2F	5'- GGTTTCCGTAGTGAACCTGCAATTCAAAAAAAGCCGTTACTCACAT -3'	Forward
3R	5'- AAGGCCGTCCTGTTCAATCATCTAGCCTTCCTTTGCCGCTGCTTGCT -3'	Reverse
3F	5'- CAGCGGCAAAGGAAGGCTAGATGATTGAACAGGACGGCCTTCACGC -3'	Forward
4R	5'- GCGCATAGCCGGCGCGGATCTCAAAAGAACTCGTCCAGGAGGCGGT -3'	Reverse
4F	5'- TCCTGGACGAGTTCTTTTGAGATCCGCGCCGGCTATGCGCCCGTGC -3'	Forward
5R	5'- CACTGCAGCGAAAGACGGGCCGTAAGGACG -3'	Reverse
Ub-pro-F1	5'- TCGGTACCCGTTAGAACGCGTAATACGAC -3'	Forward
ub-pro-R1	5'- TCCTCGCCCTTGCTCACCATGTTGGCTAGTGTTGCTTAGGT -3'	Reverse
ub-GFP-F	5'- ACCTAAGCAACACTAGCCAACATGGTGAGCAAGGGCGAGGA -3'	Forward
ub-GFP-R	5'- AGCACATACTACAGATAGCTTAGTTTTACTTGTACAGCTCGTCCA -3'	Reverse
ub-term-F1	5'- TGGACGAGCTGTACAAGTAAAACTAAGCTATCTGTAGTATGTGCT -3'	Forward
Ub-term-R1	5'- ATCTAGAACCGCGTAATACGACTCACTATAGGGAGAC -3'	Reverse
Ub-term-R2	5'- TCGGTACCACCGCGTAATACGACTCACTATAGGGAGACTGCAGTT -3'	Reverse
pUC18-R	5'- AACAGCTATGACCATGATTACGAATTCGAGCTCGG -3'	Reverse

5R includes *Pst* I site (underlined).

Ub-pro-F1 and Ub-term-R2 also have *Kpn* I site (underlined).

CHAPTER 2

Molecular cloning of a *Pinguiochrysis pyriformis* oleate-specific microsomal Δ12-fatty acid desaturase and functional analysis in yeasts and thraustochytrids

2-1. INTRODUCTION

A body of accumulating evidence shows the cardiovascular benefits of omega-3 polyunsaturated fatty acids (PUFA) such as eicosapentaenoic acid (EPA, C20:5$^{\Delta 5, 8, 11, 14, 17}$) and docosahexaenoic acid (DHA, C22:6$^{\Delta 4, 7, 10, 13, 16, 19}$) (75). Actually, cardiac societies including the American Heart Association and the European Society for Cardiology recommend the intake of 1 g/day of EPA and DHA for the prevention of cardiovascular disease and sudden cardiac death (76). Additionally, DHA, a major fatty acid of phospholipids in the human brain and retina, is thought integral to the growth and development of the brain (77). The major source of EPA and DHA is fish oils such as sardine oil but recent decreases in fish resources require a substitute (78). This has stimulated plant biotechnology aiming to accumulate beneficial PUFA in seed oils of transgenic plants (79). An alternative approach to the production of omega-3 fatty acids may target thraustochytrids, unicellular eukaryotic marine protists including the genera *Thraustochytrium*, *Ulkenia*, and *Aurantiochytrium* (formerly *Schizochytrium*) (80). Thraustochytrids are known to accumulate PUFA especially DHA and omega-6 docosapentaenoic acid (DPA, C22:5$^{\Delta 4, 7, 10, 13, 16}$), mainly in their lipid droplets. Compared to plants such as arabidopsis and tobacco, however, basic genetic information is still lacking for thraustochytrids.

In the present study, a cDNA encoding a putative fatty acid desaturase (PpDes12) was isolated from the marine microalga *Pinguiochrysis pyriformis* MBIC 10872 belonging to a new class of Pinguiophyceae, which was found to accumulate EPA in cells (28). The PpDes12 was identified to be a microsomal Δ12-fatty acid desaturase which converts oleic acid (OA, C18:1$^{\Delta 9}$) to linoleic acid (LA, C18:2$^{\Delta 9,\ 12}$). The Δ12-fatty acid desaturase is a key enzyme in the standard (desaturase/elongase) pathway for production of omega-3 as well as omega-6 fatty acids (Fig. 2-1A). To express the PpDes12 in thraustochytrids, a construct driven by the ubiquitin promoter from *Thraustochytrium aureum* ATCC 34304 was used. *A. limacinum* mh0186 transformed with the PpDes12 gene, but not with empty construct, converted exogenously added OA to LA, indicating that the gene product functions as a Δ12-fatty acid desaturase in thraustochytrids. This report, the first to describe the heterozygous expression of a fatty acid desaturase in thraustochytrids, could facilitate a genetic approach to the synthesis of fatty acids in thraustochytrids.

2-2. MATERIALS AND METHODS

Materials

TOPO TA Cloning vector was purchased from Invitrogen (California, USA). Lambda cDNA Library Construction Kits was purchased from Stratagene (California, USA). Synthetic oligonucleotides and all other reagents are the same as described in CHAPTER 1.

Strains and culture

P. pyriformis MBIC 10872 was obtained from the Marine Biotechnology Institute, Kamaishi (Japan) and American Type Culture Collection (USA), respectively. *T. aureum* ATCC 34304 and *A. limacinum* mh0186 were obtained and cultured as described in CHAPTER 1.

Molecular cloning of PpDes 12 from *P. pyriformis* MBIC 10872

P. pyriformis was grown at 25℃ in ESM medium (81). Cells in a late logarithmic phase of growth were harvested by centrifugation (6,000 x g, 4℃, 15 min), and total RNA was extracted by the phenol-SDS method (82). Poly(A)$^+$RNA was purified and subjected to the first-strand cDNA synthesis. A pair of degenerate primers targeting the conserved region for fatty acid desaturases, F1 (5'-GGI TGG MGI ATH WSI CAY MGN ACI CAY CA-3'; corresponding to the amino acid sequence GWRISHRTHH) and R1 (5'-CCR TAR TCN CKR TCN AYI GT-3'; corresponding to T(V/I)DRDYG). PCR was then performed using these primers with first-strand cDNA as a template (PCR cycle: 95℃/30 s, 50℃/30 s, 68℃/2 min, 40 cycles). The amplified PCR

products were subcloned into the TOPO TA Cloning vector and sequenced. The sequence of an insert showed high identity to known Δ12-fatty acid desaturases, and thus was used as a probe to screen a cDNA library of *P. pyriformis* MBIC 10872. A cDNA library was constructed using Lambda cDNA Library Construction Kits. Phage was packaged and used to infect *Escherichia coli* XL1-Blue MRF'. Subsequently, a cDNA library was screened by plaque hybridization with a HRP-labeled probe prepared by ECL Direct Nucleic Labeling. After several rounds of screening, positive clones were excised as a pBluescript SK (-) phargemid by *in vivo* excision. Finally, a full-length cDNA clone encoding Δ12-fatty acid desaturase, named PpDes12, was obtained. The plasmid containing PpDes12 cDNA was designated pBCN8.

Expression of PpDes12 in yeasts

A cDNA of PpDes12 ORF was amplified by PCR using a 5' primer containing a *Hin*d III site (P.pyr-F, 5'-TTA AGC TTC AAA ATG TCT CGT GGA GGA AAC CTC TC-3') and a 3' primer containing a *Xba* I site (P.pyr-R, 5'-GTC TAG ATT TAG TCG TGC GCC TTG TAG AAC A-3'), and pBCN8 as a template (94℃/30 s, 61℃/30 s, 72℃/2 min, 30 cycles). The PCR-amplified PpDes12 ORF was digested with *Hin*d III and *Xba* I, and cloned into the same sites of pYES2/CT (Invitrogen). The resulting PpDes12-expression vector, designated pYpΔ12Des, was introduced into the *Saccharomyces cerevisiae* INVSc1 (Invitrogen) by the lithium-acetate method (83). The transformants were selected by plating on synthetic agar plates lacking uracil (SC-ura). *S. cerevisiae* harboring *PpDes12* was cultured in uracil-lacking SC medium containing 2% glucose at 25℃ for 3 days, and then cultured for an additional 1 day in uracil-lacking SC medium containing 2% galactose. Cells were collected by

centrifugation at 3,500 g for 10 min.

Western blotting of FLAG-tagged PpDes12

The Flag tag sequence was inserted just after the initiation codon of PpDes12 gene by PCR. The PCR was conducted using a forward primer containing the FLAG tag sequences (P.pyr-FLAG-F, 5'-CTA AGC TTC AAA ATG *GAT TAC AAG GAT GAC GAT GAC AAG* TCT CGT GGA-3') and reverse primer (P.pyr-R, 5'-GTC TAG ATT TAG TCG TGC GCC TTG TAG AAC A-3'). The underline and italics indicate the *Hin*d III site and FLAG tag sequence, respectively. The PCR fragment was directly subcloned into the yeast expression vector pYES2/CT and subsequencely introduced into *S. cerevisiae* by the method described above. After incubation of the transformant in SC-ura medium, the cells were harvested and suspended in 0.1 M potassium phosphate buffer, pH 7.2, containing 0.33 M sucrose, 0.1% BSA, 1000 units/ml catalase, and a protease inhibitor coctail (Roche Diagnostics K.K.). Glass beads were added and the resultant slurry was sonicated for 20 sec and centrifuged (3,000 x g for 10 min). The supernatant (cell lysate) was centrifuged at 100,000 x g for 60 min. The supernatant was used as a cytosolic fraction and the resultant pellet was suspended in 0.1 M potassium phosphate buffer, pH 7.2, containing glycerol (20% by vol.) and used as a microsomal fraction. Ten micrograms of protein was loaded onto a 10% SDS-PAGE gel and transferred to a PVDF membrane (0.45 μm) using a Bio-Rad Trans-Blot® SD Cell. The membrane was incubated with 5% (w/v) skim milk in TBS buffer containing 0.1% Tween 20 (Tween-TBS) for 1 hour at room temperature, washed with Tween-TBS three times, and incubated at room temperature for 3 hour with an anti-DYKDDDDK tag monoclonal antibody (Wako, Osaka, Japan, 1:5000). It was

then washed with Tween-TBS 3 more times and incubated for 3 hours at room temperature with an HRP-conjugated anti-mouse IgG [H+L] goat antibody (Nacalai Tesque; 1:10000). The membrane was again washed with Tween-TBS 3 times. Protein expression was visualized using a peroxidase staining kit (Nacalai Tesque, Kyoto, Japan; 1:20).

Expression of PpDes12 in thraustochytrids

To express the PpDes12 gene in thraustochytrids, an expression construct (Neo^r/PpDes12 construct, Fig. 2-6A) was prepared. For control, PpDes 12 gene with ubiquitin promoter/terminator was omitted from the expression construct (Neo^r construct, Fig. 2-6B). The EF-1α promoter/terminator and ubiquitin promoter/terminator were obtained from *T. aureum* ATCC 34304. The codons of Neo^r were adjusted according to the codon usage of *T. aureum* ATCC 34304 (84). The primers for PCR amplification of these sequences are shown in supplemental Table 2-2. The expression construct was introduced into *A. limacinum* mh0186 cells by electrophoration as described in CHAPTER 1. The cells were then immediately re-suspended in 1 ml of GY medium and incubated at 25℃ for 1 day, and spread on potato-dextrose agar plates containing G418 at 0.5 mg/ml. After incubation at 25℃ for 2-5 days, colonies that appeared on the plates were regarded as putative transformants. *A. limacinum* mh0186 harboring *PpDes12* gene was cultured in GY medium at 25℃ for 4 days. Cells were collected by centrifugation at 3,500 g for 10 min.

Genomic PCR and southern blot hybridization of thraustochytrid transformants

Genomic PCR was performed using the forward primer 2F and reverse primer pUC18-R (Table 2-2) (96℃/2 min, 98℃/20 sec, 60℃/30 sec, 72℃/5 min, 30 cycles). For Southern blot hybridization, 5 μg of genomic DNA was digested at 37℃ with *Xba* I overnight. The digested DNA was separated on 1% agarose gel and transferred onto a Hybond-N^+. The membrane was hybridized with a probe prepared using the DIG DNA Labeling Kit (Roche Diagnostics K.K.). PCR primers used were PD12d-probe-F (5'-CTG CCC GGC CCG CCG CGA CGA CTA-3') and PD12d-probe-R (5'-CGG CGT GAA GCT ACG GTC GAT GGT-3'). Genomic DNA hybridized with probe was detected with an anti-Digoxigenin-AP Fab fragment and an NBT/BCIP stock solution (Roche Diagnostics K.K.).

RT-PCR of Neo^r and PpDes12 in the thraustochytrid transformants

Total RNA was prepared from transformants, grown in GY medium containing appropriate amounts of G418, with a Sepasol RNA I Super (Nacalai Tesque), RNeasy Mini Kit (QIAGEN) and DNase I (Takara Bio Inc.), and used to produce first-strand cDNA with PrimeScript™ Reverse Transcriptase (Takara Bio Inc.). PCR was performed using the forward primer 3F and reverse primer 4R for amplification of Neo^r cDNA and forward primer ub pro-D12d-F and reverse primer ub term-D12d-R for amplification of PpDes12 cDNA (96℃/2 min, 98℃/20 sec, 60℃/30 sec, 72℃/90 sec, 30 cycles) (Table 2-2).

Fatty acid analysis

The preparation and extraction of fatty acid methyl esters (FAME) were carried out as

described previously (17). The resulting FAMEs were analyzed by gas chromatography (GC) by the method described in (85). The FAMEs were also subjected to gas chromatography-mass spectrometry (GC-MS) using a Shimadzu GC-MS QP-5000 (SHIMADZU Co., Kyoto, Japan) equipped with a capillary column (DB-1, 0.25 mm i.d. x 30 m, film thickness 0.25 μm, Agilent). The column temperature was programmed to increase at 4℃/min from 160℃ to 260℃. The injection-port temperature was 250℃. The rate of conversion of substrates to products was calculated as follows; conversion rate (%) = GC peak area of product / (GC peak area of product + GC peak area of substrate) x 100. Furthermore, picolinyl esters were prepared from the FAME as described previously (86) and subjected to GC-MS using the equipment described above. The column temperature was programmed to increase at 2.5℃/min from 240℃ to 260℃ and maintained for 15 min, then increased at 2.5℃/min to 280℃.

2-3. RESULTS

Molecular cloning of PpDes12 from *P. pyriformis* MBIC 10872

P. pyriformis MBIC 10872 has been reported to accumulate omega-3 PUFA, especially EPA, in cells (28). In this study, the author isolated the cDNA fragment (516-bp) of a putative desaturase (PpDes12) from this organism by degenerate PCR as described in MATERIALS AND METHODS. The DNA fragment was used as a probe to isolate a full-length cDNA clone through plaque hybridization with a *P. pyriformis* MBIC 10872 cDNA library. After the screening of 5.5 x 10^5 recombinants, a cDNA clone including the putative PpDes12 ORF was isolated and designated pBCN8.

Nucleotide and deduced amino acid sequences of PpDes12

The author sequenced 1,494 nucleotides of pBCN8, and found a 1,314-bp ORF of PpDes12 encoding a putative 437 amino acid residues. As shown in Fig. 2-2, the deduced amino acid sequence of PpDes12 exhibited a high degree of identity with fungal and protozoan Δ12-fatty acid desaturases, such as those from *Mortierella alpina* (43.4%) (87), *Mucor circinelloides* (45.3%) (88), *Rhizopus oryzae* (44.6%) (89), *Saprolegnia diclina* (48.0%) (90) and *Trichoderma brucei* (37.2%) (91) (the number in parentheses shows the identity relative to PpDes12). Three histidine boxes, conserved in almost all fatty acid desaturases, were found in the deduced amino acid sequence of PpDes12 (Fig. 2-2, underlined), whereas the cytochrome b_5 motif, characteristic of front-end desaturases, was not.

Phylogenetic analysis

Δ12- and Δ12/Δ15-fatty acid desaturases have been classified into the following groups based on sequence similarity: a fungal & protozoan group, a plant group, a cyanobacterial group, and a chloroplast-localized plant group. The evolutionary relationship between PpDes12 and other Δ12- and Δ12/Δ15-fatty acid desaturases was examined in a phylogenetic analysis. PpDes12 was found to be clustered with the fungal & nematode group in which it was most closely related to the *S. diclina* Δ12-fatty acid desaturase (Fig. 2-3).

Expression of PpDes12 in *S. cerevisiae*

To clarify the function of PpDes12, a PpDes12-expression construct (pYpΔ12Des) and an empty-control construct (pYES2/CT) were separately introduced into the INVSc1 strain of *S. cerevisiae* and the fatty acid composition of pYpΔ12Des and mock transformants was analyzed by GC using fatty acid methyl esters. The peak corresponding to standard LA ($18:2^{\Delta 9,\ 12}$) methyl ester was found in pYpΔ12Des transformants but not in mock transformants, although OA ($18:1^{\Delta 9}$), the precursor of LA, was found in both transformants (Fig. 2-4A, B). On the other hand, amounts of endogenous palmitic acid (C16:0), stearic acid (C18:0) and palmitoleic acid ($C16:1^{\Delta 9}$) were unchanged in pYpΔ12Des and mock transformants. GC-MS of the new peak in pYpΔ12Des transformants revealed its molecular mass (m/z 294) and fragmentation pattern to be identical to those of the standard LA methyl ester (Fig. 2-4C, D). The rate of conversion of OA to LA was calculated to be 14.3 ± 2.71 % under the conditions used (average from duplicate experiments using 3 different transformants). These results indicate that endogenous OA was converted to LA in pYpΔ12Des transformants.

However, no double bonds were introduced into myristoleic acid ($14:1^{\Delta 9}$), palmitoleic acid ($16:1^{\Delta 9}$), elaidic acid ($18:1^{\Delta 9\ trans}$), LA, γ-linolenic acid ($C18:3^{\Delta 6,\ 9,\ 12}$), dihomo-γ-linolenic acid ($C20:3^{\Delta 8,\ 11,\ 14}$), arachidonic acid ($C20:4^{\Delta 5,\ 8,\ 11,\ 14}$) and docosatetraenoic acid ($C22:4^{\Delta 7,\ 10,\ 13,\ 16}$) when they were added to the culture of pYpΔ12Des or mock transformants at 40 μM (data not shown). Taken together, the PpDes12 gene of *P. pyriformis* MBIC 10872 encodes a Δ12-fatty acid desaturase that catalyzes the conversion of OA to LA by introducing a double bond at the Δ12 position of OA.

Western blotting of FLAG-tagged PpDes12 expressed in the yeasts

The author examined the expression of PpDes12 at the protein level. Yeast cells expressing FLAG-tagged PpDes12 were lysed and fractionated into a microsomal fraction and cytosolic fraction, which were subjected to Western blotting using anti DYKDDDDK-tag antibody. A 51.1-kDa protein band was detected in the cell lysate and microsomal fraction but not cytosolic fraction (Fig. 2-5). The molecular weight (51.1-kDa) was well consistent with that estimated from the deduced amino acid sequence of the desaturase with a FLAG tag. This result indicates that PpDes12 can be classified as a microsomal fatty acid desaturase.

Expression of PpDes12 in *A. limacinum*

Thraustochytrids are potentially an alternative to fish for the production of omega-3 PUFAs (80). However, the genetic approach to the synthesis of fatty acids in thraustochytrids has not been fully established due to a lack of molecular tools for gene manipulation. In this study, the author designed a thraustochytrid-specific expression

construct to express the heterozygous gene in thraustochytrids using a promoter and a terminator of house-keeping genes derived from *T. aureum* ATCC 34304. To select the transformants, the author used neomycin (G418) and a neomycin-resistance (Neo^r) gene after adjusting the codons according to the codon usage of *T. aureum* ATCC 34304.

To confirm whether the PpDes12 is able to function in thraustochytrids, a Neo^r/PpDes12-expression construct (Fig. 2-6A) and a Neo^r control construct (Fig. 2-6B) were separately injected into *A. limacinum* mh0186 by electroporation. Transformants grown on a G418-containing GY agar medium were subjected to genomic PCR to examine whether a full-length Neo^r/PpDes12 DNA was integrated into the genome of the mh0186 strain. As shown in Fig. 2-6C, a 5,425-bp PCR product (corresponding to Neo^r/PpDes12 construct, Fig. 2-6A) was detected in the Neo^r/PpDes12 transformants, whereas a 2,717-bp PCR product (corresponding to Neo^r construct, Fig. 2-6B) was amplified for control Neo^r transformants. Southern blot hybridization using a PpDes12 DNA probe confirmed that the PpDes12 gene was integrated into the mh0186 genome (Fig. 2-6D). Furthermore, RT-PCR revealed that transcripts of both Neo^r gene (835-bp) and PpDes12 gene (1,354-bp) were present in Neo^r/PpDes12 transformants while the transcript of Neo^r gene, but not PpDes12, was detected in control Neo^r transformants (Fig. 2-6E and F). These results clearly indicate that the PpDes12 and Neo^r genes were integrated into the genome of *A. limacinum* mh0186 and then translated to the respective mRNA.

Finally, the fatty acid composition of Neo^r/PpDes12 transformants and control Neo^r transformants was analyzed by GC using methyl ester derivatives. The peak corresponding to standard LA methyl ester appeared in Neo^r/PpDes12 transformants (Fig. 2-7B) but not in control Neo^r transformants (Fig. 2-7A) after adding OA to the

culture of both transformants. GC-MS of this new peak revealed its molecular mass (m/z) and fragmentation pattern to be identical to those of the LA picolinyl ester (Fig. 2-7C). The rate of conversion of OA to LA was calculated to be 7.28 ± 1.33 % (average from duplicate experiments using 5 different transformants). No significant change in fatty acid composition except OA and LA was observed in Neo^r/PpDes12 transformants, compared to control Neo^r transformants (data not shown).

Additionally, ^{14}C-LA was detected in Neo^r/PpDes12 transformants but not in control Neo^r transformants when ^{14}C-oleoyl-CoA was added to the culture of transformants (Fig. 2-8).

Collectively, the *Pinguiochrysis* gene encoding PpDes12 was integrated into the genome of *A. limacinum* mh0186 (Fig. 2-6C and D), translated into PpDes12 mRNA (Fig. 2-6F) and functioned as a Δ12-fatty acid desaturase in thraustochytrid cells (Fig. 2-7).

2-4. DISCUSSION

In this study, the author cloned a putative fatty acid desaturase (PpDes12) gene from *P. pyriformis* MBIC 10872 that accumulates omega-3 PUFAs especially EPA (28). The gene was found to encode an enzyme capable of catalyzing the introduction of a double bond at the Δ12 position of OA but not other fatty acids tested. Western blotting of FLAG-tagged PpDes12 expressed in the yeast revealed that the enzyme was recovered in the microsomal fraction. Furthermore, analysis using TMHMM (http://www.cbs.dtu.dk/services/TMHMM/) suggested that the enzyme has two transmembrane domains. These results indicate that PpDes12 is an oleate-specific microsomal Δ12-fatty acid desaturase. The deduced amino acid sequence of PpDes12 contains three histidine boxes (Fig. 2-2, underlined), commonly conserved in fatty acid desaturases. This region may act as di-iron co-ordinating centers for catalytic activity (54). Meanwhile, PpDes12 possesses no cytochrome b_5-like domain which is usually present in front-end desaturases and functions as an electron donor. It has been reported that a *T. brucei* oleate desaturase did not carry a cytochrome b_5-like domain but might use a microsomal cytochrome or the cytochrome b_5-like domain of other desaturases as an electron donor (91). PpDes12 could accept electrons in a similar manner to the *T. brucei* oleate desaturase.

The phylogenetic analysis of Δ12- and bifunctional Δ12/Δ15-fatty acid desaturases by the maximum-likelihood method (92) revealed that PpDes12 is a member of a fungal & nematode Δ12-fatty acid desaturase group. Among the organisms belonging to this group, only *P. pyriformis* is a “photosynthetic” stramenopile. Although PpDes12 was recovered in the microsomal fraction when expressed in the yeast (Fig. 2-5), its

intracellular distribution remains to be clarified. However, PpDes12 could be present in chloroplasts like other Δ12-fatty acid desaturases of higher plants, because the strain MBIC 10872 cells used in this study have one or two typical chloroplasts and accumulate PUFA in the chloroplasts (28, 29). It is worth noting that the activity of Δ12-fatty acid desaturase could not be detected *in vitro* using the cell lysate or microsomal fraction as an enzyme source possibly because of difficulty with the solubilization of the protein. Thus, reconstitution of the enzyme reaction *in vitro* remains to be achieved.

Although thraustochytrids accumulate PUFA mainly in lipid droplets, their pathway for production of PUFA has not been well documented. Accumulating evidence, however, suggests that two distinct pathways of fatty acid synthesis are present in thraustochytrids, *i.e.*, polyketide synthase-like (PUFA synthase) and the desaturase/elongase (standard) pathway. The former pathway has been well documented in marine bacteria (93) and thraustochytrids (30), and the latter, in animals from nematodes to mammals (94, 95). It is worth noting that targeted mutagenesis of a PUFA synthase gene of *Schizochytrium* sp. resulted in auxotrophic mutants that required supplementation with PUFA (26). This result suggests that the regular pathway in *Schizochytrium* sp. was not capable of synthesizing adequate amount of PUFA under the conditions used, probably due to the absence of a Δ12-fatty acid desaturase (26). The author also found in the present study that *A. limacinum* mh0186 does not have OA and LA, the former being the substrate of Δ12-fatty acid desaturase, and the latter, the product of Δ12-fatty acid desaturase. Furthermore, exogenously added OA was not converted to LA in mh0186 cells until a *Pinguiochrysis* Δ12-fatty acid desaturase was expressed in the strain. The author's observations may indicate that *A. limacinum*

(formerly *Schizochytrium* sp.) has no Δ12-fatty acid desaturase activity. It is note worthy that the expression of Δ12-fatty acid desaturase did not alter the PUFA composition of *A. limacinum* mh0186 except for OA and LA, suggesting the standard pathway of fatty acid synthesis is not sufficiently working in mh0186 cells.

On the other hand, several fatty acid desaturases (17) and elongases (18) possibly associated with the regular pathway of fatty acid synthesis have been identified in thraustochytrids. Thus, the relationship between the PUFA synthase pathway and standard pathway, and/or the mutual relationships of each enzyme in the standard pathway should be carefully examined using several different species of thraustochytrids. The thraustochytrid-specific gene expression system developed in this study could help us to understand the mechanics of fatty acid synthesis in thraustochytrids and facilitate the biotechnology of thraustochytrids.

In conclusion, the author isolated a gene encoding an oleate-specific microsomal Δ12-fatty acid desaturase from *P. pyriformis* MBIC 10872 and successfully expressed it in yeasts as well as thraustochytrids.

2-5. SUMMARY

The author isolated a putative desaturase gene from a marine alga, *P. pyriformis* MBIC 10872, which is capable of accumulating eicosapentaenoic acid (C20:5$^{\Delta 5, 8, 11, 14, 17}$). The gene possessed an open reading frame of 1,314-bp encoding a putative 437 amino acid residues showing high sequence identity (37-48%) with fungal and nematode Δ12-fatty acid desaturases. Yeast cells transformed with the gene converted endogenous OA (C18:1$^{\Delta 9}$) to LA (C18:2$^{\Delta 9, 12}$). However, no double bonds were introduced into other endogenous fatty acids or exogenously added fatty acids. FLAG-tagged enzyme was recovered in the micosome fraction when expressed in yeast cells. To express the gene in thraustochytrids, a construct driven by the thraustochytrid-derived ubiquitin promoter was used. Interestingly, exogenously added OA was converted to LA in the gene transformants but not mock transformants of *A. limacinum* mh0186. These results clearly indicate that the gene, encoding a microsomal Δ12-fatty acid desaturase, was expressed functionally in not only yeasts but also thraustochytrids. This is the first report describing the heterozygous expression of a fatty acid desaturase in thraustochytrids, and could facilitate a genetic approach toward fatty acid synthesis in thraustochytrids which are expected to be an alternative source of PUFAs.

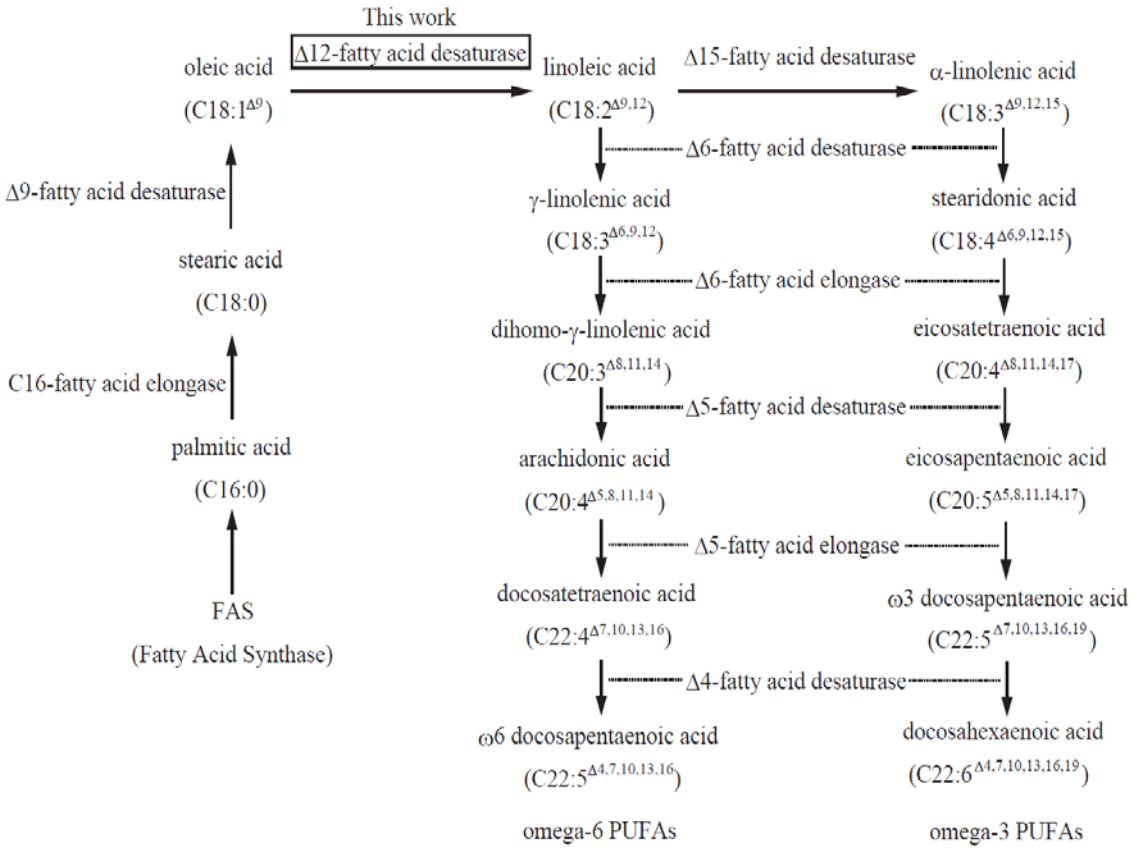

Fig. 2-1. Putative PUFA synthetic pathway involving PpDes12.

PpDes12 would convert OA to LA in *P. pyriformis.*

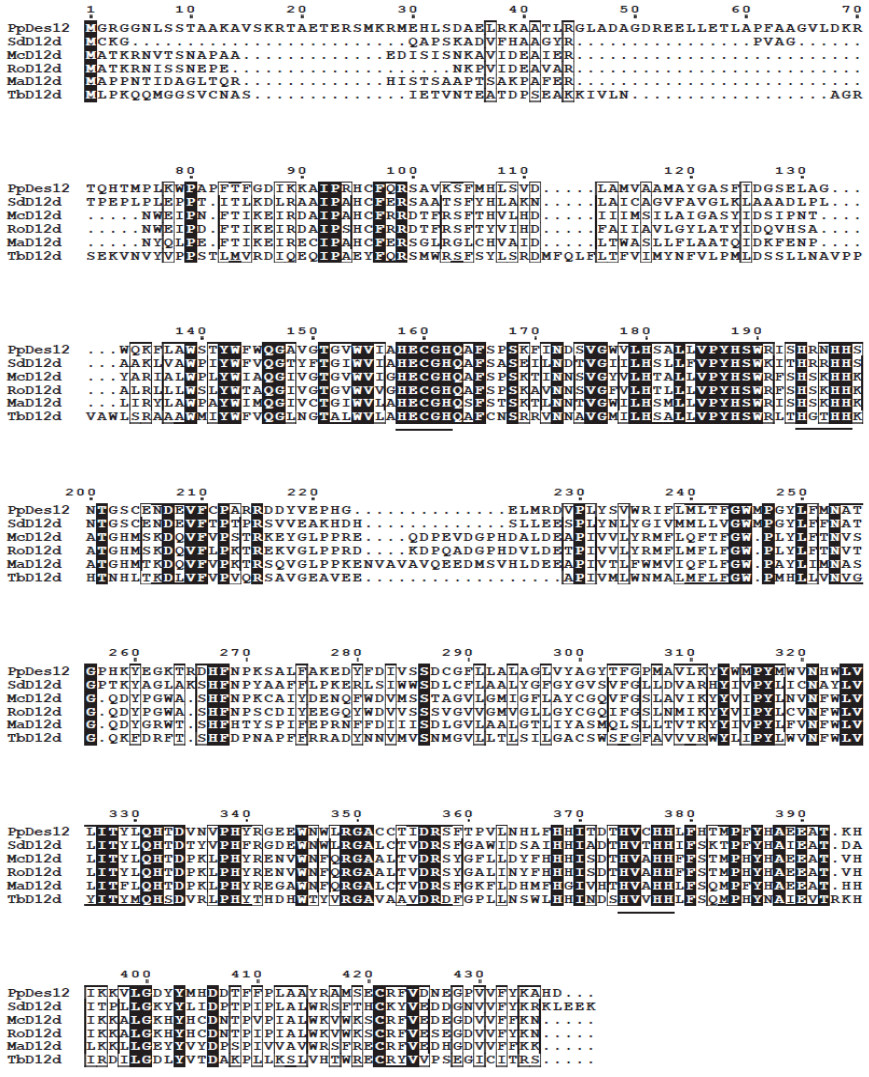

Fig. 2-2. Alignment of the deduced amino acid sequence of PpDes12 with sequences of fungal and protozoan Δ12-fatty acid desaturases.

PpDes12 and fungal and protozoan Δ12-fatty acid desaturases were aligned using ClustalW 1.81 (96) and the alignment was shaded in ESPript 2.2 (http://espript.ibcp.fr/ESPript/cgi-bin /ESPript.cgi). Identical and similar amino acid residues are shown by white letters on a black background and bold face with a black box, respectively. The histidine boxes commonly conserved in fatty acid desaturases are underlined. MaD12d, *M. alpina* Δ12-fatty acid desaturase (87); McD12d, *M. circinelloides* Δ12-fatty acid desaturase (88); PpD12d, *P. pyriformis* Δ12-fatty acid desaturase (this study); RoD12d, *R. oryzae* Δ12-fatty acid desaturase (89); SdD12d, *S. diclina* Δ12-fatty acid desaturase (90); TbD12d, *T. brucei* Δ12-fatty acid desaturase (91).

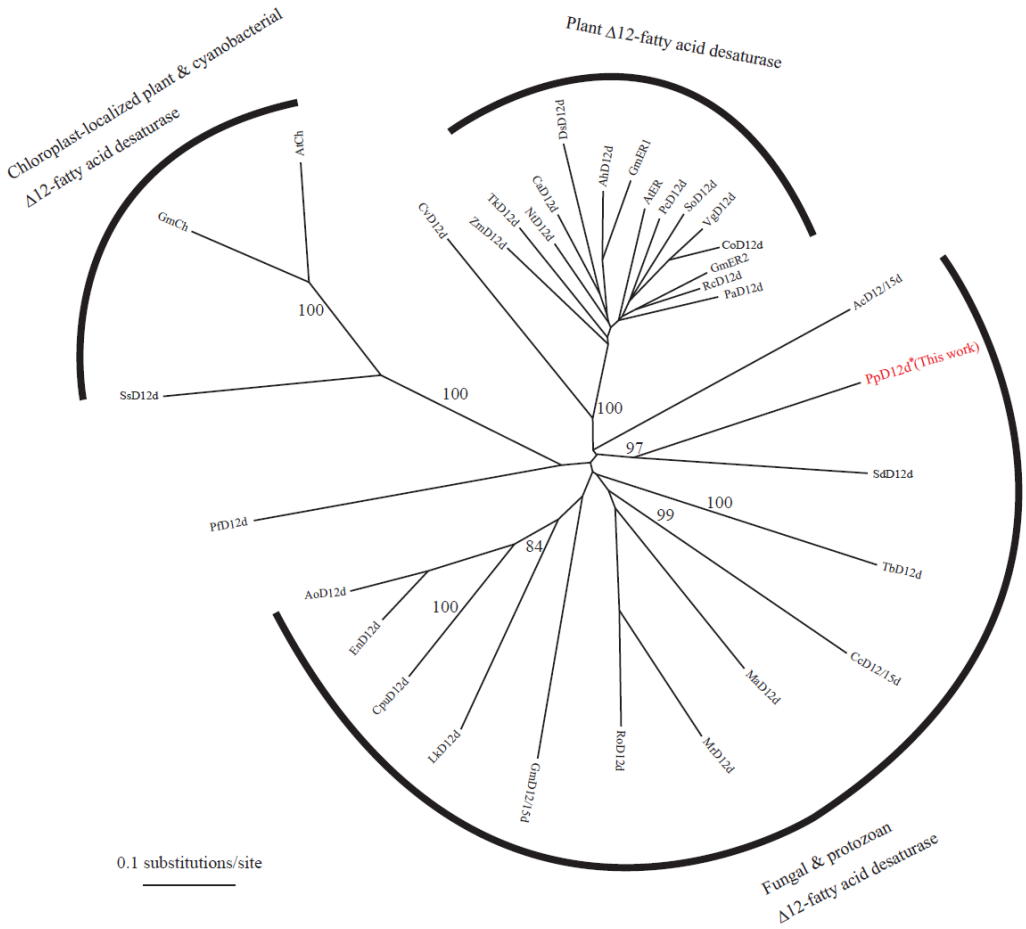

Fig. 2-3. The phylogenetic analysis of Δ12- and bifunctional Δ12/Δ15-fatty acid desaturases.

Phylogenetic tree was constructed by maximum-likelihood method (92) using MOLPHY version 2.3 computer program package. The scale bar represents a distance of 0.1 substitutions per site in the protein sequence. The abbreviations and origins of desaturases used are summarized in Table 2-1.

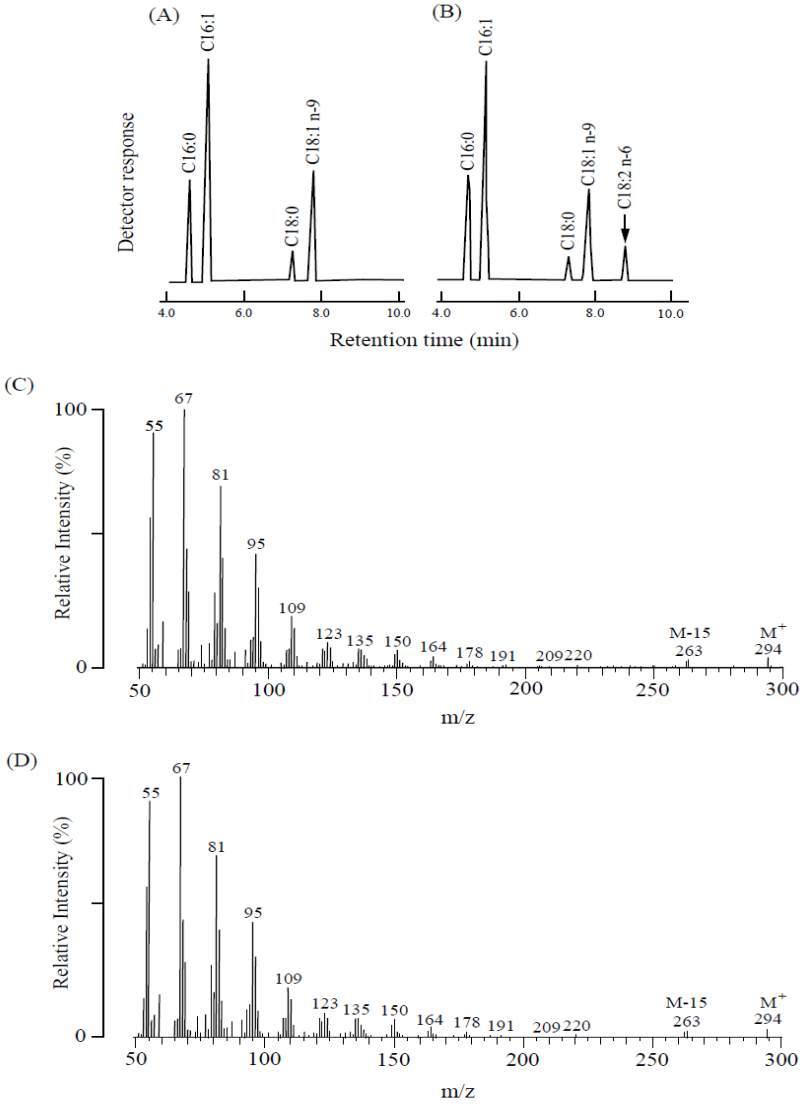

Fig. 2-4. GC and GC-MS of FAME from *S. cerevisiae* transformants.

Gas chromatograms showing the FAME from *S. cerevisiae* transformed with (A) empty vector, pYES2/CT (mock transformants) and (B) PpDes12-containing vector, pYpΔ12Des (PpDes12 transformants). The arrow indicates the new peak in PpDes12 transformants (B). (C), Mass spectrum of the standard LA methyl ester. (D), Mass spectrum of FAME generated in PpDes12 transformants. The cells were cultured in uracil-lacking SC medium containing 2% glucose at 25℃ for 3 days, and then cultured for an additional 1 day in uracil-lacking SC medium containing 2% galactose with or without exogenous fatty acids. When fatty acids were added to the culture, 0.1% tergitol was also added. Fatty acids were extracted from freeze-dried cells and subjected to GC and GC-MS as described in MATERIALS AND METHODS.

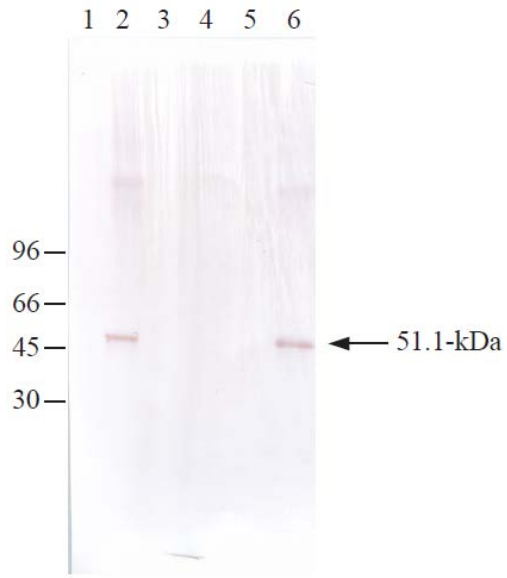

Fig. 2-5. Western blot analysis of FLAG-tagged PpDes12 expressed in the yeast.
1, cell lysate from mock transformant; 2, cell lysate from transformant expressing the FLAG-tagged PpDes12; 3, cytsol fraction from mock transformant; 4, cytsol fraction from transformant expressing the FLAG-tagged PpDes12; 5, microsome fraction from mock transformant; 6, microsome fraction from transformant expressing the FLAG-tagged PpDes12. *S. cerevisiae* cells harboring a vector containing the FLAG-tagged PpDes12 gene or an empty vector (mock control) were cultured in SC-ura medium and the cell lysates were subjected to the procedure for preparation of micosomes. Western blotting was carried out using 10% SDS-PAGE and anti-DYKDDDDK tag mouse monoclonal antibody and HRP-conjugated anti mouse IgG goat antibody. Details are described in MATERIALS AND METHODS.

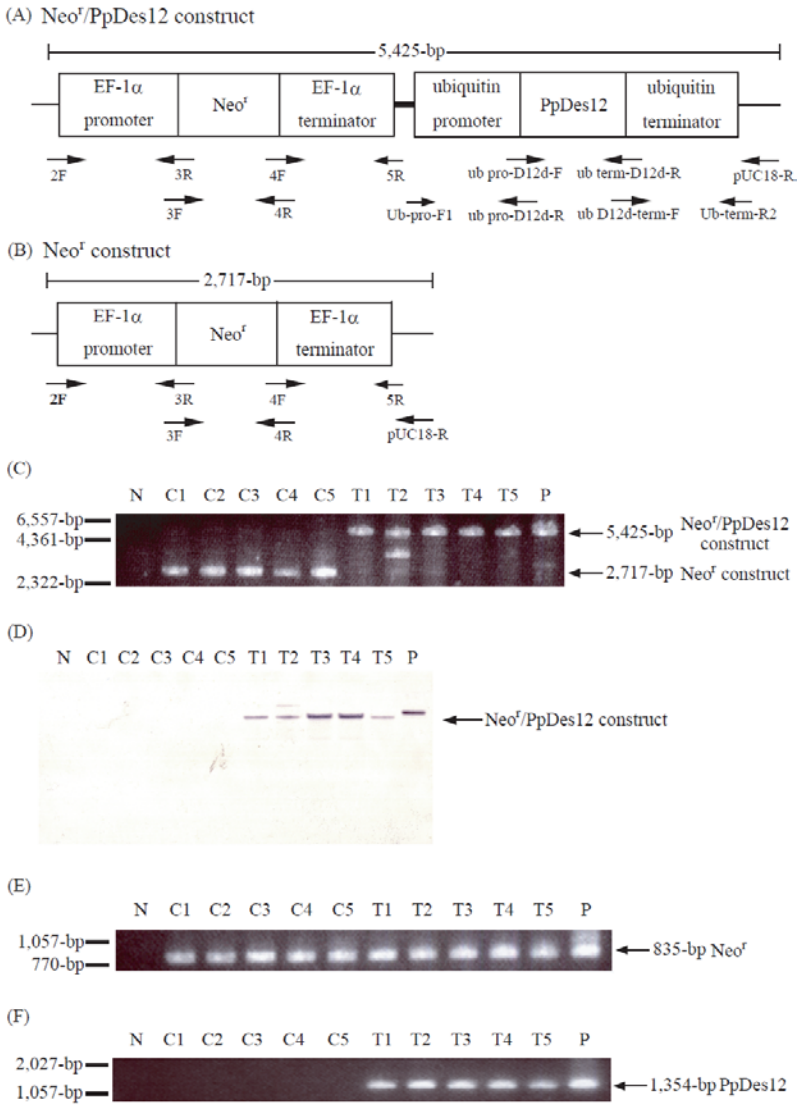

Fig. 2-6. Molecular characterization of *A. limacinum* mh0186 transformants.
(A), thraustochytrid-specific exprerssion construct containing Neo^r and PpDes12 genes (Neo^r/PpDes12 construct) with sites for primers used. (B), thraustochytrid-specific exprerssion construct containing Neo^r gene (Neo^r construct, control vector) with sites for primers used. Neo^r and PpDes12 genes were drived with thraustochytorid-derived EF-1α promoter/terminator and ubiquitin promoter/terminator, respectively. (C), Genomic PCR showing Neo^r construct and Neo^r/PpDes12 construct. (D), Southern blot hybridization using PpDes12-specific probe. RT-PCR amplifying Neo^r mRNA (E) and PpDes12 mRNA (F). N, negative control (wild-type mh0186); C1-C5, Neo^r transformants (mock transformants); T1-T5, Neo^r/PpDes12 transformants; P, positive control (pNeoDes12). The details are shown in MATERIALS AND METHODS.

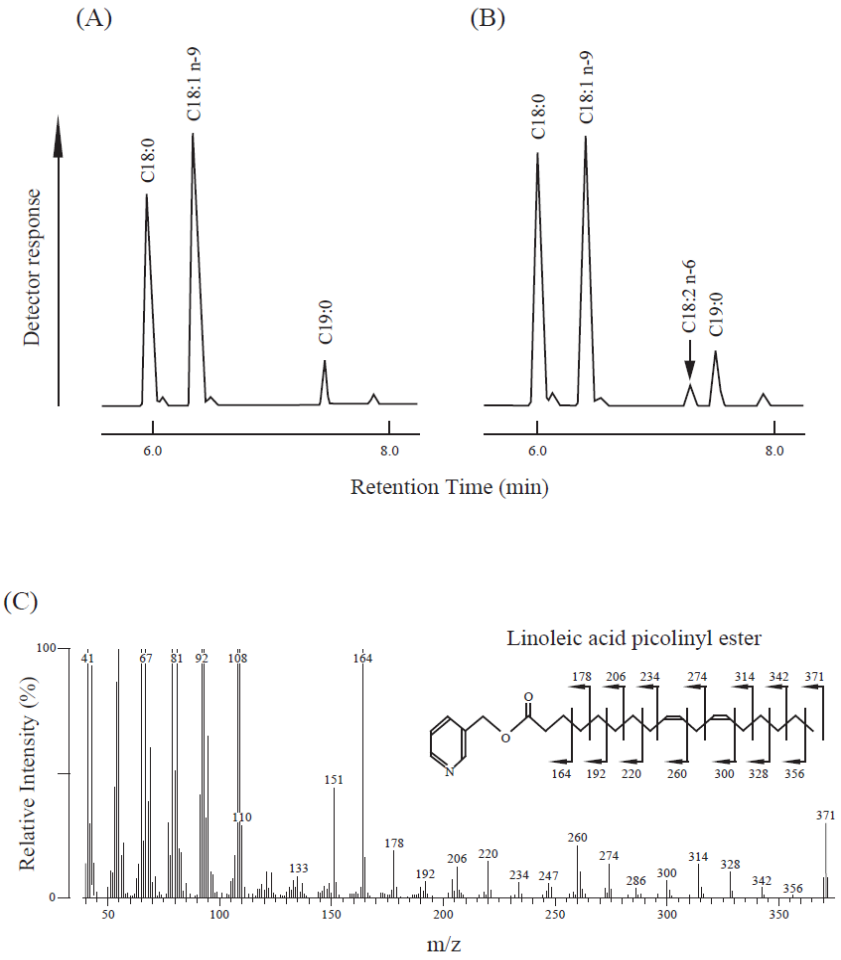

Fig. 2-7. GC and GC-MS analysis of fatty acid derivatives from *A. limacinum* transformants.

Gas chromatograms showing the FAME from *A. limacinum* mh0186 transformed with (A) control Neo^r construct (mock transformants) and (B) Neo^r /PpDes12 construct (PpDes12 transformants). The arrow indicates the new peak in PpDes12 transformants. (C), Mass spectrum of the picolinyl ester derivatives of the fatty acids generated in mh0186 cells transformed with a Neo^r/PpDes12 construct. Cells were cultured in a GY medium containing G418 at a concentration of 0.5 mg/ml at 25℃ for 3 days, and then cultured for an additional 1 day with 100 μM OA. Fatty acids were extracted from freeze-dried cells and subjected to GC and GC-MS as described in MATERIALS AND METHODS.

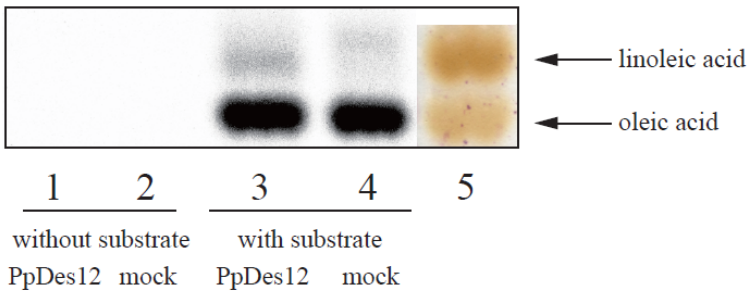

Fig. 2-8. *In vivo* conversion of ^{14}C-OA to ^{14}C-LA in *A. limacinum* mh0186 harboring PpDes12 gene.

A. limacinum mh0186 was cultured at 25˚C for 1 day in GY medium containing 5 nmol of ^{14}C-oleoyl CoA (0.29 μCi). The fatty acids were extracted as FAMEs and then applied to a reverse phase TLC plate which was developed with methanol/acetonitrile/water (90.5/14/7, v/v/v). ^{14}C-fatty acids were detected by FLA5000.

Table 2-1. Abbreviations of desaturase genes described in this chapter.

Abbreviations	Origins and desaturase names
MrD12d	*M. rouxii* Δ12-fatty acid desaturase
RoD12d	*R. oryzae* Δ12-fatty acid desaturase
MaD12d	*M. alpina* Δ12-fatty acid desaturase
CcD12/15d	*C. cinerea* Δ12/Δ15-fatty acid desaturase
EnD12d	*E. nidulans* Δ12-fatty acid desaturase
AoD12d	*A. oryzae* Δ12-fatty acid desaturase
CpuD12d	*C. purpurea* Δ12-fatty acid desaturase
LkD12d	*L. kluyveri* Δ12-fatty acid desaturase
GmD12/15d	*G. moniliformis* Δ12/Δ15-fatty acid desaturase
TbD12d	*T. brucei* Δ12-fatty acid desaturase
SdD12d	*S. diclina* Δ12-fatty acid desaturase
CoD12d	*C. officinalis* Δ12-fatty acid desaturase
VgD12d	*V. galamensis* Δ12-fatty acid desaturase
SoD12d	*S. oleracea* Δ12-fatty acid desaturase
PcD12d	*P. crispum* Δ12-fatty acid desaturase
RcD12d	*R. communis* Δ12-fatty acid desaturase
GmER2	*G. max* ER isozyme2 Δ12-fatty acid desaturase
AtER	*A. thaliana* ER Δ12-fatty acid desaturase
PfD12d	*P. fendleri* Δ12-fatty acid desaturase
PaD12d	*P. americana* Δ12-fatty acid desaturase
NtD12d	*N. tabacum* Δ12-fatty acid desaturase
CaD12d	*C. alpina* Δ12-fatty acid desaturase
DsD12d	*D. sinuata* Δ12-fatty acid desaturase
AhD12d	*A. hypogaea* Δ12-fatty acid desaturase
GmER1	*G. max* ER isozyme1 Δ12-fatty acid desaturase
TkD12d	*T. kirilowii* Δ12-fatty acid desaturase
ZmD12d	*Z. mays* Δ12-fatty acid desaturase
CvD12d	*C. vulgaris* Δ12-fatty acid desaturase
AcD12/15d	*A. castellanii* Δ12/Δ15-fatty acid desaturase
GmCh	*G. max* chloroplast precursor Δ12-fatty acid desaturase
AtCh	*A. thaliana* chloroplast Δ12-fatty acid desaturase
SsD12d	*Synechocystis* sp. Δ12-fatty acid desaturase

Table 2-2. PCR primers used in this chapter.

Name	Sequence	Direction
2F	5'- GGTTTCCGTAGTGAACCTGCAATTCAAAAAAAGCCGTTACTCACAT -3'	Forward
3R	5'- AAGGCCGTCCTGTTCAATCATCTAGCCTTCCTTTGCCGCTGCTTGCT -3'	Reverse
3F	5'- CAGCGGCAAAGGAAGGCTAGATGATTGAACAGGACGGCCTTCACGC -3'	Forward
4R	5'- GCGCATAGCCGGCGCGGATCTCAAAAGAACTCGTCCAGGAGGCGGT -3'	Reverse
4F	5'- TCCTGGACGAGTTCTTTTGAGATCCGCGCCGGCTATGCGCCCGTGC -3'	Forward
5R	5'- CACTGCAGCGAAAGACGGGCCGTAAGGACG -3'	Reverse
Ub-pro-F1	5'- TCGGTACCCGTTAGAACGCGTAATACGAC -3'	Forward
ub pro-D12d-R	5'- AGGTTTCCTCCACGACCCATGTTGGCTAGTGTTGCTTAGGTCGCT -3'	Reverse
ub pro-D12d-F	5'- CCTAAGCAACACTAGCCAACATGGGTCGTGGAGGAAACCTCTCCA -3'	Forward
ub term-D12d-R	5'- ATACTACAGATAGCTTAGTTTTAGTCGTGCGCCTTGTAGAACACA -3'	Reverse
ub D12d-term-F	5'- TCTACAAGGCGCACGACTAAAACTAAGCTATCTGTAGTATGTGCT -3'	Forward
Ub-term-R2	5'- TCGGTACCACCGCGTAATACGACTCACTATAGGGAGACTGCAGTT -3'	Reverse
pUC18-R	5'- AACAGCTATGACCATGATTACGAATTCGAGCTCGG -3'	Reverse
D12d-F2	5'- CGCGGTGGG***C***ACCGGTGTCTGGGTCATCGC -3'	Forward
D12d-R2	5'- ACACCGGT***G***CCCACCGCGCCCTGCCAGAA -3'	Reverse

5R includes *Pst* I site (underlined).

Ub-pro-F1 and ub-term-R2 also have *Kpn* I site (underlined).

The bold and italic letters in D12d-F2 and D12d-R2 sequences indicate the altered nucleotides.

CHAPTER 3

The analysis of Δ12-fatty acid desaturase function revealed that two distinct pathways are active for the synthesis of polyunsaturated fatty acids in *Thraustochytrium aureum* ATCC 34304

3-1. INTRODUCTION

n-3 PUFAs, such as EPA and DHA and their metabolites, have attracted increasing attention for the development of medicines and nutritional supplements based on their serological, cardiovascular and anti-inflammatory benefits (41-43). For example, EPA is used as a medicine for hyperlipidemia and arteriosclerotic diseases. Furthermore, DHA plays important roles in the development of the retina and the brain in infants and possibly in the maintenance of normal brain function in adults (45, 46). Fish oils such as sardine and tuna oils are the major commercial sources of EPA and DHA. However, there is a concern that fish oils will be insufficient to meet the increasing global demand for these PUFAs in the future. Thus, several microorganisms and plants have been explored as alternative sources of PUFAs (68).

Thraustochytrids are eukaryotic marine protists including the typical genera *Thraustochytrium* and *Aurantiochytrium* (formerly *Schizochytrium*), which belong to the Stramenopiles, class Labyrinthulomycetes, family Thraustochytriaceae. These organisms are commonly found in marine and estuarine environments and play important roles in the degradation and mineralization of organic materials in marine ecosystems. Thraustochytrids have recently received increasing attention for their

ability to produce and accumulate high amounts of n-3 PUFAs in cellular lipid droplets; thus, they are under consideration as an alternative industrial source of n-3 PUFAs.

Two distinct pathways for the production of PUFAs have been proposed in thraustochytrids; the polyketide synthase-like (PUFA synthase) pathway, which occurs in several marine bacteria (32), and the desaturase/elongase (standard) pathway, which occurs widely in eukaryotes (68, 97). Gene clusters in the PUFA synthase pathway have been isolated from *Schizochytrium* (now reclassified as *Aurantiochytrium*), in which the disruption of one gene in the synthase pathway resulted in the loss of DHA and n-6 DPA, indicating that these PUFAs are produced solely by the PUFA synthase pathway (24, 26). Several genes encoding fatty acid desaturases and elongases, which may be involved in the standard pathway, have been isolated from thraustochytrids (17, 20, 21). However, the genes encoding the Δ12- and Δ15-fatty acid desaturases, which are key enzymes in the standard pathway, have not yet been identified in thraustochytrids. Thus, it is unclear whether the standard pathway is actually responsible for the production of PUFAs in thraustochytrids.

In this study, the author isolated a putative Δ12-fatty acid desaturase (TauΔ12des) gene from *Thraustochytrium aureum* ATCC 34304. TauΔ12des was identified as a microsomal Δ12-fatty acid desaturase that converts oleic acid (OA, C18:1$^{\Delta 9}$) into linoleic acid (LA, C18:2$^{\Delta 9,\ 12}$) when expressed in the budding yeast *Saccharomyces cerevisiae*. Interestingly, this enzyme also displays a weak ν+3-fatty acid desaturase activity, which converts C19:1$^{\Delta 10}$ into C19:2$^{\Delta 10,\ 13}$ in yeast cells. The *tauΔ12des*-disruption mutants of *T. aureum* ATCC 34304, generated by the homologous recombination of *tauΔ12des* with marker genes, resulted in the accumulation of OA and a significant decrease in the levels of LA and the downstream PUFAs that can be

generated via the standard pathway. In contrast, the amount of DHA in these mutants increased slightly, indicating that DHA is generated through the PUFA synthase pathway. These results clearly indicate, for the first time, that two distinct pathways for the synthesis of PUFAs are active in *T. aureum*. The author also stresses that this report is the first describing the disruption of a fatty acid desaturase gene in thraustochytrids. Thus, this study opens the door for elucidating these entire biosynthetic pathways and the biological functions of PUFAs in thraustochytrids and facilitates the genetic modification of thraustochytrids for the production of beneficial PUFAs.

3-2. MATERIALS AND METHODS

Materials

The antibiotics hygromycin B and blasticidin were purchased from Nacalai Tesque. The synthetic oligonucleotides and all the other reagents were obtained from the same sources as described in CHAPTERS 1 and 2.

Strains and culture

T. aureum ATCC 34304 was cultured as described in CHAPTER 1.

Molecular cloning of TauΔ12des from *T. aureum* ATCC 34304

T. aureum was grown at 25°C in GY medium. Cells in the late logarithmic growth phase were harvested by centrifugation (3,500 × *g*, 4°C, 10 min), and the genomic DNA was extracted.

The primers were designed based on our local genome database. The open reading frame (ORF) of the predicted Δ12-fatty acid desaturase was amplified with the forward primer Tw3-F1 and the reverse primer Tw3-R1. The primer sequences are listed in Table 3-4. PCR was then performed using these primers with *T. aureum* genomic DNA as a template in a master mix that included LA Taq DNA polymerase (Takara Bio Inc.). The amplified PCR products were purified and cloned into the pGEM®-T Easy Vector (Promega, Tokyo, Japan) and sequenced. The full-length genomic DNA clone encoding a Δ12-fatty acid desaturase was named TauΔ12des.

Expression of the *tauΔ12des* in yeast

The ORF of the *tauΔ12des* was amplified by PCR using a 5′ primer containing a *Hin*d III site (Tw3-*Hind*3-F) and a 3′ primer containing an *Xba* I site (Tw3-*Xba*1-R), and genomic DNA as a template (98°C/20 s, 60°C/30 s, 72°C/1.5 min, 30 cycles). The PCR-amplified TauΔ12des ORF was digested with *Hin*d III and *Xba* I and then purified and cloned into the same sites in pYES2/CT (Invitrogen). The resulting TauΔ12des expression vector, designated pYTauΔ12Des, was introduced into *S. cerevisiae* INVSc1 (Invitrogen) using the lithium acetate method (83). The transformants were selected by plating on synthetic agar plates lacking uracil (SC-ura). *S. cerevisiae* transformants harboring the *tauΔ12des* were cultured in SC-ura medium containing 2% glucose at 25°C for 3 days and then cultured for an additional 1 day in SC-ura medium containing 2% galactose. The cells were collected by centrifugation at 3,500 × *g* for 10 min.

Western blotting of FLAG-tagged TauΔ12des

The FLAG tag sequence was inserted immediately after the initiation codon of the *tauΔ12des* by PCR. The PCR was conducted using a forward primer containing the FLAG tag sequences (TD12d-FLAG-F, 5′- GG AAG CTT ATG *GAT TAC AAG GAT GAC GAT GAC AAG TGC AAG* GTC GAT G-3′) and the reverse primer Tw3-*Xba*1-R; the underlining and italics here indicate the *Hin*d III site and the FLAG tag sequence, respectively. The PCR fragment was cloned directly into the yeast expression vector pYES2/CT and subsequently introduced into *S. cerevisiae* by the method described above. After the incubation of the transformants in SC-ura medium, the proteins were extracted, and a western blotting assay was performed as described in CHAPTER 2. Briefly, 10 μg of protein was loaded onto a 10% SDS-PAGE gel and transferred to a

PVDF membrane (0.45 μm) using a Bio-Rad Trans-Blot® SD Cell. The membrane was incubated with 5% (w/v) skim milk in TBS buffer containing 0.1% Tween 20 (Tween-TBS) for 1 hour at room temperature with constant agitation. After three washes with Tween-TBS, the membrane was incubated at room temperature for 3 hours with an anti-DYKDDDDK tag monoclonal antibody (Wako; 1:5,000). The membrane was then washed with Tween-TBS three more times and incubated for 3 hours at room temperature with an HRP-conjugated anti-mouse IgG [H+L] goat antibody (Nacalai Tesque; 1:10,000). The membrane was again washed thrice with Tween-TBS. Protein expression was visualized using a peroxidase staining kit (Nacalai Tesque; 1:20).

Targeted disruption of the *tauΔ12des* in *T. aureum*

The *tauΔ12des*-disruption mutants were generated by homologous recombination. Because *T. aureum* is apparently diploid, two different markers were employed for the disruption of the gene in the two different alleles. The disruption constructs consisted of either the Hyg^r or Bla^r expression cassette sandwiched between the 1,001-bp 5′- and 3′-flanking sequences of the *tauΔ12des* (Fig. 3-6). First, the 5′- and 3′-flanking sequences were amplified using the TD12d-up-F and TD12d-up-R primers and the TD12d-down-F and TD12d-down-R primers, respectively. Next, these amplified fragments were connected by fusion PCR and cloned into the pGEM®-T easy vector. The Hyg^r and Bla^r expression cassettes were cloned into the *Bgl* II site of the vector. The ubiquitin promoter and SV40 terminator were cloned from *T. aureum* ATCC 34304 and the pcDNA 3.1 Myc-His vector (Invitrogen), respectively. The hyg^r and bla^r were obtained from pcDNA 3.1/Hygro (Invitrogen) and pTracer-CV/Bsd/lacZ (Invitrogen),

respectively. The primers used for the PCR amplification of these sequences are listed in Table 3-1. Homologous recombination was performed using the modified split marker system (98). The disruption construct was separated into 5′- and 3′-fragments by PCR and introduced into *T. aureum* cells by microprojectile bombardment as described in CHAPTER 1. A PDS-1000/He Particle Delivery System (Bio-Rad) was used for the transformation. Gold particles (0.6 μm in diameter) were coated with the disruption construct. The 1st allele of TauΔ12des was replaced with the disruption construct containing the Hyg^r expression cassette (1st-allele knock-out construct), and the 2nd allele was replaced with the construct containing the Bla^r expression cassette (2nd-allele knock-out construct). The transformants were selected by their ability to grow on PDA plates containing hygromycin B or hygromycin B plus blasticidin. The concentrations of hygromycin B and blasticidin in the PDA plates were 2 mg/ml and 0.2 mg/ml, respectively.

Complementation of the *tauΔ12des*-disruption mutants with the *tauΔ12des*

To express the *tauΔ12des* in the *tauΔ12des*-disruption mutants, the Neo^r/TauΔ12des construct (Fig. 3-12A) was prepared. For the control experiment, the *tauΔ12des* with the ubiquitin promoter/terminator was omitted from the expression construct (Neo^r construct, Fig. 3-12B). The ubiquitin terminator was obtained from *T. aureum* ATCC 34304. The codons of Neo^r were adjusted to match the codon usage of *T. aureum* ATCC 34304. The primers used for the PCR amplification are listed in Table 3-4 and Table 2-2. The expression construct was introduced into *T. aureum* cells by the method described above. The cells were incubated on a PDA plate at 25°C for 3 hours, after which the colonies were collected and spread on a PDA plate containing G418 at 2

mg/ml. After incubation at 25°C for 7 days, any colonies that appeared on the plates were regarded as putative transformants. The *T. aureum* transformants were cultured in GY medium containing G418 at 2 mg/ml at 25°C for 5 days. The cells were collected by centrifugation at 3,500 × *g* for 10 min.

Genomic PCR and southern blot hybridization

Genomic PCR was performed using the Hyg-F and Hyg-R primers for the amplification of the *hyg*^{r}, the Bla-F and Bla-R primers for the *bla*^{r}, the forward primer ub pro-Tw3-F with the reverse primer ub term-Tw3-R for the *tauΔ12des*, and the forward primer 2F with the reverse primer pUC18-R for the Neo^r/TauΔ12des construct. For Southern blot hybridization, 1.5 μg of genomic DNA was digested with restriction enzymes at 37°C overnight. The digested DNA was separated on a 0.7% agarose gel and transferred onto a Hybond-N$^+$ membrane (GE healthcare). The membrane was hybridized with a probe prepared using the DIG DNA Labeling Kit (Roche Diagnostics K.K.). The probes were amplified with the KO up-probe-F1 and KO up-probe-R1 primers (for the 5′-flanking region), the KO down-probe-F3 and KO down-probe-R3 primers (for the 3′-flanking region), and the TD12d-probe-F1 and TD12d-probe-R1 primers (for the Neo^r/TauΔ12des construct). The genomic DNA hybridized with each probe was detected with the anti-Digoxigenin-AP Fab fragment and an NBT/BCIP stock solution (Roche Diagnostics K.K.).

Detection of Hyg^r, Bla^r, Neo^r and TauΔ12des mRNA by RT-PCR

Total RNA was prepared from transformants grown in GY medium containing appropriate amounts of antibiotics with Sepasol RNA I Super (Nacalai Tesque), an

RNeasy Mini Kit (QIAGEN) and DNaseI (Takara Bio Inc.) and used to produce first-strand cDNA with PrimeScript^{TM} Reverse Transcriptase (Takara Bio Inc.). PCR was performed using the Hyg-F and Hyg-R primers for the amplification of Hyg^{r} cDNA, the Bla-F and Bla-R primers for the Bla^{r} cDNA, the 3F and 4R primers for the Neo^{r} cDNA and the ub pro-Tw3-F and ub term-Tw3-R primers for the TauΔ12des cDNA.

Growth curve and dry cell weight

Precultured cells were inoculated into 250 ml GY medium in a 500-ml flask. After incubating the culture at 25°C with shaking at 150 rpm, the absorbance measurements were performed at a wavelength of 600 nm with an Ultrospec 3000 spectrophotometer. Spectrophotometric readings of the optimal density (OD) were taken every hour. The dry cell weight (DCW) was determined by transferring 10 ml of the culture to a preweighed centrifuge tube and then centrifuging at 3,500 × *g* for 10 min. The cell pellet was then washed twice with 50% ASW and once with distilled water. The washed cell pellets were freeze-dried and weighed.

Fatty acid analysis

Precultured cells were incubated in a 50-ml flask containing 25 ml of GY medium at 25°C for 5 days with shaking at 150 rpm. The harvested cells were washed twice with 50% ASW and once with distilled water. The preparation and extraction of FAMEs were performed as described in CHAPTER 2. The resulting FAMEs were analyzed by GC using the method described in CHAPTER 2. The FAMEs were also subjected to GC-MS using a Shimadzu GC-MS QP-5000 (SHIMADZU Co.) equipped with a capillary column (DB-1, 0.25 mm i.d. × 30 m, film thickness 0.25 μm, Agilent). The

column temperature was programmed to increase from 160°C to 260°C at 4°C/min. The injection-port temperature was 250°C. Using lignoceric acid (C24:0) as an internal standard, the FAME samples were analyzed and quantified based on their peak areas on the chromatogram relative to the peak area of the internal standard. Furthermore, picolinyl esters prepared from the FAMEs as described in CHAPTER 2 were subjected to GC-MS using the equipment described above. The column temperature was programmed to increase from 240°C to 260°C at 2.5°C/min, hold at 260°C for 15 min and then increase to 280°C at 2.5°C/min.

Lipid extraction and the separation of lipid classes

Precultured cells were incubated in a 500-ml flask containing 200 ml of GY medium at 25°C for 5 days with shaking at 150 rpm. The cells were harvested by centrifugation at 3,000 × *g* for 10 min and washed twice with 50% ASW and once with distilled water. The total lipids were extracted using the Folch method (99) after freeze-drying the cells.

The separation of the total lipids into neutral lipid, glycolipid, and phospholipid fractions using a Sep-Pak Plus Silica cartridge (2 ml) and TLC analysis was performed as described previously (85). The FAMEs in each fraction were prepared and analyzed by GC as described above.

3-3. RESULTS

Molecular cloning of a Δ12-fatty acid desaturase from *T. aureum* ATCC 34304

Several fatty acid desaturase genes have been cloned from thraustochytrids (20); however, a Δ12-fatty acid desaturase gene has not yet been cloned from these organisms. In this study, the author isolated a putative Δ12-fatty acid desaturase (TauΔ12des) gene from *T. aureum* ATCC 34304, as described in MATERIALS AND METHODS. The gene, named *tauΔ12des,* contains a 1,185-bp ORF encoding a putative 395 amino acid residues. As illustrated in Fig. 3-1, the deduced amino acid sequence of the *tauΔ12des* exhibits a high degree of identity with Δ12-fatty acid desaturases found in diatoms and picophytoplankton such as those from *Thalassiosira pseudonana* (41%) (XP_002292071), *Micromonas* sp. (44%) (XP_002507091), and *Phaeodactylum tricornutum* (41%) (3503348AJJ) (the number in parentheses indicates the sequence identity relative to TauΔ12des). Three histidine boxes, which are conserved in almost all membrane-bound fatty acid desaturases, are found in the deduced amino acid sequence of TauΔ12des (Fig. 3-1, underlined), whereas the cytochrome b_5 motif, a characteristic of front-end desaturases, is not present in the enzyme.

Phylogenetic analysis of TauΔ12des

The Δ12- and Δ12/Δ15-fatty acid desaturases have been classified into the following groups based on sequence similarity: a fungal and protozoan group, a plant group, a cyanobacterial group, and a chloroplast-localized plant group. The evolutionary relationships among TauΔ12des and other Δ12- and Δ12/Δ15-fatty acid desaturases were examined in a phylogenetic analysis. Although TauΔ12des was not clustered

with any group, it was most closely related to the Δ12-fatty acid desaturase found in the diatom *P. tricornutum* (Fig. 3-2).

Exploring the specificity of TauΔ12des expressed in the budding yeast *S. cerevisiae*

To elucidate the specificity of TauΔ12des activity, a TauΔ12des expression construct (pYTauΔ12Des) and an empty-control construct (pYES2/CT) were separately introduced into the *S. cerevisiae* strain INVSc1, and the fatty acid compositions of these transformants were analyzed by GC using their corresponding FAMEs. The peak corresponding to the LA ($18:2^{\Delta 9, 12}$) methyl ester standard was found in the GC spectra of the pYTauΔ12Des transformants (Fig. 3-3B) but not in those of the mock transformants (Fig. 3-3A). GC-MS analysis of the newly generated peak in the pYTauΔ12Des transformants revealed the presence of a molecular ion (m/z 294) and fragment ions identical to those of the LA methyl ester standard (Fig. 3-4A, B). These results indicated that endogenous OA was converted into LA in the transformants harboring pYTauΔ12Des. Moreover, a new peak was generated in pYTauΔ12Des-harboring transformants, but not in mock transformants, when nonadecanoic acid ($C19:1^{\Delta 10}$) was added to the culture (Fig. 3-3A, B). The new peak was determined to be nonadecadienoic acid ($C19:2^{\Delta 10, 13}$) by GC-MS (Fig. 3-4C, D). This result indicates that TauΔ12des is a Δ12-fatty acid desaturase with ν+3 regioselectivity. However, no double bonds were introduced into myristoleic acid ($14:1^{\Delta 9}$), palmitoleic acid ($16:1^{\Delta 9}$), heptadecenoic acid ($17:1^{\Delta 10}$), elaidic acid ($18:1^{\Delta 9\ trans}$), LA, γ-linolenic acid ($C18:3^{\Delta 6, 9, 12}$), dihomo-γ-linolenic acid ($C20:3^{\Delta 8, 11, 14}$), arachidonic acid ($C20:4^{\Delta 5, 8, 11, 14}$) or docosatetraenoic acid ($C22:4^{\Delta 7, 10, 13, 16}$) when they were added to cultures of either pYTauΔ12Des-harboring transformants or mock transformants at 50

μM (data not shown). Taken together, it was concluded that the *tauΔ12des* encodes a fatty acid desaturase with the dual specificities of a Δ12-fatty acid desaturase and a ν+3-fatty acid desaturase, which catalyze the conversions of OA to LA and C19:1$^{\Delta 10}$ to C19:2$^{\Delta 10, 13}$, respectively.

Western blotting of FLAG-tagged TauΔ12des expressed in yeast

The author examined the expression of TauΔ12des at the protein level when expressed in *S. cerevisiae*. Yeast cells expressing FLAG-tagged TauΔ12des were lysed and fractionated into microsomal and cytosolic fractions followed by analysis with Western blotting using an anti-DYKDDDDK-tag antibody. A 45.3-kDa protein band was detected in the cell lysate and the microsomal fractions but not in the cytosolic fraction (Fig. 3-5). This molecular weight was consistent with that estimated from the deduced amino acid sequence of TauΔ12des with a FLAG tag. These results indicate that TauΔ12des is classified as a microsomal fatty acid desaturase.

Generation of *tauΔ12des*-disruption mutants

To address the question of whether TauΔ12des is involved in the standard pathway in *T. aureum*, the *tauΔ12des* was disrupted in the thraustochytrid by homologous recombination using a disruption construct containing *hyg*^{r} or *bla*^{r} as a marker gene flanked with the 5′ and 3′ sequences of the Tau Δ12des genomic locus (Fig. 3-6). Because *T. aureum* ATCC 34304 appears to be diploid, two loci harboring the *tauΔ12des* should be disrupted by different marker genes to create a full deletion mutant. Transformants grown on GY medium containing hygromycin B (1st-allele disrupted mutants) or hygromycin B plus blasticidin (1st-/2nd-allele disrupted mutants) were

subjected to genomic PCR and RT-PCR to confirm the disruption of the *tauΔ12des*. As shown in Fig. 3-7A, B, 1,026-bp and 399-bp PCR products (corresponding to the *hyg*^{r} and *bla*^{r}, respectively) were detected in the 1st-/2nd-allele disrupted mutants (*tauΔ12des*-disruption mutants) but not in the wild-type strain. In contrast, an 1,185-bp PCR product (corresponding to *tauΔ12des*) was amplified in the wild-type strains and the 1st-allele disrupted mutants but not in the 1st-/2nd-allele disrupted mutants (Fig. 3-7C). Furthermore, RT-PCR revealed that transcripts of both the *hyg*^{r} (1,026 bp) and the *bla*^{r} (399 bp), but not the *tauΔ12des*, were present in 1st-/2nd-allele disrupted mutants, whereas the transcript of *tauΔ12des* (1,185 bp) was detected in both the wild-type strains and the 1st-allele disrupted mutants (Fig. 3-7D, E, F). Transcripts of the *hyg*^{r}, but not the *bla*^{r}, were detected in the 1st-allele disrupted mutants, and no transcripts of the *hyg*^{r} or *bla*^{r} were detected in the wild-type strain.

Southern blot hybridization using the DIG-labeled 5′-upstream and 3′-downstream regions of the *tauΔ12des* as the probes was conducted to further characterize the *tauΔ12des*-disruption mutants. When hybridized with the 5′-upstream-specific probe, a single 2,028-bp band was detected in the wild-type strain, whereas 5,880- and 5,253-bp bands, corresponding to the two disruption constructs containing each marker gene, were detected in the 1st-/2nd-allele disrupted mutants, respectively (Fig. 3-8D). Hybridization with a 3′-downstream-specific probe resulted in the generation of single a 2,334-bp band in the wild-type strain, whereas a single 1,496-bp band was detected in the 1st-/2nd-allele disrupted mutants (Fig. 3-8E). These results clearly indicate that the *tauΔ12des* was disrupted by homologous recombination with the two marker genes and that *T. aureum* is diploid under the growth conditions used.

Characterization of the *tauΔ12des*-disruption mutants from the perspective of fatty acid biosynthesis

The compositions of the fatty acids in the wild-type strain and the *tauΔ12des*-disruption mutants were analyzed by GC using their methyl ester derivatives. The picolinyl esters, prepared from the FAMEs, were also analyzed by GC-MS to identify each fatty acid (data not shown). In contrast to the wild type, the mutants had no LA ($C18:2^{\Delta 9,\ 12}$), the major product of TauΔ12des, whereas they accumulated a significant amount of OA ($C18:1^{\Delta 9}$), the major substrate for TauΔ12des (Fig. 3-9A, B, Table 3-2). Importantly, the downstream derivatives of LA in the standard pathway also decreased drastically in *tauΔ12des*-disruption mutants, except for DHA, which was instead slightly increased. Furthermore, the $C17:1^{\Delta 9}$ and $C19:1^{\Delta 9}$ contents significantly increased in the *tauΔ12des*-disruption mutants, indicating that these odd-chain fatty acids are substrates for TauΔ12des. The loss of Δ12-fatty acid desaturase activity was also confirmed by the metabolic labeling of mutants using ^{14}C-oleoyl-CoA (Fig. 3-10); no ^{14}C-LA was found in the mutants, in contrast to the wild type. As shown in Table 3-3, the accumulation of OA and the decrease of LA and its downstream PUFAs in the standard pathway were observed not only in the total fatty acid fraction but also in each lipid class (*i.e.*, neutral lipids, phospholipids, and glycolipids) of the *tauΔ12des*-disruption mutants.

Despite the significant changes in the fatty acid profiles in the total fatty acid and complex lipid fractions, no difference was observed in cell growth between the wild-type strain and the *tauΔ12des*-disruption mutants under our cultivation conditions (Fig. 3-11).

Restoration of the fatty acid profile in revertants of the *tauΔ12des*-disruption mutants

To complement the *tauΔ12des* in the *tauΔ12des*-disruption mutants, a Neo^r/TauΔ12des-expression construct (Fig. 3-12A) was injected into the disruption mutants by microprojectile bombardment. As a control, a Neo^r-expression construct was injected into other *tauΔ12des*-disruption mutants (Fig. 3-12B). Transformants grown on GY medium containing G418 were selected as transformants and subjected to genomic PCR to determine whether a full-length Neo^r/TauΔ12des DNA was integrated into the genome of the transformants. As shown in Fig. 3-12C, a 5,306-bp PCR product (corresponding to the size of the Neo^r/TauΔ12des construct, Fig. 3-12A) was detected in the transformants harboring Neo^r/TauΔ12des DNA (tentatively designated revertants), whereas a 2,717-bp PCR product (corresponding to the size of the Neo^r construct, Fig. 3-12B) was detected in the transformants harboring the Neo^r control construct (KO/*neo*^{r}). Southern blot hybridization using a TauΔ12des DNA probe confirmed that the *tauΔ12des* was integrated into the genomes of the revertants (Fig. 3-12D). Furthermore, RT-PCR revealed that transcripts of the *neo*^{r} (835-bp) and the *tauΔ12des* (1,185-bp) were present in the revertants, whereas the transcript of the *neo*^{r}, but not the *tauΔ12des*, was detected in the KO/*neo*^{r} (Fig. 3-12E, F). These results clearly indicate that *tauΔ12des* was integrated into the genome of the revertants and then transcribed into TauΔ12des mRNA.

The fatty acid compositions of the revertant and KO/*neo*^{r} were analyzed by GC using their respective FAMEs. In contrast to the KO/*neo*^{r}, the fatty acid profile of the revertants was restored to that of the wild-type strain, *i.e.*, the levels of OA, LA and its downstream PUFAs in the revertants were similar to those of the wild-type strains (Fig.

3-13A, B, Table 3-4). Additionally, *in vivo* labeling with ^{14}C-oleoyl-CoA demonstrated the restoration of the Δ12-fatty acid desaturase activity in the revertants (Fig. 3-14). These results clearly indicate that the change in the fatty acid profile in the *tauΔ12des*-disruption mutants was entirely due to the loss of function of *tauΔ12des*.

It is shown in this CHAPTER that TauΔ12des is the Δ12-fatty acid desaturase involved in the standard pathway and that this enzyme is primarily responsible for the conversion of OA into LA in *T. aureum*. Furthermore, DHA was found to be produced in *T. aureum* primarily independently of the standard pathway, possibly via the PUFA synthase pathway. In conclusion, two working pathways for the production of PUFAs in *T. aureum* were revealed through the analysis of a native Δ12-fatty acid desaturase.

3-4. DISCUSSION

Thraustochytrids, belonging to the protist kingdom Stramenopila, are microorganisms that constitute a promising alternative to fish oils as an industrial source of PUFAs. Interestingly, the fatty acid profiles differ among the different thraustochytrid genera. The major PUFAs of the various genera are as follows: (1) DHA and omega-6 DPA; (2) DHA, omega-6 DPA and EPA; (3) DHA and EPA; (4) DHA, omega-6 DPA, EPA and ARA; and (5) DHA, omega-6 DPA, EPA, ARA and DTA (74). These different PUFA profiles may indicate the presence of different PUFA biosynthetic pathways in the various thraustochytrids. Several lines of evidence suggest the occurrence of two different pathways involved in the biosynthesis of PUFAs in thraustochytrids. The first, which is found in several marine bacteria, is the polyketide synthase-like pathway (the PUFA synthase pathway), comprising reiterative cycles including condensation, reduction, dehydration and isomerization steps, with each step catalyzed by different enzymes. Three functional ORFs of the PUFA synthase pathway have been identified in *Schizochytrium* (now reassigned to *Aurantiochytrium*) (24, 25, 30). Lippmeier *et al* suggested that the PUFA synthase pathway is the sole system responsible for PUFA production in *Schizochytrium*, as the disruption of an ORF of a PUFA synthase led to the loss of PUFAs in the thraustochytrids, which became PUFA-dependent auxotrophs (26). The other pathway, which is found in many organisms, including mammals, is the desaturase/elongase pathway (the standard pathway), comprising a series of alternating desaturation and elongation steps starting with saturated fatty acids that are produced in an FAS pathway. Although several desaturase and elongase genes have been cloned and characterized in thraustochytrids (17, 20, 21), the direct evidence that

such enzymes are operative in the standard pathway has yet been obtained. In this CHAPTER, the author demonstrated that the standard pathway is functional in *T. aureum* ATCC 34304 by disrupting the gene encoding a Δ12-fatty acid desaturase, which is a key enzyme in the standard pathway for the production of both omega-3 and omega-6 PUFAs.

In this CHAPTER, the author generated disruption mutants of *tauΔ12des* by replacing two *tauΔ12des* alleles with two different marker genes. The disruption construct was composed of the 5′ and 3′ regions of the *tauΔ12des* as homologous recombination sites and an antibiotic-resistance gene (*hyg*^{r} or *bla*^{r}) as a marker gene (Fig. 3-6). Molecular analysis of the *tauΔ12des*-disruption mutants showed that the *tauΔ12des* ORFs of two alleles were replaced by *hyg*^{r} or *bla*^{r} (Figs. 3-7 and 3-8). This result indicates that *T. aureum* is diploid, at least under the conditions used in this study. In contrast, *Schizochytrium* sp. ATCC 20888 appeared to be haploid (26).

Unexpectedly, the *tauΔ12des*-disruption mutants of *T. aureum* were indistinguishable from the wild-type strain in morphology and cell growth under the conditions used in this study (Fig. 3-11). However, the disruption of the *tauΔ12des* led to a dramatic change in the fatty acid profile, in which an increase of OA (C18:1$^{\Delta 9}$) was observed in combination with the disappearance of LA (C18:2$^{\Delta 9,\ 12}$) (Fig. 3-9, Table 3-2). Furthermore, the *tauΔ12des*-disruption mutants showed decreased levels of the omega-6 and omega-3 PUFAs that are downstream of LA in the standard pathway. In contrast, DHA levels were slightly increased in the disruption mutants. These results demonstrate that TauΔ12des functions in the standard pathway for the production of PUFAs, whereas DHA is primarily produced by a nonstandard pathway in *T. aureum*, possibly by the PUFA synthase pathway. However, we observed that the disruption of

the PUFA synthase gene in *T. aureum* resulted in a marked decrease in DHA but not in other PUFAs such as LA, ARA (C20:4$^{\Delta5, 8, 11, 14}$) and EPA (C20:5$^{\Delta5, 8, 11, 14, 17}$) (data not shown). Notably, a small amount of DHA was still present in the PUFA synthase-disrupted mutants, suggesting that DHA is produced not only by the PUFA synthase pathway but also by the standard pathway. Neither TauΔ12des nor PUFA-synthase disruption mutants of *T. aureum* were auxotrophs, in contrast to PUFA-synthase mutants of *Schizochytrium* spp.

Interestingly, the author observed the accumulation of C17:1$^{\Delta9}$ and C19:1$^{\Delta9}$ in the *tauΔ12des*-disruption mutants, and this accumulation was eliminated by introducing *tauΔ12des* into the disruption mutants. This result indicates that TauΔ12des also accepts odd-chain fatty acids as substrates. Chang *et al* identified odd-chain PUFAs in thraustochytrids and suggested that these PUFAs are synthesized through the standard pathway (100). The accumulation of C17:1$^{\Delta9}$ and C19:1$^{\Delta9}$ in *tauΔ12des*-disruption mutants supports their hypothesis. In addition, the levels of saturated fatty acids also increased in the *tauΔ12des*-disruption mutants over those of the wild-type strain. Several recent studies have indicated that PUFAs regulate the expression of the fatty acid synthase (FAS) gene (101-103). Therefore, it is plausible that the altered PUFA profile in the disruption mutants led to upregulated expression of the FAS gene, resulting in increased amounts of saturated fatty acids.

The enzymes involved in the PUFA synthase pathway are cytosolic proteins, and the products are released from the synthetic machinery as free fatty acids (25). In contrast, the membrane desaturases accept a wide range of acyl substrates (104, 52). Therefore, the author expected that the fatty acid profiles of complex lipids from the *tauΔ12des*-disruption mutants would be somewhat different from those of the wild-type

strain, as shown in filamentous fungus (105). However, no difference was observed between the wild-type strain and the disruption mutants in their fatty acid profiles of neutral lipids, phospholipids, and glycolipids (Table 3-3). Thus, it is possible that the fatty acids produced via the standard pathway are acyl-CoA forms that are directly incorporated into different complex lipids by various acyltransferases. In other words, the desaturases and elongases that constitute the standard pathway of the thraustochytrid accept the CoA forms of fatty acids as substrates. Another possibility is that the fatty acids in each lipid class are remodeled in *T. aureum* after their incorporation into complex lipids. Further studies are necessary to elucidate the acceptor specificity of TauΔ12des *in vitro*.

In conclusion, the author presents direct evidence that TauΔ12des functions in the standard pathway and is responsible for generating certain PUFAs in *T. aureum*, although DHA is primarily produced through the PUFA synthase pathway. The results of this study also indicate that LA and its downstream products from the standard pathway are not necessary for the normal growth and morphology of *T. aureum* under our conditions, as sufficient DHA is generated through the PUFA synthase pathway.

3-5. SUMMARY

Thraustochytrids are known to accumulate PUFAs such as DHA in their lipid droplets. Accumulating evidence suggests that these organisms produce PUFAs via polyketide synthase-like (PUFA synthase) and desaturase/elongase (standard) pathways. However, it remains unclear whether the latter pathway actually functions in thraustochytrids. In this study, the author reports that the standard pathway in fact functions to produce PUFA in *Thraustochytrium aureum* ATCC 34304. The author isolated a gene encoding a putative Δ12-fatty acid desaturase (TauΔ12des) from *T. aureum* ATCC 34304. Yeast cells transformed with the *tauΔ12des* converted endogenous OA into LA. The disruption of the *tauΔ12des* in *T. aureum* by homologous recombination resulted in the accumulation of OA and a decrease in the levels of LA and its downstream PUFAs. However, the DHA content was increased slightly in *tauΔ12des*-disruption mutants, suggesting that DHA is primarily produced in *T. aureum* via the PUFA synthase pathway. The transformation of the *tauΔ12des*-disruption mutants with a TauΔ12des expression cassette restored the wild-type fatty acid profiles. These data clearly indicate that the *tauΔ12des* encodes a Δ12-fatty acid desaturase that functions in the standard pathway of *T. aureum* and demonstrate that this thraustochytrid produces PUFAs via both the PUFA synthase and the standard pathways.

Fig. 3-1. Alignment of the deduced amino acid sequence of TauΔ12des with the sequences of diatom and picophytoplankton Δ12-fatty acid desaturases.

TauΔ12des and Δ12-fatty acid desaturases from different origins were aligned using ClustalW 1.81 and the alignment was shaded in ESPript 2.2 (http://espript.ibcp.fr/ESPript/cgi-bin /ESPript.cgi). Identical and similar amino acid residues are shown as white letters on a black background and in bold face with a gray box, respectively. The histidine boxes that are commonly conserved in membrane fatty acid desaturases are underlined. TpsΔ12des, *Thalassiosira pseudonana* Δ12-fatty acid desaturase (XP_002292071); PtrΔ12des, *Phaeodactylum tricornutum* Δ12-fatty acid desaturase (3503348AJJ); TauΔ12des, *T. aureum* ATCC34304 Δ12-fatty acid desaturase (this study); and MspΔ12des, *Micromonas* sp. Δ12-fatty acid desaturase (XP_002507091).

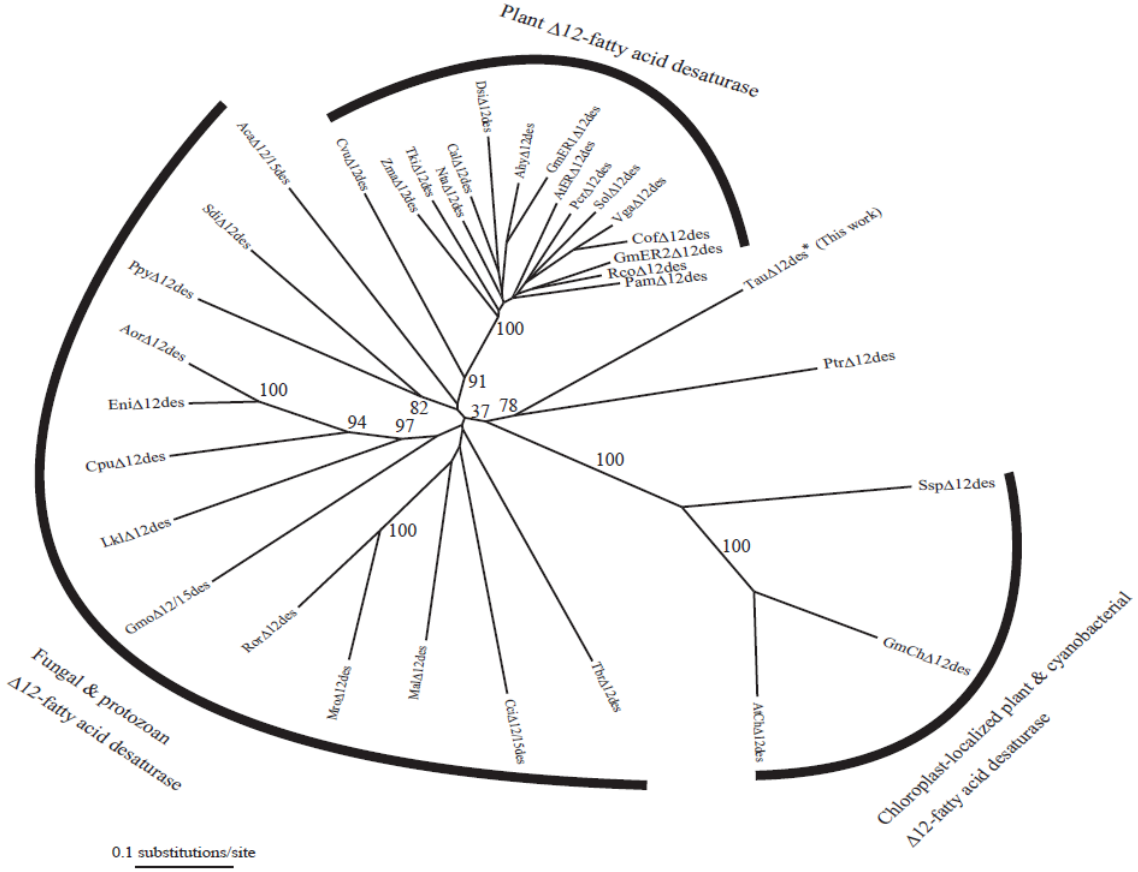

Fig. 3-2. Phylogenetic analysis of Δ12- and bifunctional Δ12/Δ15-fatty acid desaturases.

Phylogenetic tree was constructed by neighbor-joining method (http://clustalw.ddbj.nig.ac.jp/top-j.html). The scale bar represents a distance of 0.1 substitutions per site in the protein sequence. The abbreviations and origins of the desaturases used are summarized in Table 3-5.

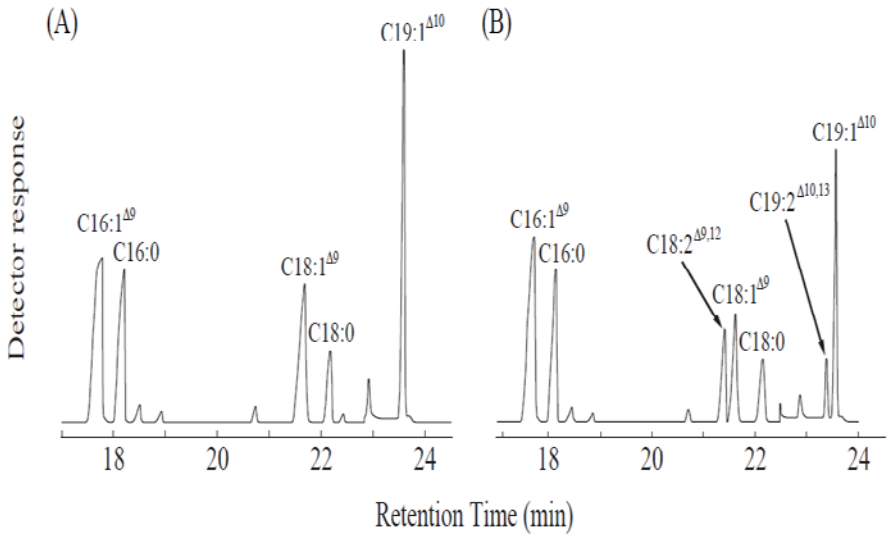

Fig. 3-3. GC analysis of FAMEs from the *S. cerevisiae* TauΔ12des transformants.

Gas chromatograms showing the FAMEs extracted from *S. cerevisiae* transformed with (A) an empty vector, pYES2/CT (mock transformants) and (B) the *tauΔ12des*-containing vector, pYTauΔ12Des (TauΔ12des transformants). The detector voltages was shifted from 1.20 to 1.50 kV at the retention time of 22.50 min. The arrows indicate the new peak observed in the TauΔ12des transformants (B). The cells were cultured in uracil-deficient SC medium containing 2% glucose at 25°C for 3 days and then cultured for an additional day in uracil-deficient SC medium containing 2% galactose with or without exogenous fatty acids. Fatty acids were added to the culture with 0.1% Tergitol. The fatty acids were extracted from freeze-dried cells and subjected to GC analysis as described in MATERIALS AND METHODS.

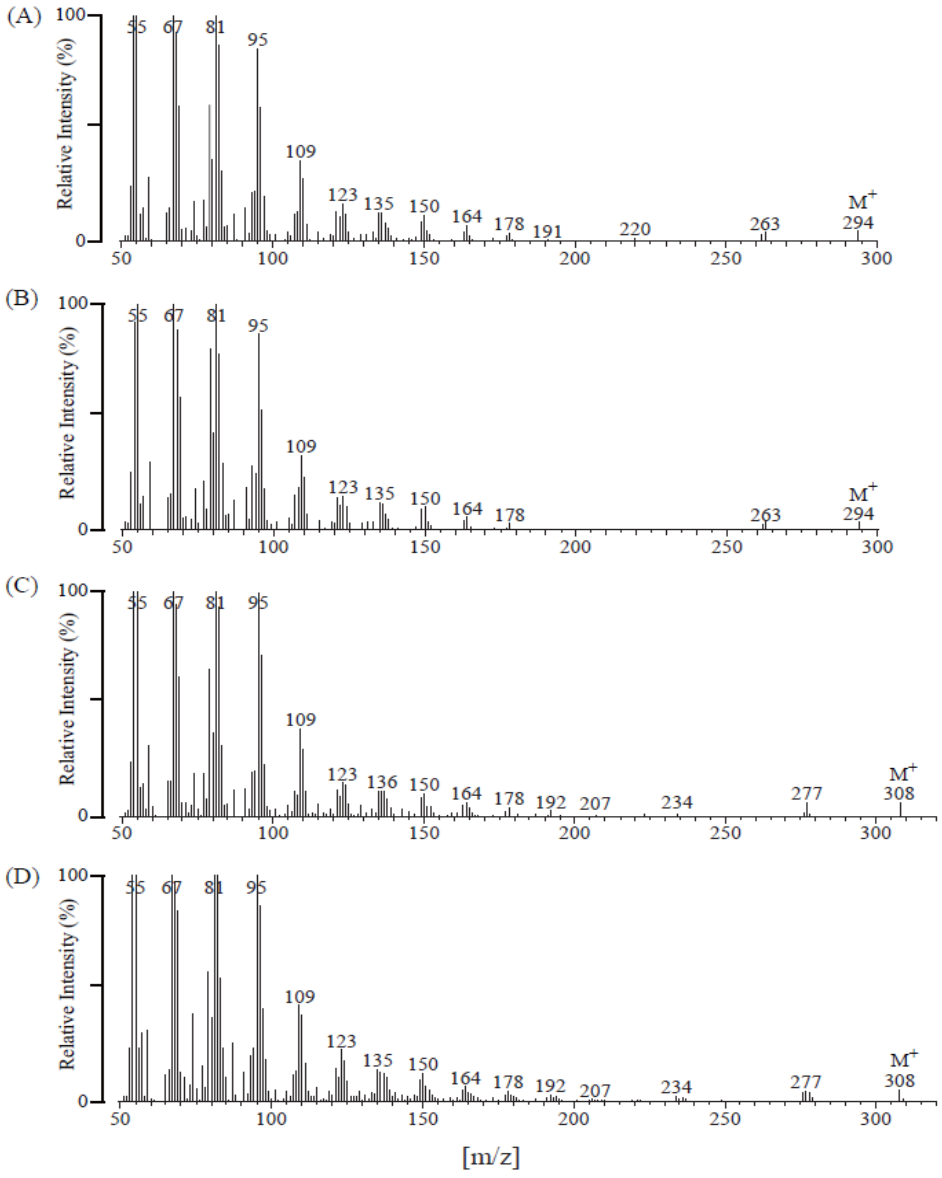

Fig. 3-4. GC-MS analysis of FAMEs from the *S. cerevisiae* TauΔ12des transformants.

(A) The mass spectrum of the new peak corresponding to the retention time of LA in the TauΔ12des transformants. (B) The mass spectrum of the LA methyl ester standard. (C) The mass spectrum of the new peak corresponding to the retention time of nonadecadienoic acid (C19:$2^{\Delta 10, 13}$) in the TauΔ12des transformants. (D) The mass spectrum of the nonadecadienoic acid (C19:$2^{\Delta 10, 13}$) methyl ester standard. The fatty acids were extracted from freeze-dried cells and subjected to GC-MS as described in MATERIALS AND METHODS.

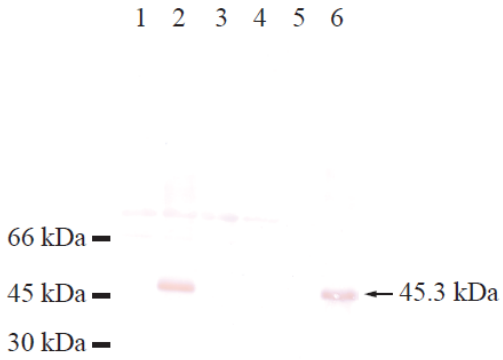

Fig. 3-5. Western blot analysis of FLAG-tagged TauΔ12des expressed in the yeast.

1, The cell lysate from the mock transformant; 2, the cell lysate from the transformant expressing the FLAG-tagged TauΔ12des; 3, the cytosolic fraction from the mock transformant; 4, the cytosolic fraction from the transformant expressing the FLAG-tagged TauΔ12des; 5, the microsomal fraction from the mock transformant; 6, the microsomal fraction from the transformant expressing the FLAG-tagged TauΔ12des. *S. cerevisiae* cells harboring a vector containing the FLAG-tagged *tauΔ12des* or an empty vector (mock control) were cultured in SC-ura medium, and their microsomes were separated from a crude cell lysate. Western blotting was conducted using 10% SDS-PAGE with an anti-DYKDDDDK tag mouse monoclonal antibody and an HRP-conjugated anti mouse IgG goat antibody. The details are described in MATERIALS AND METHODS.

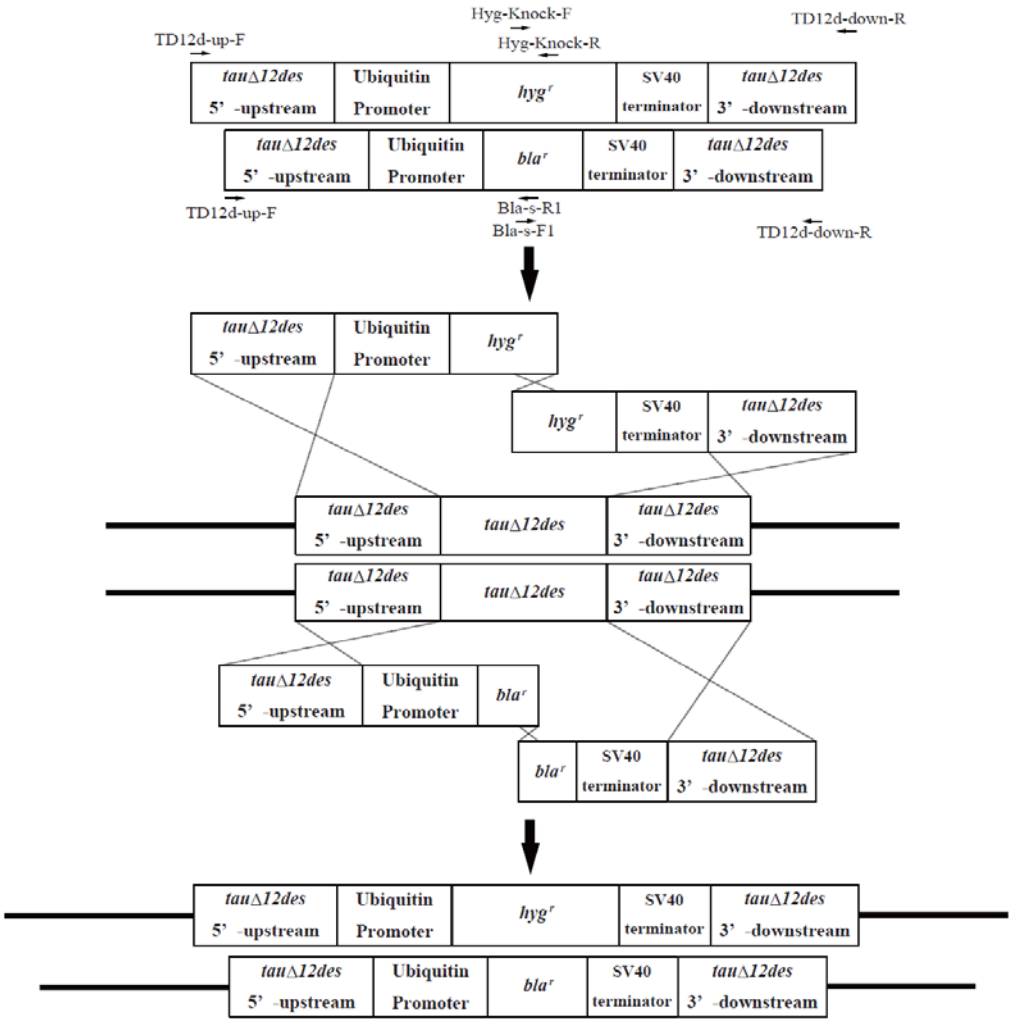

Fig. 3-6. A strategy for the disruption of TauΔ12des by homologous recombination.

The *tauΔ12des* was disrupted by homologous recombination. The 1st-allele knock-out was performed with a Hyg^r construct, and the 2nd-allele was disrupted with a Bla^r construct. The details are described in MATERIALS AND METHODS.

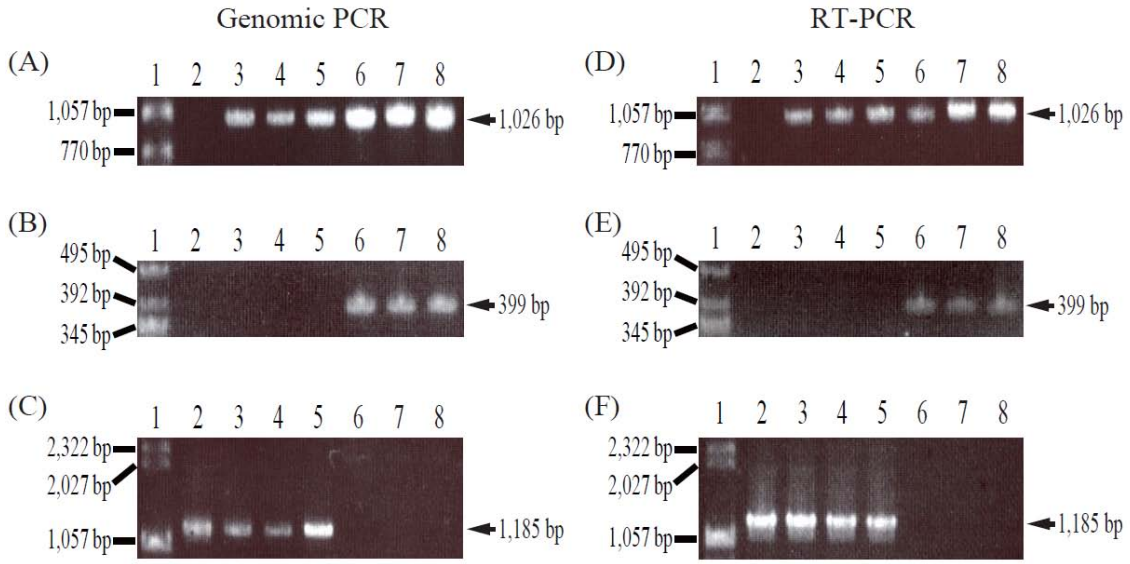

Fig. 3-7. Molecular characterization of the *tauΔ12des*-disruption mutants.

Genomic PCR showing the Hyg^r (A), Bla^r (B) and TauΔ12des (C) genes. RT-PCR amplifying Hyg^r mRNA (D), Bla^r mRNA (E) and TauΔ12des mRNA (F). 1, λ*Hin*d III digestion / ϕX174 *Hin*c II digestion marker; 2, wild-type *T. aureum*; 3-5, 1st-allele disruption mutants; 6-8, 1st/2nd-allele disruption mutants. Further details are provided in MATERIALS AND METHODS.

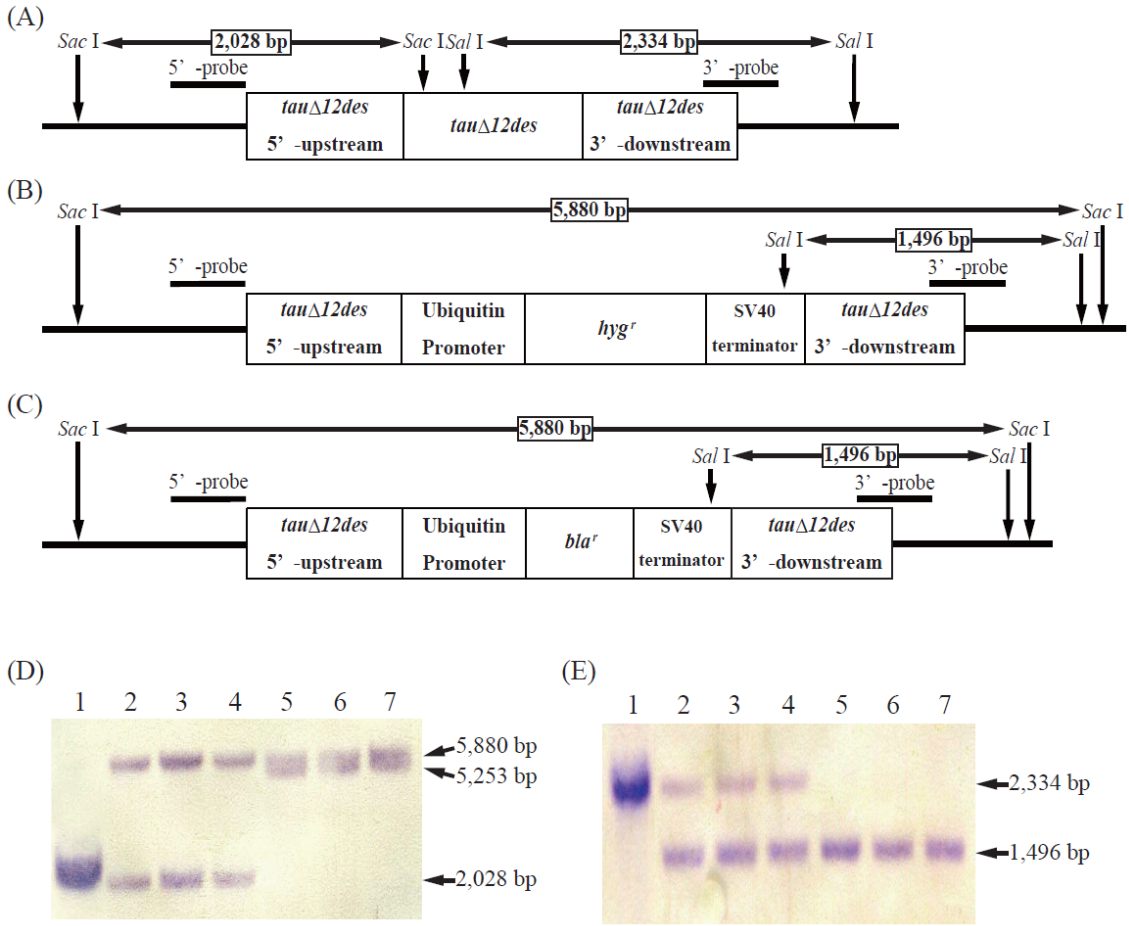

Fig. 3-8. Southern blot analysis of the *tauΔ12des*-disruption mutants.

The restriction maps for each disrupted allele. (A) wild-type allele; (B) recombinant allele with Hyg^r expression cassette; (C) recombinant allele with the Bla^r expression cassette. The confirmation of the disruption of *tauΔ12des* by Southern hybridization using a 5′-upstream-specific probe (D) or a 3′-downstream-specific probe (E). The genomic DNA was digested at 37°C overnight with *Sac* I for the 5′-upstream and with *Sal* I for the 3′-downstream Southern blot hybridization. 1, wild-type *T. aureum*; 2-4, 1st-allele disruption mutants; 5-7, 1st/2nd-allele disruption mutants. Further details are provided in MATERIALS AND METHODS.

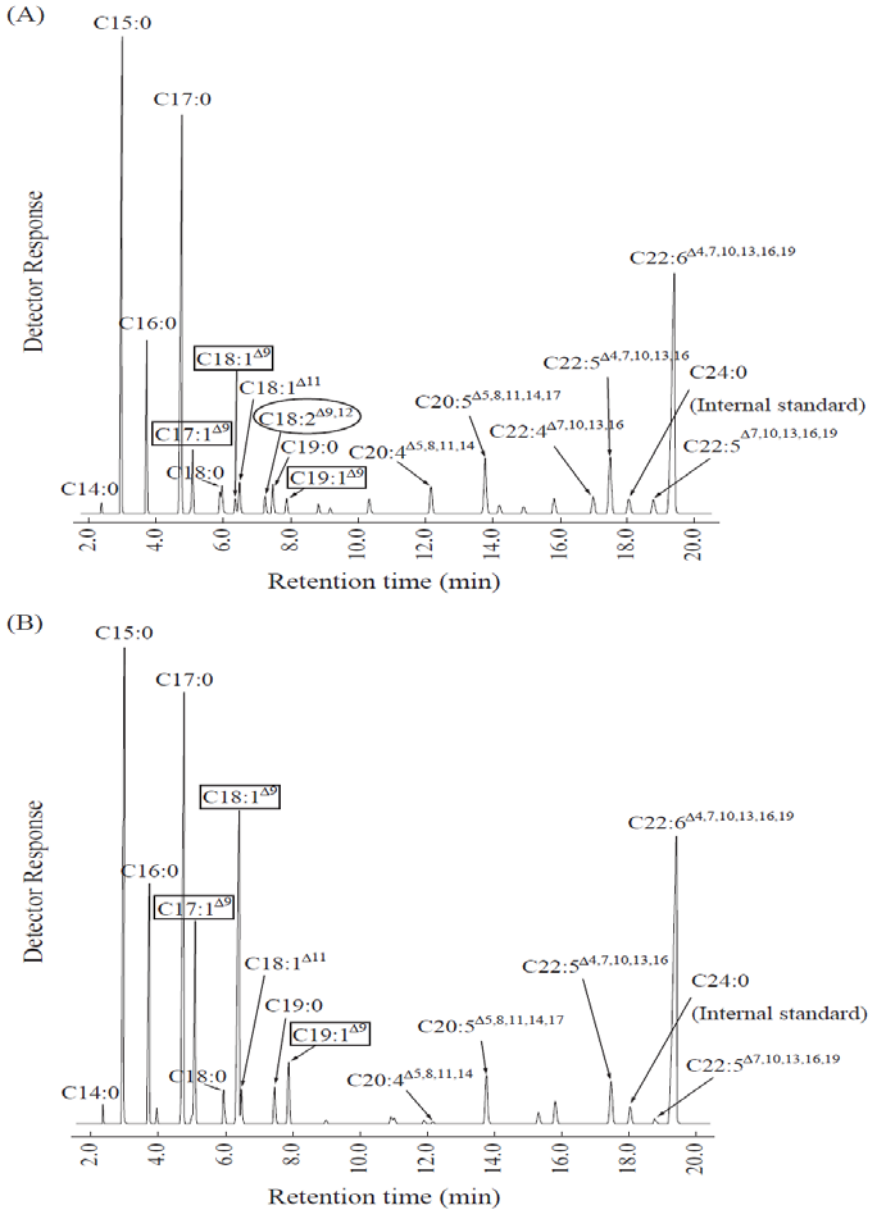

Fig. 3-9. GC of FAMEs from the wild-type strain and the *tauΔ12des*-disruption mutants.

Gas chromatograms showing the FAMEs extracted from (A) wild-type *T. aureum* and (B) *tauΔ12des*-disruption mutants (1st/2nd-allele disruption mutants). The cells were cultured in a GY medium containing ampicillin at a concentration of 0.1 mg/ml at 25°C for 5 days. The fatty acids were extracted from freeze-dried cells and subjected to GC as described in MATERIALS AND METHODS. Endogenous substrates for TauΔ12des, C17:1$^{\Delta 9}$, C18:1$^{\Delta 9}$ and C19:1$^{\Delta 9}$, are shown in the square and products, C18:2$^{\Delta 9, 12}$ is shown in the circle.

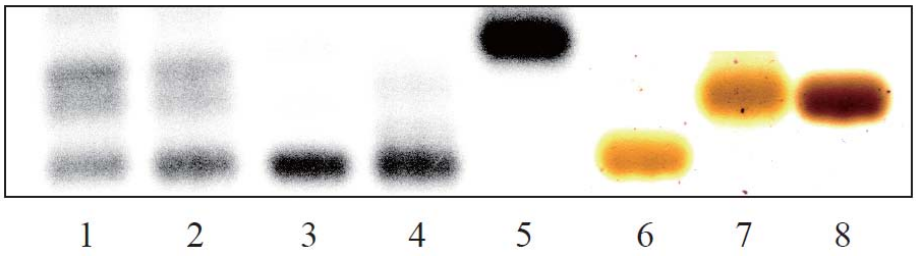

Fig. 3-10. The *in vivo* conversion of ^{14}C-oleic acid to ^{14}C-linoleic acid and downstream PUFAs in wild-type *T. aureum* and the *tauΔ12des*-disruption mutants. Wild-type *T. aureum* and *tauΔ12des*-disruption mutants were cultured at 25°C for 1 day in GY medium containing 5 nmol of ^{14}C-oleoyl CoA (0.29 μCi). The fatty acids were extracted as FAMEs and then applied to a reverse-phase TLC plate which was developed with methanol/acetonitrile/water (90.5/14/7, v/v/v). The ^{14}C-fatty acids were detected by FLA5000. 1, wild-type strain; 2, 1st-allele disruption mutant; 3, 1st/2nd-allele disruption mutant; 4, ^{14}C-oleoyl-CoA; 5, ^{14}C-DHA-CoA; 6, oleic acid; 7, linoleic acid; 8, omega-6 docosapentaenoic acid.

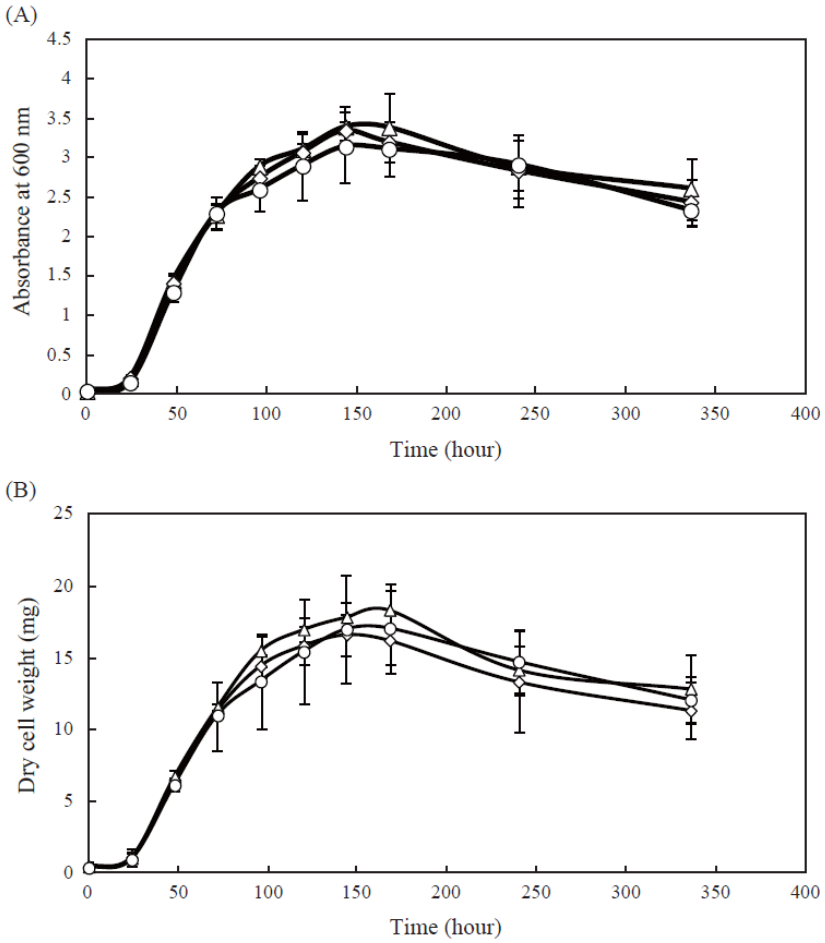

Fig. 3-11. The growth of the wild-type strain and the *tauΔ12des*-disruption mutants in GY medium.

(A) Growth curves using the optical density. (B) Growth curves using DCW. Cells from the wild-type strain (wild type, squares), 1st-allele disruption mutants (sKO, triangles), 1st/2nd-allele disruption mutants (dKO, circles) were cultured for 5 days at 25°C.

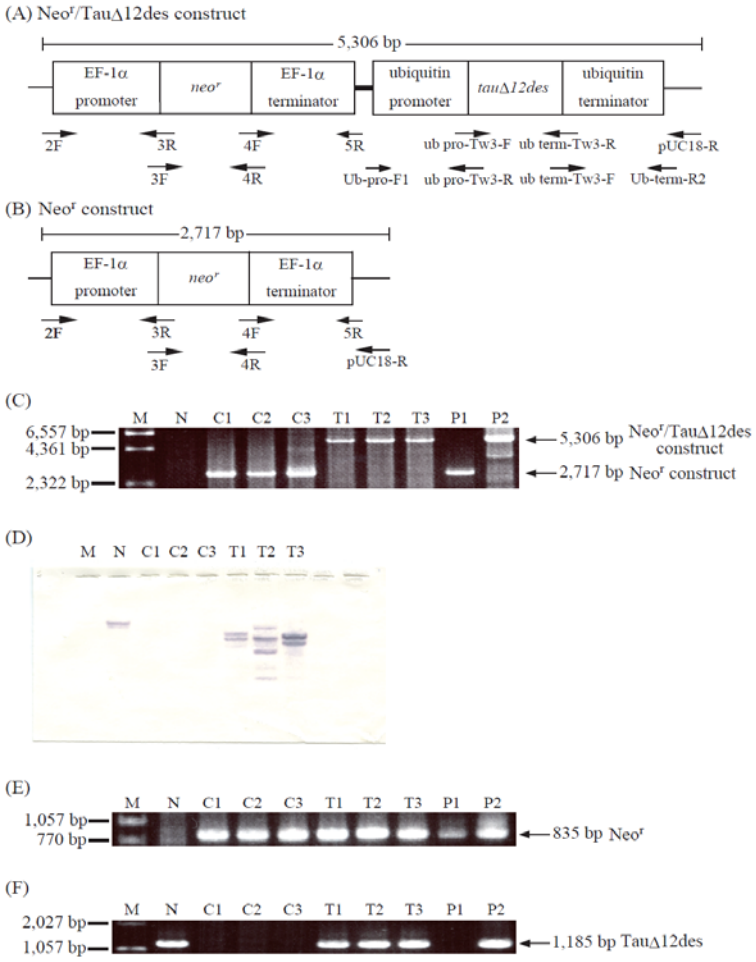

Fig. 3-12. Molecular characterization of the TauΔ12des revertants.

Neo^r/TauΔ12des construct (A) and Neo^r construct (B) were separately injected to the *tauΔ12des*-disruption mutants and then transformants obtained designated TauΔ12des revertants and Neo^r transformants (KO/neo^r). The *tauΔ12des* and *neo^r* were driven with thraustochytrid-derived ubiquitin promoter/terminator and EF-1α promoter/terminator, respectively. The primers for fusion PCR of these constructs are shown below each constructs. (C), Genomic PCR showing the Neo^r and Neo^r/TauΔ12des constructs. (D), Southern blot hybridization using a TauΔ12des-specific probe. (E, F), RT-PCR amplifying Neo^r mRNA (E) and TauΔ12des mRNA (F). M, λ*Hin*d III digestion / ϕX174 *Hin*c II digestion marker; N, control (wild-type *T. aureum*); C1-C3, Neo^r transformants (mock transformants); T1-T3, Neo^r/TauΔ12des transformants; P1, positive control (Neo^r construct); P2, positive control (Neo^r/TauΔ12des construct). These procedures are described in detail in MATERIALS AND METHODS.

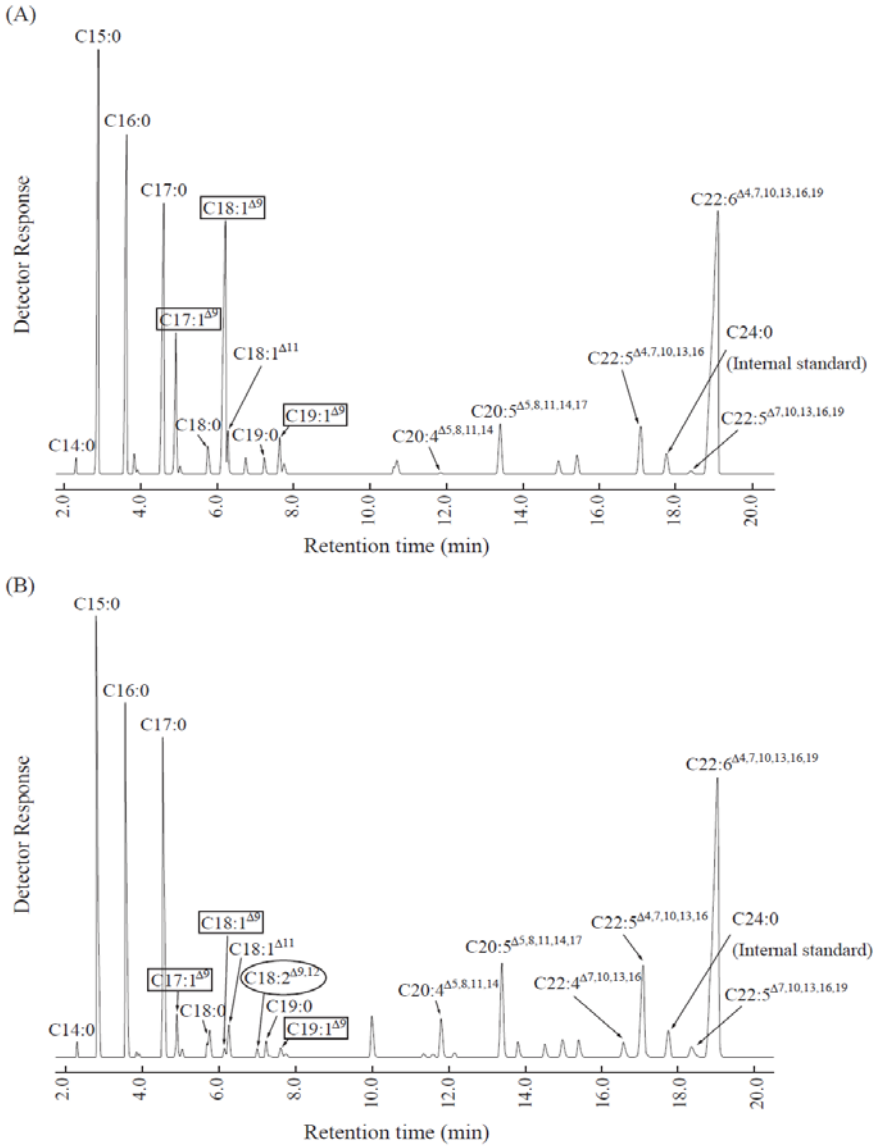

Fig. 3-13. GC analysis of FAMEs from Neo^r transformants (A) and TauΔ12des revertants (B).

Neo^r construct and Neo^r/TauΔ12des construct were separately injected to the *tauΔ12des*-disruption mutants and then transformants obtained designated Neo^r transformants (KO/*neo*^{r}) (A) and TauΔ12des revertants (B). Gas chromatograms showing the FAMEs extracted from (A) and (B). The cells were cultured in a GY medium containing G418 at a concentration of 2 mg/ml at 25°C for 5 days. The fatty acids were extracted from freeze-dried cells and subjected to GC analysis as described in MATERIALS AND METHODS. Endogenous substrates for TauΔ12des, C17:1$^{\Delta9}$, C18:1$^{\Delta9}$ and C19:1$^{\Delta9}$, are shown in the square and products, C18:2$^{\Delta9,12}$ is shown in the circle.

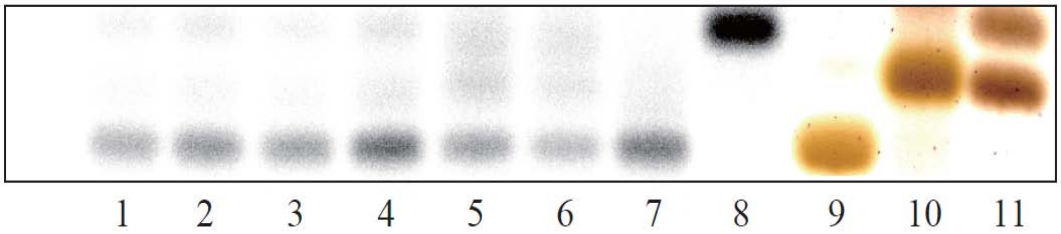

Fig. 3-14. The *in vivo* conversion of ^{14}C-oleic acid to ^{14}C-linoleic acid and downstream PUFAs in the Neo^{r} and Neo^{r}/TauΔ12des transformants.

The *tauΔ12des*-disruption mutant transformed with the Neo^{r} construct (KO/*neo*^{r}) or the Neo^{r}/TauΔ12des construct (revertant) were cultured at 25˚C for 1 day in GY medium containing 5 nmol of ^{14}C-oleoyl CoA (0.29 μCi). The fatty acids were extracted as FAMEs and then applied to a reverse-phase TLC plate, which was developed with methanol/acetonitrile/water (90.5/14/7, v/v/v). The ^{14}C-fatty acids were detected by FLA5000. 1, KO/*neo*^{r} 1; 2, KO/*neo*^{r} 2; 3, KO/*neo*^{r} 3; 4, revertant 1; 5, revertant 2; 6, revertant 3; 7, ^{14}C-oleoyl-CoA; 8, ^{14}C-DHA-CoA; 9, oleic acid; 10, linoleic acid; 11, omega-6 docosapentaenoic acid and DHA.

Table 3-1.

The PCR primers used in this chapter.

Name	Sequence	Direction
Tw3-F1	5' - ATGTGCAAGGTCGATGGGACAA -3'	Forward
Tw3-R1	5' - TCACAAACATCGCAGCCTTCGG -3'	Reverse
Tw3-*Hind*3-F	5' - GGAAGCTTATGTGCAAGGTCGATGGGACAA -3'	Forward
Tw3-*Xba*1-R	5' - TTCTAGACTAGAGCTTTTTGGCCGCACGC -3'	Reverse
TD12d-up-F	5' - AGTCAGCCCAGGCACCGATGACG -3'	Forward
TD12d-up-R	5' - AGCCAGAGCTAGATCTCTTGTGCTCCTTTTCAATCCTTT -3'	Reverse
TD12d-down-F	5' - GGAGCACAAGAGATCTAGCTCTGGCTCAAGGGACACCGT-3'	Forward
TD12d-down-R	5' - CACAGAAACTGCCTTCACGGGTCT -3'	Reverse
Bla-s-F1	5' - CAGCGTCGCCAGCGCAGCTCTC -3'	Forward
Bla-s-R1	5' - CTGCCGTCGGCTGTCCATCACT -3'	Reverse
Hyg-Knock-F	5' - TGCGATCGCTGCGGCCGATCTTAG -3'	Forward
Hyg-Knock-R	5' - TGTTATGCGGCCATTGTCCGTCAG -3'	Reverse
KO up-probe-F1	5' - GGGGTCGGCCGGTGCAGCCTTAG -3'	Forward
KO up-probe-R1	5' - GGCGGTCAGCGATCGGTCGGACTC -3'	Reverse
KO down-probe-F3	5' - GCTTGCGGCTCCTGTTGGGTGAC -3'	Forward
KO down-probe-R3	5' - ACGCCTGGCTGCCCACCATAAAC -3'	Reverse
Ub-pro-F1	5' - TCGGTACCCGTTAGAACGCGTAATACGAC -3'	Forward
ub pro-Tw3-F	5' - GCAACACTAGCCAACATGTGCAAGGTCGATGGGAC -3'	Forward
ub pro-Tw3-R	5' - ATCGACCTTGCACATGTTGGCTAGTGTTGCTTAGG -3'	Reverse
ub term-Tw3-F	5' - GCCAAAAAGCTCTAGAACTAAGCTATCTGTAGTAT -3'	Forward
ub term-Tw3-R	5' - ACAGATAGCTTAGTTCTAGAGCTTTTTGGCCGCAC -3'	Reverse
Ub-term-R2	5' - TCGGTACCACCGCGTAATACGACTCACTATAGGGAGACTGCAGTT -3'	Reverse
2F	5' - GGTTTCCGTAGTGAACCTGCAATTCAAAAAAAGCCGTTACTCACAT -3'	Forward
3F	5' - CAGCGGCAAAGGAAGGCTAGATGATTGAACAGGACGGCCTTCACGC -3'	Forward
4R	5' - GCGCATAGCCGGCGCGGATCTCAAAAGAACTCGTCCAGGAGGCGGT -3'	Reverse
pUC18-R	5' - AACAGCTATGACCATGATTACGAATTCGAGCTCGG -3'	Reverse
Hyg-F	5' - ATGAAAAAGCCTGAACTCACCGCGAC -3'	Forward
Hyg-R	5' - CTATTCCTTTGCCCTCGGACGAGTG -3'	Reverse
Bla-F	5' - ATGGCCAAGCCTTTGTCTCAAGAAGAA -3'	Forward
Bla-R	5' - TTAGCCCTCCCACACATAACCAGAGGGCAG -3'	Reverse
TD12d-probe-F1	5' - GGCACCGTGGCGACCGGGGTCTG -3'	Forward
TD12d-probe-R1	5' - TGCGGGGCGTCCTGGTCGGTGTG -3'	Reverse

Tw3-*Hind*3-F and Tw3-*Xba*1-R include *Hin*d III and *Xba* I sites, respectively (underlined).

TD12d-up-R and TD12d-down-F each include a *Bgl* II site (underlined).

Up-pro-F1 and Ub-term-R2 each include a *Kpn* I site (underlined).

Table 3-2.

The fatty acid contents (μg/g DCW) of the wild-type strain and the *tauΔ12des*-disruption mutants. The means ± SD. values based on three replicates are indicated (n = 3).

Fatty acid	Wild type	1st-allele KO	1st/2nd-allele KO
14:0	1.35 ± 0.179	1.44 ± 0.122	2.52 ± 0.308
15:0	63.0 ± 4.58	66.2 ± 5.25	78.9 ± 10.6
16:0	29.0 ± 4.16	32.1 ± 3.08	47.4 ± 10.5
17:0	81.8 ± 8.89	87.5 ± 9.39	87.0 ± 9.70
$17:1^{\Delta 9}$	11.8 ± 0.573	17.9 ± 2.77	36.3 ± 4.46
18:0	11.5 ± 1.41	10.9 ± 0.756	10.3 ± 0.930
$18:1^{\Delta 9}$	3.50 ± 0.272	7.61 ± 0.865	76.5 ± 2.14
$18:1^{\Delta 11}$	6.09 ± 0.594	7.01 ± 1.16	6.01 ± 1.69
$18:2^{\Delta 9,12}$	4.50 ± 0.492	4.35 ± 0.260	N.D.
19:0	8.02 ± 0.775	8.11 ± 0.799	8.35 ± 0.961
$19:1^{\Delta 9}$	4.20 ± 0.162	6.19 ± 0.665	13.8 ± 5.35
$20:4^{\Delta 5,8,11,14}$	8.37 ± 0.488	8.77 ± 0.491	0.226 ± 0.391
$20:5^{\Delta 5,8,11,14,17}$	18.5 ± 1.14	20.6 ± 0.945	15.4 ± 0.713
$22:4^{\Delta 7,10,13,16}$	6.15 ± 0.793	5.90 ± 0.519	N.D.
$22:5^{\Delta 4,7,10,13,16}$	20.3 ± 1.25	21.2 ± 1.26	15.3 ± 0.374
$22:5^{\Delta 7,10,13,16,19}$	6.26 ± 0.801	6.54 ± 0.588	2.67 ± 0.516
$22:6^{\Delta 4,7,10,13,16,19}$	104 ± 6.79	114 ± 6.23	135 ± 30.4

N. D., Not Detected; indicates values below the limit of detection.

Table 3-3.

The fatty acid contents (μg/g lipid) in each lipid fraction of the wild-type strain and the *tauΔ12des*-disruption mutants. The means ± SD. values based on three replicates are indicated (n = 3).

	Neutral lipid fraction		Glycolipid fraction		Phospholipid fraction	
Fatty acid	Wild type	1st/2nd-allele KO	Wild type	1st/2nd-allele KO	Wild type	1st/2nd-allele KO
14:0	2.31 ± 2.04	6.48 ± 2.02	N.D.	0.540 ± 0.940	N.D.	N.D.
15:0	189 ± 89.0	235 ± 46.0	36.7 ± 21.2	22.5 ± 4.77	124 ± 15.0	116 ± 11.2
16:0	60.5 ± 27.6	74.9 ± 16.2	15.5 ± 8.72	10.0 ± 3.48	68.0 ± 5.23	53.0 ± 9.99
17:0	346 ± 114	251 ± 34.4	47.6 ± 21.6	18.7 ± 6.66	162 ± 10.2	91.5 ± 7.94
$17:1^{\Delta9}$	33.0 ± 18.2	137 ± 76.4	2.81 ± 0.700	15.0 ± 5.53	7.70 ± 1.64	82.7 ± 18.1
18:0	31.0 ± 20.1	30.0 ± 18.8	4.55 ± 4.40	1.78 ± 1.64	5.88 ± 1.22	N.D.
$18:1^{\Delta9}$	5.93 ± 3.12	322 ± 82.1	N.D.	26.5 ± 15.0	N.D.	96.6 ± 65.4
$18:1^{\Delta11}$	4.00 ± 4.66	3.93 ± 3.41	6.39 ± 3.66	6.66 ± 2.69	10.1 ± 8.92	10.3 ± 7.03
$18:2^{\Delta9,12}$	8.47 ± 5.18	N.D.	N.D.	N.D.	1.34 ± 2.31	N.D.
19:0	29.5 ± 12.6	25.8 ± 8.95	2.47 ± 2.57	N.D.	N.D.	N.D.
$19:1^{\Delta9}$	9.25 ± 4.72	58.9 ± 15.4	N.D.	3.13 ± 1.12	N.D.	26.3 ± 18.3
$20:4^{\Delta5,8,11,14}$	7.44 ± 5.02	N.D.	6.24 ± 3.49	N.D.	26.9 ± 13.8	1.85 ± 1.62
$20:5^{\Delta5,8,11,14,17}$	24.9 ± 11.1	7.30 ± 0.795	38.2 ± 6.42	17.2 ± 2.89	163 ± 18.6	99.5 ± 16.7
$22:4^{\Delta7,10,13,16}$	8.37 ± 4.24	N.D.	N.D.	N.D.	1.22 ± 2.11	N.D.
$22:5^{\Delta4,7,10,13,16}$	20.4 ± 7.57	10.5 ± 3.86	10.8 ± 3.52	8.46 ± 3.44	120 ± 19.1	72.6 ± 5.88
$22:5^{\Delta7,10,13,16,19}$	18.1 ± 5.15	2.72 ± 2.73	3.01 ± 0.490	0.71 ± 1.23	13.6 ± 0.830	5.19 ± 0.550
$22:6^{\Delta4,7,10,13,16,19}$	132 ± 41.9	82.1 ± 23.0	34.4 ± 11.4	28.0 ± 12.5	705 ± 59.8	702 ± 62.0

N. D., Not Detected; indicates values below the limit of detection.

Table 3-4.

The fatty acid contents (μg/g DCW) of the KO/*neo*^{r} (the 1st/2nd-allele KO + *neo*^{r}) and the revertants (the Neo^r/TauΔ12des transformants). The means ± SD. values based on three replicates are indicated (n = 3).

Fatty acid	KO/*neo*^{r}	revertant
14:0	1.71 ± 0.236	2.50 ± 1.68
15:0	40.2 ± 3.55	56.3 ± 22.4
16:0	49.1 ± 8.27	47.2 ± 8.38
17:0	32.1 ± 2.65	38.1 ± 9.73
17:1$^{\Delta 9}$	14.5 ± 0.873	12.1 ± 10.4
18:0	5.36 ± 1.11	5.29 ± 0.581
18:1$^{\Delta 9}$	50.2 ± 6.41	9.72 ± 7.84
18:1$^{\Delta 11}$	5.72 ± 0.616	4.31 ± 1.97
18:2$^{\Delta 9,12}$	N.D.	1.96 ± 1.16
19:0	2.14 ± 0.302	2.30 ± 0.723
19:1$^{\Delta 9}$	4.49 ± 1.01	3.38 ± 2.92
20:4$^{\Delta 5,8,11,14}$	0.384 ± 0.247	7.11 ± 0.509
20:5$^{\Delta 5,8,11,14,17}$	11.0 ± 1.50	21.7 ± 2.05
22:4$^{\Delta 7,10,13,16}$	N.D.	3.02 ± 0.144
22:5$^{\Delta 4,7,10,13,16}$	13.7 ± 0.556	20.5 ± 2.15
22:5$^{\Delta 7,10,13,16,19}$	1.59 ± 0.274	3.08 ± 0.423
22:6$^{\Delta 4,7,10,13,16,19}$	138 ± 3.87	114 ± 17.8

N. D., Not Detected; indicates values below the limit of detection.

Table 3-5.

The abbreviations for the desaturase genes described in this chapter.

MroΔ12des	*M. rouxii* Δ12-fatty acid desaturase
RorΔ12des	*R. oryzae* Δ12-fatty acid desaturase
MalΔ12des	*M. alpina* Δ12-fatty acid desaturase
CciΔ12/15des	*C. cinerea* Δ12/Δ15-fatty acid desaturase
EniΔ12des	*E. nidulans* Δ12-fatty acid desaturase
AorΔ12des	*A. oryzae* Δ12-fatty acid desaturase
CpuΔ12des	*C. purpurea* Δ12-fatty acid desaturase
LklΔ12des	*L. kluyveri* Δ12-fatty acid desaturase
GmoΔ12/15des	*G. moniliformis* Δ12/Δ15-fatty acid desaturase
TbrΔ12des	*T. brucei* Δ12-fatty acid desaturase
SdiΔ12des	*S. diclina* Δ12-fatty acid desaturase
PpyΔ12des	*P. pyriformis* Δ12-fatty acid desaturase
CofΔ12des	*C. officinalis* Δ12-fatty acid desaturase
VgaΔ12des	*V. galamensis* Δ12-fatty acid desaturase
SolΔ12des	*S. oleracea* Δ12-fatty acid desaturase
PcrΔ12des	*P. crispum* Δ12-fatty acid desaturase
RcoΔ12des	*R. communis* Δ12-fatty acid desaturase
GmER2Δ12des	*G. max* ER isozyme2 Δ12-fatty acid desaturase
AtERΔ12des	*A. thaliana* ER Δ12-fatty acid desaturase
PamΔ12des	*P. americana* Δ12-fatty acid desaturase
NtaΔ12des	*N. tabacum* Δ12-fatty acid desaturase
CalΔ12des	*C. alpina* Δ12-fatty acid desaturase
DsiΔ12des	*D. sinuata* Δ12-fatty acid desaturase
AhyΔ12des	*A. hypogaea* Δ12-fatty acid desaturase
GmER1Δ12des	*G. max* ER isozyme1 Δ12-fatty acid desaturase
TkiΔ12des	*T. kirilowii* Δ12-fatty acid desaturase
ZmaΔ12des	*Z. mays* Δ12-fatty acid desaturase
CvuΔ12des	*C. vulgaris* Δ12-fatty acid desaturase
AcaΔ12/15des	*A. castellanii* Δ12/Δ15-fatty acid desaturase
GmChΔ12des	*G. max* chloroplast precursor Δ12-fatty acid desaturase
AtChΔ12des	*A. thaliana* chloroplast Δ12-fatty acid desaturase
SspΔ12des	*Synechocystis* sp. Δ12-fatty acid desaturase
PtrΔ12des	*P. tricornutum* Δ12-fatty acid desaturase

GENERAL DISCUSSION

Genetic engineering of thraustochytrids for industrial applications

A number of studies have revealed PUFAs to have nutraceutical and pharmaceutical effects as membrane components, signaling molecules and gene regulatory factors. Demand for PUFAs is constantly increasing, and current sources are inadequate. Therefore, alternative sustainable sources are required. One promising approach to this problem is the genetic engineering of plants or microorganisms for selective production of beneficial PUFAs. Genes encoding desaturases and elongases, associated with PUFA biosynthesis, have been cloned and then reconstitution of the biosynthetic pathway has been attempted in plants and microbes. For example, Robert *et al* generated a transgenic *Arabidopsis thaliana* to produce DHA through transformation with a set of fatty acid desaturases and elongases. Thraustochytrids are potential candidates for a commercial source of PUFAs, because of their ability to possess prominent lipid droplets in which large amounts of PUFAs are accumulated. Over the past decade, many efforts have focused on the screening of thraustochytrids suitable for PUFA production and the investigation of optimal conditions for the production of PUFAs. However, information about gene manipulation in thraustochytrids is still lacking. As described in CHAPTER 1 and 2, the author developed a transformation system for heterologous gene expression in thraustochytrids. The Δ12-fatty acid desaturase (PpDes12)-expressing *A. limacinum* mh0186 were found to convert exogenously added OA ($C18:1^{\Delta 9}$) into LA ($C18:2^{\Delta 9,\ 12}$). Moreover, as described in CHAPTER 3, the author successfully disrupted the gene encoding a

Δ12-fatty acid desaturase (TauΔ12des) in *Thraustochytrium aureum* ATCC 34304 by homologous recombination driven with the transformation system, leading to the accumulation of OA which is a substrate for the Δ12-fatty acid desaturase. In addition, this system was applied to *A. limacinum* mh0186 to express a Δ5-fatty acid desaturase gene from *T. aureum* ATCC 34304 (23). The transformants harboring the Δ5-fatty acid desaturase gene converted exogenously added DGLA ($C20:3^{\Delta 8, 11, 14}$) and ETA ($C20:4^{\Delta 8, 11, 14, 17}$) into ARA ($C20:4^{\Delta 5, 8, 11, 14}$) and EPA ($C20:5^{\Delta 5, 8, 11, 14, 17}$), respectively. These results indicate that this transformation system makes it possible to perform the molecular breeding of thraustochytrids for selective production of PUFAs. The next step is to enhance the conversion rate of each reaction and increase the yield of PUFAs to economically viable levels in thraustochytrids.

The biosynthetic pathway for PUFA production in thraustochytrids

A growing body of evidence suggests that two distinct pathways exist in thraustochytrids, *i.e.*, the PUFA synthase pathway and the standard pathway. The genes involved in the PUFA synthase pathway were first cloned from *Schizochytrium* sp. and functionally expressed in *E. coli* by Metz *et al* (25, 65). Huang *et al* has also reported the enzymes associated with the PUFA synthase pathway in *Schizochytrium* sp. FJU-512 (24). Moreover, Lippmeier *et al* proposed that the PUFA synthase pathway is the sole pathway for PUFA biosynthesis in *Schizochytrium* sp., although enzymes involved in the standard pathway partially exist in the thraustochytrid (26). Because of the lack of a Δ12-fatty acid desaturase, *Schizochytrium* sp. is not able to synthesize PUFAs through the standard pathway using saturated fatty acids produced from the FAS

system. As shown in CHAPTER 2, *A. limacinum* mh0186 transformants harboring the Δ12-fatty acid desaturase gene could convert the exogenously added OA into LA but the wild-type mh0186 strain could not. This result indicates that the standard pathway is not working in *A. limacinum* mh0186.

The gene encoding FAS was cloned from *Schizochytrium* sp. (106). The FAS system of *Schizochytrium* sp. consists of a single large protein, resembling a fusion of fungal FAS α and β subunits. The independence of the PUFA synthase pathway from the FAS system was confirmed by Metz *et al* through the disruption of the FAS gene (25). For PUFA production, the standard pathway utilizes saturated fatty acids, synthesized by the FAS system. In the standard pathway, saturated fatty acids are converted into PUFAs by a set of desaturases and elongases. Genes encoding desaturases or elongases have also been identified in thraustochytrids. Qiu *et al* have cloned the Δ4- and Δ5-fatty acid desaturases from *Thraustochytrium* sp. (17). Δ4- and Δ5-fatty acid desaturases have also been cloned from several thraustochytrids and characterized in yeasts and thraustochytrids (18-21). Elongase genes have been identified in *Thraustochytrium* sp. FJN-10 and *T. aureum* (18, 20, 107). However, several key enzymes in the standard pathway, such as Δ12- and Δ15-fatty acid desaturases, have not been identified in thraustochytrids and thus it is still not clear whether the standard pathway actually function in thraustocytrids. In addition, it is worth noting that the genes involved in the PUFA synthase pathway have been identified in *Aurantiochytrium* but not *Thraustochytrium*. As described in CHAPTER 3, the Δ12-fatty acid desaturase (TauΔ12des) gene from *T. aureum* ATCC 34304 was cloned, expressed in yeasts and characterized. The *tauΔ12des*-disruption mutants exhibited the accumulation of the substrate OA and a marked reduction in the amount of

the product LA and its downstream PUFAs. However, the contents of DHA did not decrease in the mutants. These results indicate that the standard pathway as well as the PUFA synthase pathway is responsible for the *de novo* synthesis of PUFAs in *T. aureum* ATCC 34304, however, the production of DHA largely depends on the PUFA synthase pathway. Moreover, EDA (C20:2$^{\Delta 11,\ 14}$) was detected by GC-MS in the wild-type strain of *T. aureum* (Fig. gd-1), suggesting the presence of the Δ8-fatty acid desaturase.

Taken together, it is suggested that *Aurantiochytrium* produces PUFA via the PUFA synthase pathway, while *Thraustochytrium* produces PUFA via both the PUFA synthase and standard pathways. It has been proposed that ancestral thraustochytrids acquired the genes involved in the PUFA synthase pathway from a marine bacterium by horizontal gene transfer. The enzymes involved in the standard pathway would have been partially lost under selective pressure, because 18-carbon PUFAs are easily obtained from organic matter such as decaying leaves. Further study will be required to completely elucidate the pathway for PUFA production, and the evolutional and functional relationships between the two pathways in thraustochytrids.

The biological functions of PUFAs in thraustochytrids

PUFAs are essential components of cell membranes, maintaining membrane fluidity, and precursors for a number of biologically active molecules like eicosanoids. It was also demonstrated that *Shewanella livingstonensis* Ac10, an EPA-producing marine bacterium, requires EPA for normal membrane organization, cell division and growth at 4°C but not 18°C. However, very little is known about the physiological functions of PUFAs in thraustochytrids. Raghukumar *et al* showed that disruption of the

FAS-encoding gene resulted in the death of *Schizochytrium* sp. ATCC 20888, suggesting that saturated fatty acids are essencial for cell growth in thraustochytrids (25). On the other hand, Lippmeier *et al* demonstrated that PUFA-synthase deficient mutants required exogenously added PUFAs for the growth of *Schizochytrium* sp., while auxotrophs were able to grow in medium supplemented with PUFAs such as C18:4 n-6 which is less complex than DHA (C22:6 n-3) and DPA (C22:5 n-6) (26). This result may indicate that PUFAs are essential nutrients for the growth of thraustochytrids but highly unsaturated fatty acids, which possess more than 3 double bonds with more than 20 carbons, are not always necessary nutrients for the survival of thraustochytrids. As described in CHAPTER 3, no significant changes in growth or morphology were observed in the *tauΔ12des*-disruption mutants of *T. aureum* ATCC 34304. This result suggests that *T. aureum* could grow under normal conditions without the standard pathway, because it synthesizes DHA via the PUFA synthase pathway. Further studies will be required to elucidate the detailed physiological roles of PUFAs in thraustochytrids.

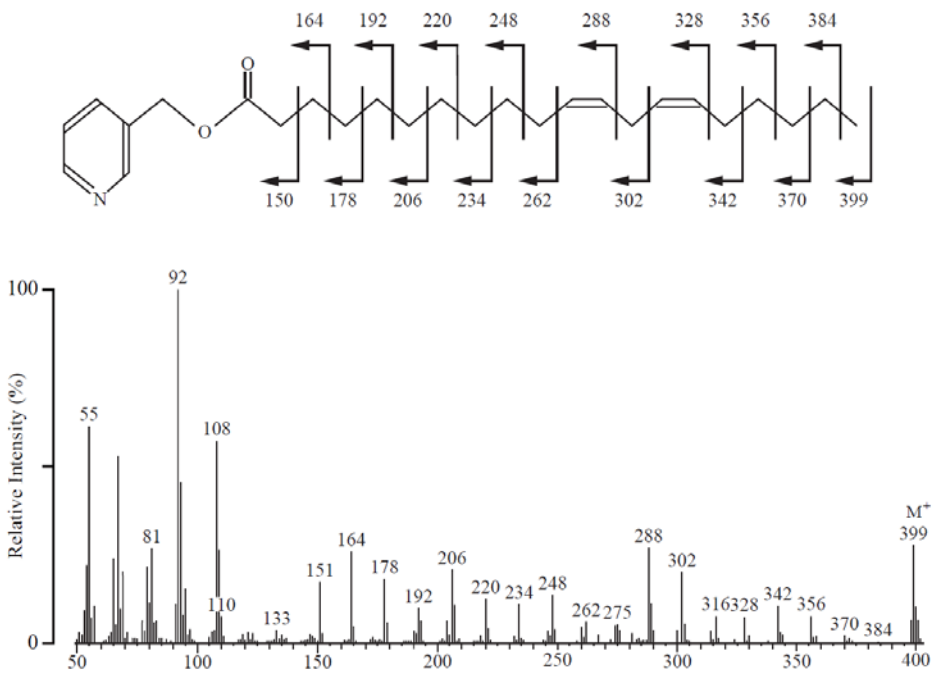

Fig. gd-1. The mass spectrum of the peak corresponding to the retention time of EDA in the wild-type *T. aureum*.

REFERENCES

(1) Tsui, C. K., W. Marshall, R. Yokoyama, D. Honda, J. C. Lippmeier, K. D. Craven, P. D. Peterson, and M. L. Berbee. 2009. *Labyrinthulomycetes* phylogeny and its implications for the evolutionary loss of chloroplasts and gain of ectoplasmic gliding. *Mol. Phylogenet. Evol.* **50:** 129-140.

(2) Yokoyama, R., D. Honda. 2007. Taxonomic rearrangement of the genus *Schizochytrium* sensu lato based on morphology, chemotaxonomic characteristics, and 18S rRNA gene phylogeny (*Thraustochytriaceae*, *Labyrinthulomycetes*): emendation for *Schizochytrium* and erection of *Aurantiochytrium* and *Oblongichytrium* gen. nov. *Mycoscience* **48:** 199-211.

(3) Fan, K. W., L. L. Vrijmoed, and E. B. Jones. 2002. Zoospore chemotaxis of mangrove thraustochytrids from Hong Kong. *Mycologia* **94:** 569-578.

(4) Taoka, Y., N. Nagano, Y. Okita, H. Izumida, S. Sugimoto, and M. Hayashi. 2009. Extracellular enzymes produced by marine eukaryotes, thraustochytrids. *Biosci. Biotechnol. Biochem.* **73:** 180-182.

(5) Anderson, R. S., B. S. Kraus, S. E. McGladdery, K. S. Reece, and N. A. Stokes. 2003. A thraustochytrid protist isolated from *Mercenaria mercenaria*: molecular characterization and host defense responses. *Fish Shellfish Immunol.* **15:** 183-194.

(6) Qian, H., Q. Liu, B. Allam, and J. L. Collier. 2007. Molecular genetic variation within and among isolates of QPX (Thraustochytridae), a parasite of the hard clam *Mercenaria mercenaria*. *Dis. Aquat. Organ.* **77:** 159-168.

(7) Harel, M., E. Ben-Dov, D. Rasoulouniriana, N. Siboni, E. Kramarsky-Winter, Y. Loya, Z. Barak, Z. Wiesman, and A. Kushmaro. 2008. A new Thraustochytrid, strain Fng1, isolated from the surface mucus of the hermatypic coral *Fungia granulosa*. *FEMS Microbiol. Ecol.* **64:** 378-387.

(8) Dykova, I., I. Fiala, H. Dvorakova, and H. Peckova. 2008. Living together: the marine amoeba *Thecamoeba hilla* Schaeffer, 1926 and its endosymbiont *Labyrinthula* sp. *Eur. J. Protistol.* **44:** 308-316.

(9) Lewis, T. E., P. D. Nichols, and T. A. McMeekin. 2001. Sterol and squalene content of a docosahexaenoic-acid-producing thraustochytrid: influence of culture age, temperature, and dissolved oxygen. *Mar. Biotechnol. (NY)* **3:** 439-447.

(10) Armenta, R. E., A. Burja, H. Radianingtyas, and C. J. Barrow. 2006. Critical assessment of various techniques for the extraction of carotenoids and co-enzyme Q10 from the Thraustochytrid strain ONC-T18. *J. Agric. Food Chem.* **54:** 9752-9758.

(11) Chen, G., K. W. Fan, F. P. Lu, Q. Li, T. Aki, F. Chen, and Y. Jiang. 2010. Optimization of nitrogen source for enhanced production of squalene from thraustochytrid *Aurantiochytrium* sp. *New Biotechnol.* **27:** 382-389.

(12) Jakobsen, A. N., I. M. Aasen, K. D. Josefsen, and A. R. Strom. 2008. Accumulation of docosahexaenoic acid-rich lipid in thraustochytrid *Aurantiochytrium* sp. strain T66: effects of N and P starvation and O_2 limitation. *Appl. Microbiol. Biotechnol.* **80:** 297-306.

(13) Chi, Z., Y. Liu, C. Frear, and S. Chen. 2009. Study of a two-stage growth of DHA-producing marine algae *Schizochytrium limacinum* SR21 with shifting dissolved oxygen level. *Appl. Microbiol. Biotechnol.* **81:** 1141-1148.

(14) Nagano, N., Y. Taoka, D. Honda, and M. Hayashi. 2009. Optimization of culture conditions for growth and docosahexaenoic acid production by a marine thraustochytrid, *Aurantiochytrium limacinum* mh0186. *J. Oleo Sci.* **58:** 623-628.

(15) Ren, L. J., X. J. Ji, H. Huang, L. Qu, Y. Feng, Q. Q. Tong, and P. K. Ouyang. 2010. Development of a stepwise aeration control strategy for efficient docosahexaenoic acid production by *Schizochytrium* sp. *Appl. Microbiol. Biotechnol.* **87:** 1649-1656.

(16) Zeng, Y., X. J. Ji, M. Lian, L. J. Ren, L. J. Jin, P. K. Ouyang, and H. Huang. 2011. Development of a temperature shift strategy for efficient docosahexaenoic acid production by a marine fungoid protist, *Schizochytrium* sp. HX-308. *Appl. Biochem. Biotechnol.* **164:** 249-255.

(17) Qiu, X., H. Hong, and S. L. MacKenzie. 2001. Identification of a Delta 4 fatty acid

desaturase from *Thraustochytrium* sp. involved in the biosynthesis of docosahexanoic acid by heterologous expression in *Saccharomyces cerevisiae* and *Brassica juncea*. *J. Biol. Chem.* **276:** 31561-31566.

(18) Lee J. C., P. Anbu, W. H. Kim, M. J. Noh, S. J. Lee, J. W. Seo and B. K. Hur. 2008. Identification of Δ9-elongation activity from *Thraustochytrium aureum* by heterologous expression in *Pichia pastoris*. *Biotechnol. Bioprocess Engineer.* **13**: 524-532.

(19) Kumon, Y., Y. Kamisaka, N. Tomita, K. Kimura, H. Uemura, T. Yokochi, R. Yokoyama, and D. Honda. 2008. Isolation and characterization of a Delta5-desaturase from *Oblongichytrium* sp. *Biosci. Biotechnol. Biochem.* **72:** 2224-2227.

(20) Kang, D. H., P. Anbu, W. H. Kim, B. K. Hur. 2008. Coexpression of elo-like enzyme and Delta 5, Delta 4-desaturases derived from *Thraustochytrium aureum* ATCC 34304 and the production of DHA and DPA in *Pichia pastoris*. *Biotechnol. Bioprocess Eng.* **13:** 483-490.

(21) Huang, J. Z., X. Z. Jiang, X. F. Xia, A. Q. Yu, R. Y. Mao, X. F. Chen, and B. Y. Tian. 2011. Cloning and functional identification of delta5 fatty acid desaturase gene and its 5'-upstream region from marine fungus *Thraustochytrium* sp. FJN-10. *Mar. Biotechnol. (NY)* **13:** 12-21.

(22) Nagano, N., K. Sakaguchi, Y. Taoka, Y. Okita, D. Honda, M. Ito, and M. Hayashi. 2011. Detection of genes involved in fatty acid elongation and desaturation in

thraustochytrid marine eukaryotes. *J. Oleo Sci.* **60:** 475-481.

(23) Kobayashi, T., K. Sakaguchi, T. Matsuda, E. Abe, Y. Hama, M. Hayashi, D. Honda, Y. Okita, S. Sugimoto, N. Okino, and M. Ito. 2011. Increase of eicosapentaenoic acid in thraustochytrids through thraustochytrid ubiquitin promoter-driven expression of a fatty acid {delta}5 desaturase gene. *Appl. Environ. Microbiol.* **77:** 3870-3876.

(24) Huang, J., X. Jiang, X. Zhang, W. Chen, B. Tian, Z. Shu, and S. Hu. 2008. Expressed sequence tag analysis of marine fungus *Schizochytrium* producing docosahexaenoic acid. *J. Biotechnol.* **138:** 9-16.

(25) Metz, J. G., J. Kuner, B. Rosenzweig, J. C. Lippmeier, P. Roessler, and R. Zirkle. 2009. Biochemical characterization of polyunsaturated fatty acid synthesis in *Schizochytrium*: release of the products as free fatty acids. *Plant Physiol. Biochem.* **47:** 472-478.

(26) Lippmeier, J. C., K. S. Crawford, C. B. Owen, A. A. Rivas, J. G. Metz, and K. E. Apt. 2009. Characterization of both polyunsaturated fatty acid biosynthetic pathways in *Schizochytrium* sp. *Lipids* **44:** 621-630.

(27) Kawachi, M. 2002. *Pinguiochrysis pyriformis* gen. et sp. nov. (*Pinguiophyceae*), a new picoplanktonic alga isolated from the Pacific Ocean. *Phycological research* **50:** 49-56.

(28) Kawachi, M. 2002. The *Pinguiophyceae* classis nova, a new class of photosynthetic stramenopiles whose members produce large amounts of omega-3 fatty acids. *Phycol. Res.* **50:** 31-47.

(29) Hsiao, T. Y., H. W. Blanch. 2006. Physiological studies of eicosapentaenoic acid production in the marine microalga *Glossomastix chrysoplasta*. *Biotechnol. Bioeng.* **93:** 465-475.

(30) Metz, J. G., P. Roessler, D. Facciotti, C. Levering, F. Dittrich, M. Lassner, R. Valentine, K. Lardizabal, F. Domergue, A. Yamada, K. Yazawa, V. Knauf, and J. Browse. 2001. Production of polyunsaturated fatty acids by polyketide synthases in both prokaryotes and eukaryotes. *Science* **293:** 290-293.

(31) Kaulmann, U., C. Hertweck. 2002. Biosynthesis of polyunsaturated fatty acids by polyketide synthases. *Angew. Chem. Int. Ed Engl.* **41:** 1866-1869.

(32) Okuyama, H., Y. Orikasa, T. Nishida, K. Watanabe, and N. Morita. 2007. Bacterial genes responsible for the biosynthesis of eicosapentaenoic and docosahexaenoic acids and their heterologous expression. *Appl. Environ. Microbiol.* **73:** 665-670.

(33) Lee, S. J., P. S. Seo, C. H. Kim, O. Kwon, B. K. Hur, and J. W. Seo. 2009. Isolation and characterization of the eicosapentaenoic acid biosynthesis gene cluster from *Shewanella* sp. BR-2. *J. Microbiol. Biotechnol.* **19:** 881-887.

(34) Shulse, C. N., E. E. Allen. 2011. Widespread occurrence of secondary lipid biosynthesis potential in microbial lineages. *PLoS One* **6:** e20146.

(35) Harizi, H., J. B. Corcuff, and N. Gualde. 2008. Arachidonic-acid-derived eicosanoids: roles in biology and immunopathology. *Trends Mol. Med.* **14:** 461-469.

(36) Chang, P. K., R. A. Wilson, N. P. Keller, and T. E. Cleveland. 2004. Deletion of the Delta12-oleic acid desaturase gene of a nonaflatoxigenic *Aspergillus parasiticus* field isolate affects conidiation and sclerotial development. *J. Appl. Microbiol.* **97:** 1178-1184.

(37) Kawamoto, J., T. Kurihara, K. Yamamoto, M. Nagayasu, Y. Tani, H. Mihara, M. Hosokawa, T. Baba, S. B. Sato, and N. Esaki. 2009. Eicosapentaenoic acid plays a beneficial role in membrane organization and cell division of a cold-adapted bacterium, *Shewanella livingstonensis* Ac10. *J. Bacteriol.* **191:** 632-640.

(38) Haeggstrom, J. Z., A. Rinaldo-Matthis, C. E. Wheelock, and A. Wetterholm. 2010. Advances in eicosanoid research, novel therapeutic implications. *Biochem. Biophys. Res. Commun.* **396:** 135-139.

(39) Levy, B. D. 2010. Resolvins and protectins: natural pharmacophores for resolution biology. *Prostaglandins Leukot. Essent. Fatty Acids* **82:** 327-332.

(40) Berquin, I. M., Y. Min, R. Wu, J. Wu, D. Perry, J. M. Cline, M. J. Thomas, T.

Thornburg, G. Kulik, A. Smith, I. J. Edwards, R. D'Agostino, H. Zhang, H. Wu, J. X. Kang, and Y. Q. Chen. 2007. Modulation of prostate cancer genetic risk by omega-3 and omega-6 fatty acids. *J. Clin. Invest.* **117:** 1866-1875.

(41) Adkins, Y., D. S. Kelley. 2010. Mechanisms underlying the cardioprotective effects of omega-3 polyunsaturated fatty acids. *J. Nutr. Biochem.* **21:** 781-792.

(42) Palacios-Pelaez, R., W. J. Lukiw, and N. G. Bazan. 2010. Omega-3 essential fatty acids modulate initiation and progression of neurodegenerative disease. *Mol. Neurobiol.* **41:** 367-374.

(43) Wall, R., R. P. Ross, G. F. Fitzgerald, and C. Stanton. 2010. Fatty acids from fish: the anti-inflammatory potential of long-chain omega-3 fatty acids. *Nutr. Rev.* **68:** 280-289.

(44) Oh, D. Y., S. Talukdar, E. J. Bae, T. Imamura, H. Morinaga, W. Fan, P. Li, W. J. Lu, S. M. Watkins, and J. M. Olefsky. 2010. GPR120 is an omega-3 fatty acid receptor mediating potent anti-inflammatory and insulin-sensitizing effects. *Cell* **142:** 687-698.

(45) Uauy, R., D. R. Hoffman, P. Peirano, D. G. Birch, and E. E. Birch. 2001. Essential fatty acids in visual and brain development. *Lipids* **36:** 885-895.

(46) Davis-Bruno, K., M. S. Tassinari. 2011. Essential fatty acid supplementation of DHA and ARA and effects on neurodevelopment across animal species: a review of the

literature. *Birth Defects Res. B. Dev. Reprod. Toxicol.* **92:** 240-250.

(47) Mohammed, B. S., S. Sankarappa, M. Geiger, and H. Sprecher. 1995. Reevaluation of the pathway for the metabolism of 7,10,13, 16-docosatetraenoic acid to 4,7,10,13,16-docosapentaenoic acid in rat liver. *Arch. Biochem. Biophys.* **317:** 179-184.

(48) Sprecher, H., Q. Chen, and F. Q. Yin. 1999. Regulation of the biosynthesis of 22:5n-6 and 22:6n-3: a complex intracellular process. *Lipids* **34 Suppl:** S153-6.

(49) Sprecher, H. 2000. Metabolism of highly unsaturated n-3 and n-6 fatty acids. *Biochim. Biophys. Acta* **1486:** 219-231.

(50) Chu, F. L., E. D. Lund, E. Harvey, and R. Adlof. 2004. Arachidonic acid synthetic pathways of the oyster protozoan parasite, *Perkinsus marinus*: evidence for usage of a delta-8 pathway. *Mol. Biochem. Parasitol.* **133:** 45-51.

(51) Sayanova, O., R. Haslam, B. Qi, C. M. Lazarus, and J. A. Napier. 2006. The alternative pathway C20 Delta8-desaturase from the non-photosynthetic organism *Acanthamoeba castellanii* is an atypical cytochrome *b5*-fusion desaturase. *FEBS Lett.* **580:** 1946-1952.

(52) Pereira, S. L., A. E. Leonard, and P. Mukerji. 2003. Recent advances in the study of fatty acid desaturases from animals and lower eukaryotes. *Prostaglandins Leukot. Essent. Fatty Acids* **68:** 97-106.

(53) Lindqvist, Y., W. Huang, G. Schneider, and J. Shanklin. 1996. Crystal structure of delta9 stearoyl-acyl carrier protein desaturase from castor seed and its relationship to other di-iron proteins. *EMBO J.* **15:** 4081-4092.

(54) Shanklin, J., E. Whittle, and B. G. Fox. 1994. Eight histidine residues are catalytically essential in a membrane-associated iron enzyme, stearoyl-CoA desaturase, and are conserved in alkane hydroxylase and xylene monooxygenase. *Biochemistry* **33:** 12787-12794.

(55) Sakuradani, E., T. Abe, K. Iguchi, and S. Shimizu. 2005. A novel fungal omega3-desaturase with wide substrate specificity from arachidonic acid-producing *Mortierella alpina* 1S-4. *Appl. Microbiol. Biotechnol.* **66:** 648-654.

(56) Meesapyodsuk, D., D. W. Reed, P. S. Covello, and X. Qiu. 2007. Primary structure, regioselectivity, and evolution of the membrane-bound fatty acid desaturases of *Claviceps purpurea*. *J. Biol. Chem.* **282:** 20191-20199.

(57) Hoffmann, M., M. Wagner, A. Abbadi, M. Fulda, and I. Feussner. 2008. Metabolic engineering of omega3-very long chain polyunsaturated fatty acid production by an exclusively acyl-CoA-dependent pathway. *J. Biol. Chem.* **283:** 22352-22362.

(58) Meesapyodsuk, D., X. Qiu. 2011. The Front-end Desaturase: Structure, Function, Evolution and Biotechnological Use. *Lipids* in press.

(59) Wang, J., L. Yu, H. Wang, Y. Gao, J. P. Schrementi, R. K. Porter, D. A. Yurek, M. Kuo, C. S. Suen, G. Cao, J. S. Bean, R. F. Kauffman, and Y. Qian. 2008. Identification and characterization of hamster stearoyl-CoA desaturase isoforms. *Lipids* **43:** 197-205.

(60) Zhou, X. R., I. Horne, K. Damcevski, V. Haritos, A. Green, and S. Singh. 2008. Isolation and functional characterization of two independently-evolved fatty acid Delta12-desaturase genes from insects. *Insect Mol. Biol.* **17:** 667-676.

(61) Jackson, F. M., T. C. Fraser, M. A. Smith, C. Lazarus, A. K. Stobart, and G. Griffiths. 1998. Biosynthesis of C18 polyunsaturated fatty acids in microsomal membrane preparations from the filamentous fungus *Mucor circinelloides. Eur. J. Biochem.* **252:** 513-519.

(62) Oura, T., S. Kajiwara. 2008. Disruption of the sphingolipid Delta8-desaturase gene causes a delay in morphological changes in *Candida albicans. Microbiology* **154:** 3795-3803.

(63) Jakobsson, A., R. Westerberg, and A. Jacobsson. 2006. Fatty acid elongases in mammals: their regulation and roles in metabolism. *Prog. Lipid Res.* **45:** 237-249.

(64) Millar, A. A., L. Kunst. 1997. Very-long-chain fatty acid biosynthesis is controlled through the expression and specificity of the condensing enzyme. *Plant J.* **12:** 121-131.

(65) Yazawa, K. 1996. Production of eicosapentaenoic acid from marine bacteria. *Lipids* **31 Suppl:** S297-300.

(66) Napier, J. A. 2002. Plumbing the depths of PUFA biosynthesis: a novel polyketide synthase-like pathway from marine organisms. *Trends Plant Sci.* **7:** 51-54.

(67) Qiu, X. 2003. Biosynthesis of docosahexaenoic acid (DHA, 22:6-4, 7,10,13,16,19): two distinct pathways. *Prostaglandins Leukot. Essent. Fatty Acids* **68:** 181-186.

(68) Alonso, D. L., F. G. Maroto. 2000. Plants as 'chemical factories' for the production of polyunsaturated fatty acids. *Biotechnol. Adv.* **18:** 481-497.

(69) Graham, I. A., T. Larson, and J. A. Napier. 2007. Rational metabolic engineering of transgenic plants for biosynthesis of omega-3 polyunsaturates. *Curr. Opin. Biotechnol.* **18:** 142-147.

(70) Errampalli, D., K. Leung, M. B. Cassidy, M. Kostrzynska, M. Blears, H. Lee, and J. T. Trevors. 1999. Applications of the green fluorescent protein as a molecular marker in environmental microorganisms. *J. Microbiol. Methods* **35:** 187-199.

(71) March, J. C., G. Rao, and W. E. Bentley. 2003. Biotechnological applications of green fluorescent protein. *Appl. Microbiol. Biotechnol.* **62:** 303-315.

(72) Rakosy-Tican, E., C. M. Aurori, C. Dijkstra, R. Thieme, A. Aurori, and M. R.

Davey. 2007. The usefulness of the gfp reporter gene for monitoring *Agrobacterium*-mediated transformation of potato dihaploid and tetraploid genotypes. *Plant Cell Rep.* **26:** 661-671.

(73) Taoka, Y., N. Nagano, Y. Okita, H. Izumida, S. Sugimoto, and M. Hayashi. 2009. Influences of culture temperature on the growth, lipid content and fatty acid composition of *Aurantiochytrium* sp. Strain mh0186. *Mar. Biotechnol. (NY)* **11:** 368-374.

(74) Huang, J., T. Aki, T. Yokochi, T. Nakahara, D. Honda, S. Kawamoto, S. Shigeta, K. Ono, and O. Suzuki. 2003. Grouping newly isolated docosahexaenoic acid-producing thraustochytrids based on their polyunsaturated fatty acid profiles and comparative analysis of 18S rRNA genes. *Mar. Biotechnol. (NY)* **5:** 450-457.

(75) Vrablik, M., M. Prusikova, M. Snejdrlova, and L. Zlatohlavek. 2009. Omega-3 fatty acids and cardiovascular disease risk: do we understand the relationship? *Physiol. Res.* **58 Suppl 1:** S19-26.

(76) von Schacky, C., W. S. Harris. 2007. Cardiovascular benefits of omega-3 fatty acids. *Cardiovasc. Res.* **73:** 310-315.

(77) Innis, S. M. 2008. Dietary omega 3 fatty acids and the developing brain. *Brain Res.* **1237:** 35-43.

(78) Lee, J. H., J. H. O'Keefe, C. J. Lavie, and W. S. Harris. 2009. Omega-3 fatty acids: cardiovascular benefits, sources and sustainability. *Nat. Rev. Cardiol.* **6:** 753-758.

(79) Sayanova, O. V., J. A. Napier. 2004. Eicosapentaenoic acid: biosynthetic routes and the potential for synthesis in transgenic plants. *Phytochemistry* **65:** 147-158.

(80) Raghukumar, S. 2008. Thraustochytrid Marine Protists: production of PUFAs and Other Emerging Technologies. *Mar. Biotechnol. (NY)* **10:** 631-640.

(81) Watanabe, M.M., M. Kawachi, M. Hiroki and F. Kasai. 2000 NIES-collection list of strains, Microalgae and protozoa, 6th ed. NIES, Japan.

(82) Bijli, K. M., B. P. Singh, S. Sridhara, and N. Arora. 2001. Isolation of total RNA from pollens. *Prep. Biochem. Biotechnol.* **31:** 155-162.

(83) Chen, D. C., B. C. Yang, and T. T. Kuo. 1992. One-step transformation of yeast in stationary phase. *Curr. Genet.* **21:** 83-84.

(84) Nakamura, Y., T. Gojobori, and T. Ikemura. 2000. Codon usage tabulated from international DNA sequence databases: status for the year 2000. *Nucleic Acids Res.* **28:** 292.

(85) Abe, E., Y. Hayashi, Y. Hama, M. Hayashi, M. Inagaki, and M. Ito. 2006. A novel phosphatidylcholine which contains pentadecanoic acid at sn-1 and docosahexaenoic

acid at sn-2 in *Schizochytrium* sp. F26-b. *J. Biochem.* **140:** 247-253.

(86) Dubois, N., C. Barthomeuf and J. P. Berge. 2006. Convenient preparation of picolinyl derivatives from fatty acid esters. *Eur. J. Lipid Sci. Technol.* **108**: 28-32.

(87) Sakuradani, E., M. Kobayashi, T. Ashikari, and S. Shimizu. 1999. Identification of Δ12-fatty acid desaturase from arachidonic acid-producing *Mortierella* fungus by heterologous expression in the yeast *Saccharomyces cerevisiae* and the fungus *Aspergillus oryzae*. *Eur. J. Biochem.* **261:** 812-820.

(88) Passorn, S., K. Laoteng, S. Rachadawong, M. Tanticharoen, and S. Cheevadhanarak. 1999. Heterologous expression of *Mucor rouxii* delta(12)-desaturase gene in *Saccharomyces cerevisiae*. *Biochem. Biophys. Res. Commun.* **263:** 47-51.

(89) Wei, D., M. Li, X. Zhang, Y. Ren, and L. Xing. 2004. Identification and characterization of a novel Δ12-fatty acid desaturase gene from *Rhizopus arrhizus*. *FEBS Lett.* **573:** 45-50.

(90) Pereira, S. L., Y. S. Huang, E. G. Bobik, A. J. Kinney, K. L. Stecca, J. C. Packer, and P. Mukerji. 2004. A novel omega3-fatty acid desaturase involved in the biosynthesis of eicosapentaenoic acid. *Biochem. J.* **378:** 665-671.

(91) Petrini, G. A., S. G. Altabe, and A. D. Uttaro. 2004. *Trypanosoma brucei* oleate desaturase may use a cytochrome *b5*-like domain in another desaturase as an electron

donor. *Eur. J. Biochem.* **271:** 1079-1086.

(92) Felsenstein, J. 1996. Inferring phylogenies from protein sequences by parsimony, distance, and likelihood methods. *Methods Enzymol.* **266:** 418-427.

(93) Orikasa, Y., A. Yamada, R. Yu, Y. Ito, T. Nishida, I. Yumoto, K. Watanabe, and H. Okuyama. 2004. Characterization of the eicosapentaenoic acid biosynthesis gene cluster from *Shewanella* sp. strain SCRC-2738. *Cell. Mol. Biol. (Noisy-le-grand)* **50:** 625-630.

(94) Napier, J. A., L. V. Michaelson. 2001. Genomic and functional characterization of polyunsaturated fatty acid biosynthesis in *Caenorhabditis elegans*. *Lipids* **36:** 761-766.

(95) Nakamura, M. T., T. Y. Nara. 2003. Essential fatty acid synthesis and its regulation in mammals. *Prostaglandins, Leukotrienes and Essential Fatty Acids* **68:** 145-150.

(96) Chenna, R., H. Sugawara, T. Koike, R. Lopez, T. J. Gibson, D. G. Higgins, and J. D. Thompson. 2003. Multiple sequence alignment with the Clustal series of programs. *Nucleic Acids Res.* **31:** 3497-3500.

(97) Warude, D., K. Joshi, and A. Harsulkar. 2006. Polyunsaturated fatty acids: biotechnology. *Crit. Rev. Biotechnol.* **26:** 83-93.

(98) Fu, J., E. Hettler, and B. L. Wickes. 2006. Split marker transformation increases homologous integration frequency in *Cryptococcus neoformans*. *Fungal Genetics and*

Biology **43:** 200-212.

(99) Folch, J., M. Lees, and G. H. Sloane stanley. 1957. A simple method for the isolation and purification of total lipides from animal tissues. *J. Biol. Chem.* **226:** 497-509.

(100) Lee Chang, K. J., M. P. Mansour, G. A. Dunstan, S. I. Blackburn, A. Koutoulis, and P. D. Nichols. 2011. Odd-chain polyunsaturated fatty acids in thraustochytrids. *Phytochemistry* **72:** 1460-1465.

(101) Worgall, T. S., S. L. Sturley, T. Seo, T. F. Osborne, and R. J. Deckelbaum. 1998. Polyunsaturated fatty acids decrease expression of promoters with sterol regulatory elements by decreasing levels of mature sterol regulatory element-binding protein. *J. Biol. Chem.* **273:** 25537-25540.

(102) Teran-Garcia, M., C. Rufo, M. T. Nakamura, T. F. Osborne, and S. D. Clarke. 2002. NF-Y Involvement in the Polyunsaturated Fat Inhibition of Fatty Acid Synthase Gene Transcription. *Biochem. Biophys. Res. Commun.* **290:** 1295-1299.

(103) Teran-Garcia, M., A. W. Adamson, G. Yu, C. Rufo, G. Suchankova, T. D. Dreesen, M. Tekle, S. D. Clarke, and T. W. Gettys. 2007. Polyunsaturated fatty acid suppression of fatty acid synthase (FASN): evidence for dietary modulation of NF-Y binding to the Fasn promoter by SREBP-1c. *Biochem. J.* **402:** 591-600.

(104) Domergue, F., A. Abbadi, C. Ott, T. K. Zank, U. Zahringer, and E. Heinz. 2003. Acyl carriers used as substrates by the desaturases and elongases involved in very long-chain polyunsaturated fatty acids biosynthesis reconstituted in yeast. *J. Biol. Chem.* **278:** 35115-35126.

(105) Jareonkitmongkol, S., E. Sakuradani, and S. Shimizu. 1993. A Novel Delta5-Desaturase-Defective Mutant of *Mortierella alpina* 1S-4 and Its Dihomo-gamma-Linolenic Acid Productivity. *Appl. Environ. Microbiol.* **59:** 4300-4304.

(106) Hauvermale, A., J. Kuner, B. Rosenzweig, D. Guerra, S. Diltz, and J. G. Metz. 2006. Fatty acid production in *Schizochytrium* sp.: Involvement of a polyunsaturated fatty acid synthase and a type I fatty acid synthase. *Lipids* **41:** 739-747.

(107) Jiang, X., L. Qin, B. Tian, Z. Shu, and J. Huang. 2008. Cloning and expression of two elongase genes involved in the biosynthesis of docosahexaenoic acid in *Thraustochytrium* sp. FJN-10. *Wei Sheng Wu Xue Bao* **48:** 176-183.

ACKNOWLEDGEMENTS

The author would like to express heartfelt gratitude to Dr. Makoto Ito, Professor of Kyushu University Graduate School, for ardent instruction, enthusiastic discussions, and warm encouragements throughout of this study.

The author would also like to express profound gratitude to Dr. Nozomu Okino, Associate Professor of Kyushu University Graduate School, for invaluable help and encouragements throughout of this study.

The author extends sincere appreciation to Dr. Miki Nakao, Professor of Kyushu University Graduate School, for making a thorough review of the thesis.

The author expresses hearty thanks to Dr. Keishi Sakaguchi at Kyushu University for constructive advice, technical assistance and training throughout of this study.

The author acknowledges a great debt to Dr. Yoichiro Hama, Associate Professor of Saga University, for GC-MS analysis, precise suggestions and sincere encouragements.

The author appreciates Dr. Masahiro Hayashi, Associate Professor of Miyazaki University, and Dr. Daisuke Honda, Associate Professor of Konan University, for providing thraustochytrids and advice for cultivating the organisms.

The author expresses gratitude to Dr. Norihide Kurano and Dr. Akira Sato, Marine

Biotechnology Institute Co., Ltd., for providing invaluable samples, and Dr. Shinichi Sugimoto and Mr. Yuji Okita, Nippon Suisan Kaisha, Ltd., for valuable suggestions and encouragements.

Heartfelt thanks to Dr. Yohei Ishibashi, Dr. Eriko Abe and Dr. Naoyuki Matsunaga for generous support throughout of this work.

The author would like to thank Dr. Kuniko Yamaguchi, Ms. Noriko Nakahara, each and every one of other members in the Laboratory of Marine Resource Chemistry, Department of Bioscience and Biotechnology, Graduate School of Bioresource and Bioenvironmental Sciences, Kyushu University, for encouragements throughout of this study.

Finally, the author owes the deepest gratitude to my family for support and encouragement throughout of my life.